WASHINGTON UNIVERSITY
SEVER INSTITUTE OF TECHNOLOGY
DEPARTMENT OF CHEMICAL ENGINEERING

MODELING OF GAS AND LIQUID PHASE MIXING WITH REACTION IN BUBBLE COLUMN REACTORS

by

QINGQI WANG

Prepared under the direction of Professor M. P. Dudukovič

A thesis presented to the Sever Institute of
Washington University in partial fulfillment
of the requirements of the degree of
MASTER OF SCIENCE

August, 1996
Saint Louis, Missouri

WASHINGTON UNIVERSITY
SEVER INSTITUTE OF TECHNOLOGY
DEPARTMENT OF CHEMICAL ENGINEERING

ABSTRACT

MODELING OF GAS AND LIQUID PHASE MIXING WITH REACTION IN BUBBLE COLUMN REACTORS

by Qingqi Wang

ADVISER: Professor Milorad P. Dudukovič

August, 1996
St. Louis, Missouri

Bubble column reactors are widely used in industry. The knowledge of gas and liquid phase mixing and flow pattern in bubble columns is critical to their design, scale up and operations. In this work, a two phase phenomenological model, based on the physical description of the bubble column system in both bubbly and churn turbulent flow, is developed and presented. The model accounts for observed large scale recirculation of liquid and gas phase and for crossmixing between the upflow and the downflow regions.

A bimodal bubble size distribution is assumed. A bubble column is represented by nine different regions: upflow region for large bubbles, upflow and downflow regions for small bubbles, upflow and downflow regions for the liquid phase, the distributor and disengagement zones for the gas phase, and liquid inlet and outlet mixing zones. The interactions between the upflow and downflow of liquid, between the upflow and downflow of small bubbles and between large and small bubbles, are all incorporated in this model based on available fundamental and phenomenological relations. Coupling between the phases is brought in through the mass transfer terms. A weighting factor, describing the relative contribution to mass transfer for different size bubbles and in different regions, is defined. Liquid phase chemical reaction is also accounted for.

The model is presented for two cases: one with continuous flow of both liquid and gas, and the other for batch liquid with continuous flow of gas. An implicit finite difference routine is developed to obtain the residence time distribution numerically for tracer data analysis. Concentration profiles in different regions as a function of time on stream are predicted. The comparison of model predictions with data from the literature in various bubble column sizes is presented. It is found that the model can satisfactorily represent a variety of operating conditions.

The developed recycle with cross flow model (RCFM) is used to predict bubble column performance for a number of liquid phase reaction schemes. In addition, tracer impulse responses are predicted based on the model at various column locations subject to tracer injection at different positions in the column for both batch and continuous flow of liquid.

TABLE OF CONTENTS

No. Page

TABLE OF CONTENTS

(continued)

No. Page

TABLE OF CONTENTS

(continued)

No. Page

LIST OF TABLES

No. Page

LIST OF FIGURES

No. Page

LIST OF FIGURES

(continued)

No. Page

LIST OF FIGURES

(continued)

No. Page

LIST OF FIGURES

(continued)

No. Page

LIST OF FIGURES

(continued)

GLOSSARY

a = interfacial area (m^2/m^3)

Ar = free area of gas distribution (m^2)

C = concentration (mol/m^3)

d = bubble diameter (m)

D = column diameter (m)

E(t) = derivative of residence time distribution

F(t) = step input response

g = gravitational acceleration (m/s^2)

H = Henry's constant

H(t) = Heaviside's step function

k = reaction rate constant for first order reaction ($1/s$)

k_e = exchange coefficient (m^2/s)

k_l = mass transfer coefficient (m/s)

K = dimensionless crossmixing coefficient

l = Prantl's mixing length (m)

L = column height (m)

Q = volumetric flow rate (m^3/s)

r = recycle ratio

R = column radius (m)

t = time (s)

Sc = Schmidt number

U = superficial velocity (m/s)

u = interstitial velocity (m/s)

$\bar{u}$ = mean interstitial velocity (m/s)

u_S = slip velocity (m/s)

V = volume (m^3)

x = dimensionless position along longitudinal direction

Greek letters

ε = gas hold up

$\bar{\varepsilon}$ = average gas hold up

ρ = density (kg/m^3)

$\Delta\rho$ = density difference between liquid and gas (kg/m^3)

η = viscosity (cp)

σ = surface tension of liquid (N/m^2)

τ = residence time (sec)

μ_l = liquid viscosity (cp)

η_l = liquid viscosity (cp)

ν_m = molecular viscosity (m^2/s)

ν_t = turbulent kinematic viscosity (m^2/s)

δ = delta function

Subscript

b = bubble

g = gas

gl = large bubble

gs = small bubble

g_{in} = inlet of gas

g_{out} = outlet of gas

g_o = gas at t=0

g_1 = small bubble in upflow region

g_{12} = between small bubbles in upflow and downflow

g_{13} = between small bubbles in upflow and large bubbles

g_2 = small bubble in downflow region

g_3 = large bubble in upflow region

l = liquid

l_{in} = inlet of liquid

l_0 = liquid at t=0

l_{out} = outlet of liquid

LB = large bubble

l_1 = liquid in upflow region

l_{1a} = liquid a in upflow region

l_{1b} = liquid b in upflow region

l_{1c} = liquid c in upflow region

l_{12} = between upflow and downflow of liquid

l_2 = liquid in downflow region

l_{2a} = liquid a in downflow region

l_{2b} = liquid b in downflow region

l_{2c} = liquid c in downflow region

large = large bubble

o = central

s = small bubble

SB = small bubble

total = t

trans = transition

w = wall

Superscript

l = large

s = small

ACKNOWLEDGMENTS

I would like to deeply express my gratitude to my adviser Dr. Milorad P. Dudukovic' for his support, constructive criticism through all the work of my thesis. His tremendous source of inspiration conducts me to develop new models. The discussion between us and his critical review of my thesis help me to dive into the world of bubble column reactors, enhance my research ability and also improve my English proficiency. The way to study and work I learned from him definitely benefits for my future career.

I am very thankful to my colleagues, Dr. Salesh Kumar for the discussion of one dimensional liquid phase model and the source of some important reference to initiate the bubble column research. Ms. Sujatha Degalessan for her help in developing the two phase recycle with cross flow mixing model, providing the liquid phase tracer data and critical review of my thesis. My appreciation also goes to Mr. Puneet Guopta and Mr. Shantanu Roy for their critical review of my thesis and Dr. Baisheng Zhou for the helpful discussion. Dr. Al-Dahhan Muthanna for the review of my thesis.

I am also grateful for the support received from the industrial participants of the Chemical Reaction Engineering Laboratory (CREL) consortium and the Fellowship from the Department of Chemical Engineering during my study at Washington University. In addition, I would like to thank the support of the Department of Energy via Air Product Contract No. DOE-FC 22-95 PC 95051.

Finally, I wish to deeply express my thanks to my wife Yehua (Emily) Yang for her love and support. The encouragement of my parents is also greatly appreciated.

Modeling of Gas and Liquid Phase Mixing with Reaction in Bubble Column Reactors

1. Introduction

Bubble column reactors are widely used in diverse engineering applications. Typical uses in chemical industry include hydrogenation, chlorination, oxidation, sulphonation, gas purification and etc. (Deckwer, (1985), Menzel et al. (1990) and Shetty et al. (1992)). In petrochemical applications, bubble column reactors have a distinct advantage over other processes such as fixed bed reactors in their uniform temperature distribution and effective heat transfer. They are also frequently being used in fermentation such as beer production (Lübbert and Larson, (1990), (Lübbert, (1991)), Fischer-Tropsch synthesis (Bukur, et al. (1986)) and production of liquid fuels from biological materials and natural gas (Toseland et al. (1994)). Recently, the increasing demand for bubble columns in the field of biotechnology, biochemical engineering as well as in waste water treatment and in syngas conversion processes makes extensive studies of bubble column reactors more and more important.

The ultimate goal in bubble column research is to rapidly scale up from laboratory size to pilot plant size and finally to industrial bubble column scale. It has been found that both gas and liquid phase mixing behavior, turbulent intensity and residence time distribution of both phases are critical to the design, scale-up and operation. During the past two decades, modeling of the mixing behavior of both gas and liquid phases has been widely investigated but it is not yet completely successful. This is due to the difficulties in describing the following: 1. complexities of liquid backmixing behavior including chaotic phenomena; 2. bubble size distribution in the churn turbulent regime (heterogeneous regime); 3. the difference in the mixing caused by large and small bubbles, and the

interaction among bubbles in churn turbulent regime due to coalescence and break-up of bubbles; and 4. interfacial mass transfer process coupled with chemical reaction.

It is believed that the ultimate representation of physical phenomena in a bubble column system relies on the complete solution of fundamental governing hydrodynamic equations. Improved understanding of many effects results from the use of computational fluid dynamic codes (e.g. CFDLIB codes from Los Alamos by Kashiwa and Core (1991) and Lübbert and Lapin (1994)). Although extensive studies of computational hydrodynamic models continue in this field, due to the complexities of the system and the limitations of the current computer, it may take quite a long time to achieve a complete solution of the fundamental models. Therefore, a phenomenological model, which captures the observed phenomena and physically describes the bubble column system is urgently required to meet our current needs.

A review of the past literature reveals that most of the models for mixing in bubble column reactors are often restricted to the liquid phase, and modeling of gas phase mixing is much less frequently described. Furthermore, modeling of both gas and liquid phase mixing with the impact on chemical reaction and mass transfer is even more scarcely reported. Nearly all the reported models for the gas phase and for the liquid phase are based on the axial dispersion model (ADM) such as those of Field and Davidson (1980), Towell and Ackerman (1981), Kawaoe et al. (1988), Van Vuuren (1991), Shetty et al. (1992), Modak et al. (1993) and Toseland et al. (1994). In Shetty et al.'s (1992) paper, a bimodal bubble size distribution is incorporated in the ADM. Furthermore, Modak et al. (1993) illustrated through regression analysis that the exchange coefficient between large and small bubbles in the churn turbulent regime is very large, which implies that the concentration in the large bubbles and the surrounding small bubbles is similar.

Very few papers have relied on a phenomenological backmixing model, such as papers by Myers et al. (1987) and Degalessan et al. (1996), but these are only applied to the liquid phase in a bubble column reactor. Although the axial dispersion model has been successfully used in many situations, as has been pointed out by Levenspiel and Fizgerald (1983) and Deckwer and Schumpe (1993), this model is over simplified and is not a good choice for bubble column reactors. This is because the axial dispersion model usually describes a small deviation from the plug flow. Experimental observations recently reported by Lübbert and Larson (1990) and Devanathan et al. (1990) indicated that the liquid behavior is dominated by large scale convection rather than random and small scale phenomena. In the churn turbulent regime with high superficial gas velocity, the bimodal bubble size distribution was assumed for the gas phase by Vermeer and Krishna (1981) and Shah and Joseph (1985). The flow in that regime becomes chaotic, and is characterized by fast moving large bubbles in the presence of small bubbles which are carried with the recirculated liquid. The gas phase mixing is also one of the important hydrodynamic parameters to be considered in the scale-up of a bubble column system, which physically, can't be simply modeled by ADM! It is noteworthy that the reason for selecting ADM in the past has been the fact that ADM is simple and only has one parameter and, from the mathematical point of view, it can sometimes fit the experimental residence time distribution (RTD) data. Therefore, a new phenomenological model that relies on the realistic physical picture of a bubble column reactor, and also fits the experimental RTD curves, needs to be developed.

Recycle with cross flow model (RCFM) is a good choice. It was first developed in 1970 by Hochman and McCord and was successfully applied for tall tanks with a number of axial impellers. Myers et al. (1987) and Degalessan et al. (1996) extended its application by successfully implementing the model to describe backmixing of the liquid phase in bubble column reactors. Froment and Bischoff (1990) have also noted the applicability of this model for the bubble column system. However, a reaction scheme has

never been included in the model, only the injection point of tracer at the bottom or at the top of the column was considered. In addition, the model was only used previously in the liquid phase. The applicability of the model for gas phase mixing is unknown.

Recent experimental evidence (Devanathan et al. (1990), Yang et al. (1993) and Degalessan et al. (1996)), confirms the existence of large single liquid recirculation cell in bubble columns. Data obtained by Computer Aided Radioactive Particle Tracking (CARPT) also indicates the existence of radial eddy diffusivity which can be modeled by a cross flow exchange coefficient. Hence, a recycle with cross flow model represents a good physical basis for modeling bubble column system. In this work, we prepare to use such a physical basis and develop a model for gas and liquid phase mixing with mass transfer and reaction. The capabilities of the model for predicting tracer test results and reactant conversions will then be tested.

2. Research Objectives

The overall objective of this work is the development of a new phenomenological model, two phase recycle with cross flow model (TRCFM), to describe, based on the available physical evidence, the two phase bubble column reactors in both churn turbulent and bubbly flow regimes.

Specifically, the following goals have been set:

1. Development of a two phase recycle with cross flow model (TRCFM).

2. Determination of model parameters from experimental observations and empirical correlations.

3. Development of TRCFM subcases for representation of liquid phase mixing together with different chemical reaction schemes (single irreversible reaction, series reactions and parallel reactions) in the liquid phase for both continuous liquid flow and batch liquid processing.

4. Development of a TRCFM subcase for representation of gas phase mixing.

5. Test of the model with tracer experimental data for different size of bubble column reactors.

3. Review of the Recycle with Cross Flow Model (RCFM)

Hochman and McCord (1970) proposed a liquid phase mixing model, the recycle with cross flow model (RCFM) to describe residence time distributions in a tall stirred tank with multiple axial impellers. Later, this model was extended to be used for liquid phase mixing in bubble columns by Myers et al.(1986). They divided the liquid phase of a bubble column into two regions: upflow in the core region (L1) and downflow in the annular region (L2). (See Figure 3-1). In such a system, the shear stress generated between the upflow and the downflow streams results in substantial crossmixing between two streams. The residence time distribution in each region and the recycle ratio, defined as the ratio of liquid phase volumetric flowrate in the downflow region to the inlet liquid volumetric flowrate, can be determined if the liquid phase interstitial velocity and the gas holdup profiles are known. The liquid phase velocity and the gas holdup profiles can be obtained either through empirical correlations, such as proposed by Miyauchi and Ueyama (1979), Anderson and Rice(1989) and etc., which will be discussed later in detail, or by experimental means. Typical examples of advanced experimental approach can be found in the studies by Devanathan et al. (1990) and Kumar et al. (1994). They used the Computer Automated Radioactive Particle Tracking (CARPT) facility together with Computer Tomography (CT) facility to experimentally determine the interstitial liquid velocity and the gas holdup profiles. The only remaining parameter of the RCFM model that needs to be fitted is the "exchange coefficient", K_{l12}. This parameter quantifies the "communication" between the upflow and downflow regions.

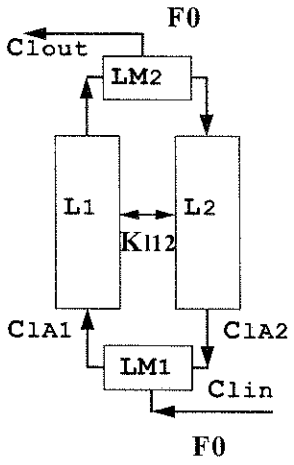

FIGURE 3-1. Liquid Phase Recycle with Cross Flow Model (RCFM)

4. Two Phase Recycle with Cross Flow Model (TRCFM)

Based on the experimental observations by Hill (1974), Devanathan et al. (1990), Grienberger and Hoffmann (1992) and Krishna and Ellenberger (1995), in bubble columns, large scale liquid circulation exists. The liquid ascends in the core region of the column and descends in the annular region close to the wall, which results in the overall liquid circulation and forms what is called a "cell pattern". In the homogeneous regime, e.g. bubbly flow regime, the superficial gas velocity is lower than the transition velocity, which is defined as the velocity where the flow pattern changes from the homogeneous regime to the heterogeneous regime (Vermeer and Krishna (1981), Krishna et al. (1994) and Krishna and Ellenberger (1995)). In the bubbly flow regime, it is assumed that only small bubbles of uniform size exist. These small bubbles, which are carried with the recirculated liquid, exhibit a slip velocity between the gas and the liquid. The motion of the small bubbles in the bubbly flow regime exhibits two different flow patterns. Small bubbles may rise in the core of the column or descend in the annular region close to the wall due to the downward velocity of liquid. In that situation, gas recirculation is induced by liquid circulation, and there is interaction between the upflow of the liquid and the downflow of the liquid and between the upflow of the small bubbles and the downflow of the small bubbles due to the shear stress between these two regions. On the other hand, in the case when the slip velocity is large enough to compensate for the downward velocity of the liquid, no small bubbles will move downward and, therefore, there will be no gas phase recirculation. In one of the cases of the new model, the first situation is assumed for representing the bubbly flow regime.

The heterogeneous regime, where the superficial gas velocity is high enough so that there is a distinct bimodal bubble size distribution, is usually called the "churn turbulent regime"(Vermeer and Krishna (1981), Krishna et al. (1994) and Krishna and Ellenberger (1995)). In this regime, because of bubble coalescence and break-up, there is interaction not only between bubbles of the same size but also among bubbles of different sizes. Due to the extreme complexities of bubble interaction and bubble size distribution, two bubble sizes (large and small bubbles) are assumed here. This is a good assumption since the bimodal bubble size distribution is seen from the experimental observations by means of dynamic gas disengagement (DGD) experiments. The large bubbles are assumed to rise in plug flow near the core region of the bubble column with higher velocity; the small bubbles, however, which are carried by the recirculated liquid, travel with lower velocity. The velocity difference for two different sizes of bubbles is due to the difference in slip velocity which is related to bubble size. The recirculation of small bubbles consists of upflow in the core region and downflow in the annular region. Figure 4-1 shows the typical velocity profiles for the small bubbles and the liquid, and for the volume occupied by each phase in each region. It is seen that the volume $V_{g1} + V_{g3} - V_{g1}^{1}$ represents the volume of small bubbles in the upflow region where the interstitial velocity of the liquid is above zero. V_{g1}^{1} represents the partial volume of the small bubbles in the upflow region where the interstitial velocity of the liquid is less than zero. V_{g2} is the volume of the small bubbles in the downflow region. V_{l1} is the volume of the liquid in the upflow region. V_{l2} is the volume of the liquid in the downflow region. V_{l2}^{1} is the partial volume of the liquid in the downflow region where the interstitial small bubble velocity is greater than zero. In addition, due to the shear stress between the upflow and the downflow of the small bubbles and the liquid itself, it is assumed that interaction exists between the small bubbles in the two flow regions as well as between the liquid in the two flow regions. This interaction is described via an exchange coefficient which will be discussed in detail

later. In addition, the exchange coefficient between the small and large bubbles is also defined in the model. This allows for the coalescence and break-up of the bubbles to be accounted for.

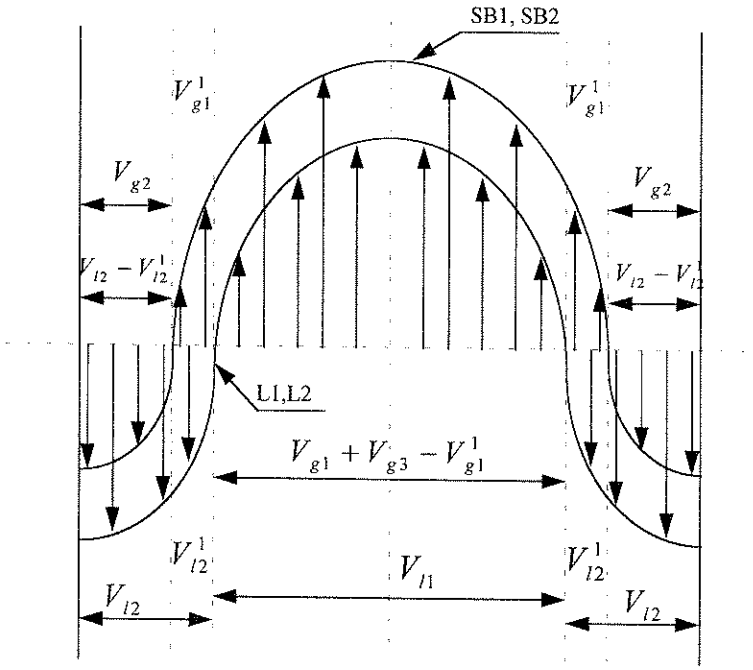

FIGURE 4.1. Schematic Diagram of Liquid and Small Bubble Time Average Interstitial Velocity Profiles in Bubble Column Reactors

The proposed model may also be applied for the case where interfacial mass transfer is present, such as for the gas component that is partially absorbed in the liquid or for a soluble gas tracer injected in the bubble column for tracer study. The mass transfer coefficients representing the large bubbles and the liquid, and the small bubbles and the liquid, are defined in the model to couple the phases. The model may also be applied for liquid phase chemical reactions when the reaction term is incorporated in the model equations.

Based on the above assumptions, a two phase recycle with cross flow model (TRCFM) emerges to physically describe gas and liquid phase mixing and numerous interactions among bubbles of the same and different size, between the liquid in upflow and downflow regions, between gas and liquid phase (mass transfer) as well as liquid phase reactions.

In churn turbulent regime (heterogeneous regime), the bubble column is assumed to be divided into nine different regions:

1. Large bubble upflow region (LB)

2. Small bubble upflow region (SB1)

3. Small bubble downflow region (SB2)

4. Liquid upflow region (L1)

5. Liquid downflow region (L2)

6. Distributor region for the gas phase at the inlet of the column (GM1)

7. Disengagement region for the gas phase at the outlet of the column (GM2)

8. Mixing zone of the liquid phase at the inlet of the bubble column (LM1)

9. Mixing zone of the liquid phase at the outlet of the bubble column (LM2)

Figure 4-2 schematically represents the phenomenological picture of a bubble column with bimodal bubble size distribution.

Figure 4-3 schematically represents the phenomenological basis for deriving the model equations for the two phase recycle with cross flow model (TRCFM). Nine regions are assumed. The soluble gas enters the bottom of the bubble column, then distributes into two bubble classes, large bubbles traveling in the upflow region (LB), small bubbles entrained by the recirculation of the liquid, traveling in both the upflow region (SB1) and the downflow region (SB2). The liquid also enters at the bottom of the bubble column and is in upflow in the L1 region and in downflow in the L2 region. The arrows shown in Figure 4-3 represent the various interactions between the large bubbles and the small bubbles in the upflow region, between the small bubbles in the upflow region and the small bubbles in the downflow region, between the liquid in the upflow region and the liquid in the downflow region, and the mass transfer effects between the large bubbles and the liquid in the upflow region, between the small bubbles in the upflow region and the liquid in the upflow region, between the small bubbles in the upflow region and the liquid in the downflow region, between the small bubbles in the downflow region and the liquid in the downflow region. GM1, LM1, GM2 and LM2 represent the gas distributor zone, the liquid inlet zone, the gas disengagement zone and the liquid outlet zone, respectively. For simplicity, it is assumed that these four regions have negligible residence times. The liquid and gas leave from the top of the bubble column.

4.1 Physical Basis for the Model and its Assumptions

The following assumptions are made:

1. Bubbles are classified into two classes, large bubbles as dilute phase and small bubbles as dense phase (Vermeer and Krishna, (1981), Krishna et al. (1991), Krishna et.

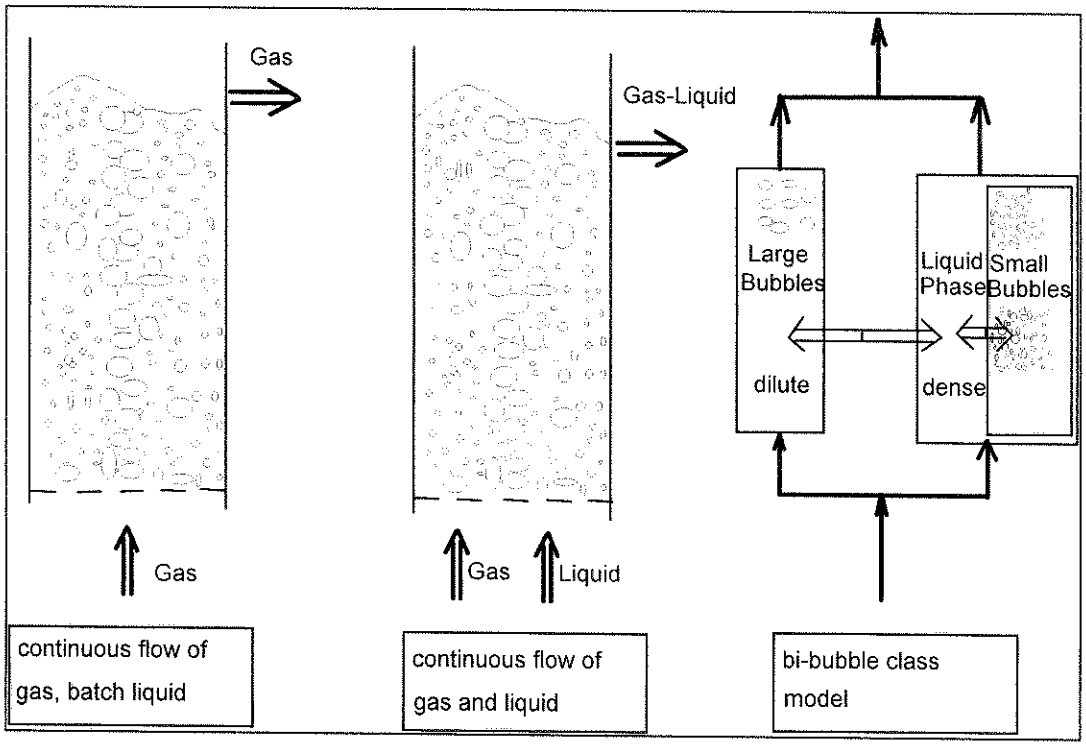

FIGURE 4-2. Typical Diagram of Gas-Liquid Bubble Column Reactors

al. (1994) and Krishna and Ellenberger, (1995)). In the bubbly flow regime, only small bubbles are assumed to exist.

2. It is assumed that large bubbles (LB) travel in plug flow near the core of the bubble column with higher rise velocity (Shetty et al. (1992), Krishna et al. (1994)) than the small bubbles.

3. The small bubbles are assumed to be partially backmixed and travel with lower velocity. Since they are recirculated along with the liquid phase (Shetty et al. (1992), Krishna et al. (1994)), it is assumed that the motion of small bubbles (SB1, SB2) can be modeled by recycle with crossflow, and the gas phase for small bubbles is, therefore, divided into two regions (upflow and downflow).

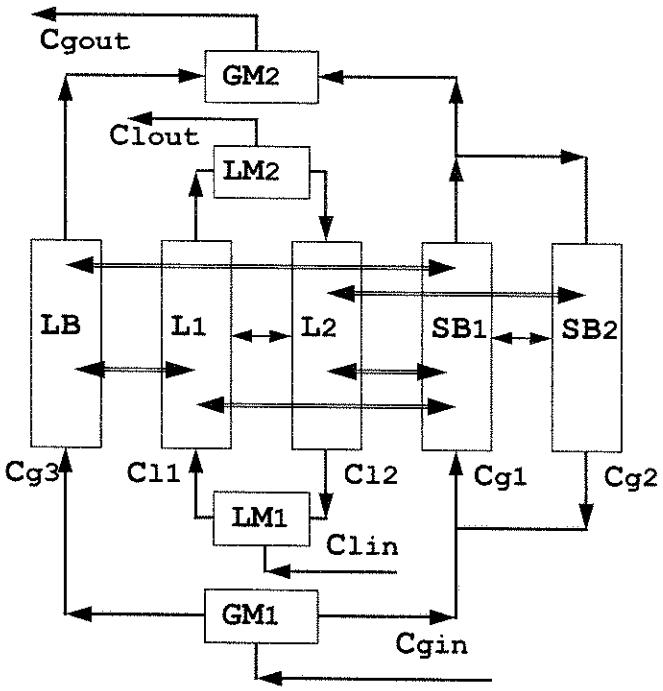

FIGURE 4-3. Schematic Diagram of TRCFM for Continuous Flow of Gas and Liquid

4. Liquid phase motion and exchange (L1, L2) are also modeled by recycle with cross flow. Liquid phase in the column is divided into two regions (upflow and downflow). This is due to the experimental observation of the overall liquid recirculation behavior in the bubble column (Myers et al. (1987), Devanathan et al. (1990) and Degalessan et al. (1996)).

5. There is no interaction among large bubbles, but interaction is allowed between small bubbles (Shetty et al. (1992)), and between large and small bubbles (Modak et al. (1993)), except for the gas disengagement zone and for the gas distributor zone. The interaction between large and small bubbles is accounted for by the coalescence and the break-up of bubbles (Modak et al. (1993)).

6. Gas is soluble, mass transfer effect is allowed.

7. The distributor zone for the gas inlet can be modeled as a perfect mixer with negligible residence time.

8. The gas disengagement zone can also be modeled as an ideal mixer with negligible residence time.

9. The liquid inlet mixing and outlet mixing zones are assumed to be perfect mixers with negligible residence times.

10. Liquid phase reactions are allowed.

4.2 Mathematical Models and Boundary Conditions

4.2.1 Churn Turbulent Regime

For the churn turbulent regime, the proposed model is presented for two cases:

1. Continuous flow of both gas and liquid.

2. Batch liquid, continuous flow of gas.

We will show later that the two phase recycle with cross flow model (TRCFM) can also be applied for the homogeneous bubbly flow regime.

4.2.1.1 Continuous Flow of Gas and Liquid

The phenomenological basis for the model equations is shown in Figure 4-1 and Figure 4-3. Figure 4-1 is a schematic of the observed liquid recirculation which dominates gas recirculation of small bubbles.

For the gas phase in small bubbles, the mass balance for a soluble gas component yields all the equations for the various regions.

Upflow region of small bubbles (SB1)

$$\tau_{g1}\frac{\partial C_{g1}}{\partial t}+\frac{\partial C_{g1}}{\partial x}+\frac{K_{g12}}{1+r_{g12}}(C_{g1}-C_{g2})+K_{g13}(C_{g1}-C_{g3})-(\frac{V_{l1}}{V_{l1}+V_{l2}^{1}})$$

$$(k_l a)^S(HC_{l1}-C_{g1})\tau_{g1}-(\frac{V_{l2}^{1}}{V_{l1}+V_{l2}^{1}})(k_l a)^S(HC_{l2}-C_{g1})\tau_{g1}=0 \qquad (4.1)$$

where τ_{g1} (s) is the mean residence time of small bubbles traveling in the SB1 section; r_{g12} is the recycle ratio for small bubbles which is defined as the ratio of the volumetric flowrate of SB2 region to the inlet volumetric flowrate of the gas into the small bubble region (SB1+SB2); K_{g12}, K_{g13} are the dimensionless exchange coefficients between the upflow of the small bubbles in the SB1 section and the downflow of the small bubbles in the SB2 section, and between the upflow of the small bubbles in the SB1 section and the upflow of the large bubbles in the LB section, respectively; H is Henry's coefficient $(mol/m^3(gas)*m^3(liquid)/mol)$; $(k_l a)^S$ is the volumetric mass transfer coefficient between the small bubbles and the liquid (s^{-1}); V_{l1}, V_{l2}^{1} (m^3) are the volume of the liquid in the L1 section, and the volume of the liquid in the L2 section where the interstitial velocity of the small bubbles is greater than zero. (See Figure 4.1).

Downflow region of small bubbles (SB2)

$$\tau_{g2}\frac{\partial C_{g2}}{\partial t}-\frac{\partial C_{g2}}{\partial x}-\frac{K_{g12}}{r_{g12}}(C_{g1}-C_{g2})-(k_l a)^{s}(HC_{l2}-C_{g2})\tau_{g2}=0 \qquad (4.2)$$

where τ_{g2} (s) is the mean residence time of the small bubbles in the SB2 section.

Upflow region of large bubbles (LB)

$$\tau_{g3}\frac{\partial C_{g3}}{\partial t}+\frac{\partial C_{g3}}{\partial x}-(k_l a)^{l}(HC_{l1}-C_{g3})\tau_{g3}+K_{g13}(C_{g3}-C_{g1})=0 \qquad (4.3)$$

where τ_{g3} (s) is the mean residence time of the large bubbles in the LB section; $(k_l a)^{l}$ is the volumetric mass transfer coefficient between the large bubbles and the liquid (s^{-1}).

The mass balance for a soluble gas component in the liquid phase yields the following equations for the various regions in the liquid phase.

Upflow region of liquid

$$\tau_{l1}\frac{\partial C_{l1}}{\partial t}+\frac{\partial C_{l1}}{\partial x}+\frac{K_{l12}}{1+r_{l12}}(C_{l1}-C_{l2})+\frac{V_{g1}-V_{g1}^{1}}{V_{l1}}\left(\frac{V_{g1}-V_{g1}^{1}}{V_{g3}+V_{g1}-V_{g1}^{1}}\right)(k_l a)^{s}(HC_{l1}$$

$$-C_{g1})\tau_{l1}+\frac{V_{g3}}{V_{l1}}\left(\frac{V_{g3}}{V_{g3}+V_{g1}-V_{g1}^{1}}\right)(k_l a)^{l}(HC_{l1}-C_{g3})\tau_{l1}+R_{l1}\tau_{l1}=0 \qquad (4.4)$$

where τ_{l1} (s) is the mean residence time of the liquid in the L1 section; r_{l12} is the recycle ratio for the liquid which is defined as the ratio of the volumetric flowrate of the L2 section to the inlet volumetric flowrate liquid to the upflow and the downflow

liquid sections (L1+L2); K_{l12} is the dimensionless exchange coefficient between the upflow of the liquid and the downflow of the liquid; $V_{g1}, V_{g3}, V_{g1}^{1}(m^3)$ are the volume of the small bubbles in the SB1, the volume of the large bubbles in the LB and the partial volume of small bubbles in the upflow section where the liquid goes downward (interstitial liquid velocity less than zero) and the small bubbles travel upward (interstitial gas velocity greater than zero); R_{l1} is the reaction term in the upflow region of the liquid. It is assumed that the reaction only occurs in the liquid phase.

In the liquid phase of the upflow region, as can be seen from Figure 4-1 and Figure 4-3, one may encounter both large bubbles and small bubbles. In order to describe the contribution to mass transfer for large and small bubbles, the weighing factor is defined to represent the mass transfer for a bimodal bubble size distribution based on the relative volume percentage of small bubbles and large bubbles.

$\frac{V_{g1}-V_{g1}^{1}}{V_{g3}+V_{g1}-V_{g1}^{1}}$ is the weighing factor for the contribution of small bubbles in the upflow section of the liquid to mass transfer.

$\frac{V_{g3}}{V_{g3}+V_{g1}-V_{g1}^{1}}$ is the weighing factor for the contribution of large bubbles in the upflow section of the liquid to mass transfer.

.

Downflow region of liquid

$$\tau_{l2}\frac{\partial C_{l2}}{\partial t}-\frac{\partial C_{l2}}{\partial x}-\frac{K_{l12}}{r_{l12}}(C_{l1}-C_{l2})+\frac{V_{g2}}{V_{l2}}\left(\frac{V_{g2}}{V_{g2}+V_{g1}^{1}}\right)(k_l a)^{s}(HC_{l2}-C_{g2})\tau_{l2}$$

$$+\frac{V_{g1}^{1}}{V_{l2}}\left(\frac{V_{g1}^{1}}{V_{g2}+V_{g1}^{1}}\right)(k_l a)^{s}(HC_{l2}-C_{g1})\tau_{l2}+R_{l2}\tau_{l2}=0 \qquad (4.5)$$

where τ_{l2} (s) is the mean residence time of the liquid in the L2 section and R_{l2} is the liquid phase reaction term in the downflow region of the liquid.

As can been seen from Figure 4-1 and Figure 4-3, in the downflow region of the liquid, one may encounter small bubbles in downflow or small bubbles in upflow. In the same way, as discussed above, a weighing factor is defined to describe the relative contribution of small bubbles in upflow and small bubbles in downflow to mass transfer.

$\frac{V_{g2}}{V_{g2}+V_{g1}^{1}}$ is the weighting factor for the contribution of the small bubbles in the downflow section to mass transfer for the downflow region of the liquid.

$\frac{V_{g1}^{1}}{V_{g2}+V_{g1}^{1}}$ is the weighting function for the contribution of the small bubbles in the upflow section to mass transfer for the downflow region of the liquid.

Initial conditions are presented in Equation 4.6 for a step injection into the gas phase at the bottom of the bubble column.

$t = 0$

$$C_{l1} = C_{l2} = C_{g1} = C_{g2} = C_{g3} = 0 \quad and \quad C_{g0} = H(t) \tag{4.6}$$

Boundary conditions are given by Equations 4.7, 4.8 and 4.9 for the small bubbles, for the liquid and for the large bubbles at the bottom of the bubble column, and by Equations 4.10 for the small bubbles and the liquid at the top of the column.

$x = 0$

$$C_{g1} = \frac{1}{1 + r_{g12}}(C_{g0} + r_{g12} C_{g2}) \tag{4.7}$$

$$C_{l1} = \frac{1}{1 + r_{l12}}(C_{l0} + r_{l12} C_{l2}) \tag{4.8}$$

$$C_{g3} = C_{g0} \tag{4.9}$$

$x = 1$

$$C_{g1} = C_{g2}, \quad C_{l1} = C_{l2} \tag{4.10}$$

The total gas phase concentration at the outlet of the bubble column is given by:

$$C_{gout} = \frac{Q_{g12}}{Q_{g12} + Q_{g3}} C_{g1} + \frac{Q_{g3}}{Q_{g12} + Q_{g3}} C_{g3} \tag{4.11}$$

$$or \quad C_{gout} = \frac{U_{g12}}{U_g} C_{g1} + \frac{U_{g3}}{U_g} C_{g3} \tag{4.12}$$

Q_{g12}, Q_{g3} are the volumetric flowrate of the gas phase in form of small bubbles and the volumetric flowrate of the gas phase in form of large bubbles, respectively. U_{g12}, U_{g3}, U_g are the superficial velocity of small bubbles, large bubbles and the total superficial gas velocity, respectively.

It is assumed that for a step input of tracer (Heaviside's step function at x = 0), the solution of all the model equations yields a F-curve for the normalized tracer response,

which on differentiating with respect to time yields an E-curve which is a derivative of the residence time distribution (Dudukovic (1987)).

Mathematically,

$$E(t) = \frac{dF}{dt} = \frac{d(C_g / C_{gin})}{dt} \tag{4.13}$$

At the outlet (x=1), it is evident,

$$E(t) = \frac{U_{g12}}{U_g} E_{SB}(t) + \frac{U_{g3}}{U_g} E_{LB}(t) \tag{4.14}$$

The normalized response can be obtained by dividing $E(t)$ in Equation 4.14 by the maximum value of $E(t)$ in Equation 4.14, which represents the normalized impulse tracer response at the outlet of the bubble column.

The gas phase distributor zone

Ideal mixer is assumed.

$$\tau_{gin} \frac{\partial C_g}{\partial t} = C_{gin} - C'_{gout} \tag{4.15}$$

Negligible residence time is assumed in this section, therefore,

$$\tau_{gin} = 0 \tag{4.16}$$

$$C_{gin} = C'_{gout} \quad or \quad C_{g0} = C_{g3_{x=0}} = C_{g12_{x=0}} \tag{4.17}$$

The disengagement zone

Ideal mixer is assumed.

$$\tau_{gout} \frac{\partial C_g}{\partial t} = C'_{gin} - C_{gout} \tag{4.18}$$

In the same way for the distributor zone it is assumed

$$\tau_{gout} = 0 \tag{4.19}$$

This leads to the followings:

$$C'_{gin} = C_{gout} \tag{4.20}$$

$$C'_{gin} = \frac{Q_{g12}}{Q_{g12} + Q_{g3}} C_{g1} + \frac{Q_{g3}}{Q_{g12} + Q_{g3}} C_{g3} \tag{4.21}$$

(refer to Equation 4.11 and Equation 4.12).

The liquid inlet zone

Ideal mixer is assumed.

$$\tau_{lin}\frac{\partial C_l}{\partial t} = C_{lin} - C'_{lout} \tag{4.22}$$

Negligible residence time is assumed in this section.

$$\tau_{lin} = 0 \tag{4.23}$$

Therefore,

$$C_{lin} = C'_{lout} \quad or \quad C_{l0} = C_{l12_{x=0}} \tag{4.24}$$

The liquid outlet zone

Ideal mixer is assumed.

$$\tau_{lout}\frac{\partial C_l}{\partial t} = C'_{lin} - C_{lout} \tag{4.25}$$

In the same way as in the distributor zone it is assumed

$$\tau_{lout} = 0 \tag{4.26}$$

Therefore,

$$C'_{lin} = C_{lout} \quad or \quad C_{l1_{x=1}} = C_{l2_{x=1}} = C_{lout} \tag{4.27}$$

4.2.1.2 Continuous Flow of Gas and Batch Liquid

In this case, the net flowrate of liquid is zero, the model equations are similar to those in the previous case, the only difference arises in the model equations for the liquid phase and in the inlet boundary conditions which are presented below (refer to Figure 4-4 for the case of batch liquid and continuous flow of gas):

The mass balance for two liquid regions (L1 and L2) is given as follows:

Upflow region of liquid

$$\tau_{l1}\frac{\partial C_{l1}}{\partial t} + \frac{\partial C_{l1}}{\partial x} + K'_{l12}(C_{l1} - C_{l2}) + \frac{V_{g1} - V^1_{g1}}{V_{l1}}\left(\frac{V_{g1} - V^1_{g1}}{V_{g3} + V_{g1} - V^1_{g1}}\right)(k_l a)^S (HC_{l1} - C_{g1})\tau_{l1} + \frac{V_{g3}}{V_{l1}}\left(\frac{V_{g3}}{V_{g3} + V_{g1} - V^1_{g1}}\right)(k_l a)^1 (HC_{l1} - C_{g3})\tau_{l1} + R_{l1}\tau_{l1} = 0 \tag{4.28}$$

Downflow region of liquid

$$\tau_{l2}\frac{\partial C_{l2}}{\partial t} - \frac{\partial C_{l2}}{\partial x} - K'_{l12}(C_{l_1} - C_{l2}) + \frac{V_{g2}}{V_{l2}}\left(\frac{V_{g2}}{V_{g2} + V^1_{g1}}\right)(k_l a)^S (HC_{l2} - C_{g2})\tau_{l2} + \frac{V^1_{g1}}{V_{l2}}\left(\frac{V^1_{g1}}{V_{g2} + V^1_{g1}}\right)(k_l a)^S (HC_{l2} - C_{g1})\tau_{l2} + R_{l2}\tau_{l2} = 0 \tag{4.29}$$

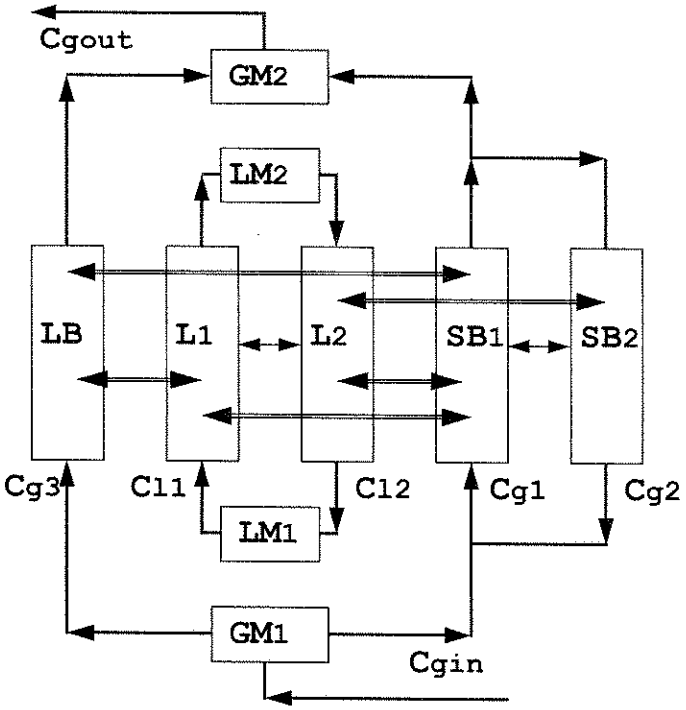

FIGURE 4-4. Schematic Diagram of TRCFM for Continuous Flow of Gas and Batch Liquid

where K'_{l12} is the dimensionless exchange coefficient between the upflow of the liquid in the L1 section and the downflow of the liquid in the L2 section for batch liquid case (see Figure 4-4).

The boundary conditions at the bottom of the bubble column are given by Equation 4.30.

$x = 0$,

$$C_{l1} = C_{l2},\ C_{g1} = \frac{1}{1+r_{g12}}(C_{g0} + r_{g12}C_{g2}),\ C_{g3} = C_{g0} \tag{4.30}$$

4.2.2 Bubbly Flow Regime

For the case of the bubbly flow regime, only small bubbles exist and the equations can, then, be simplified. In Equation 4.1, the interaction term between the large and the small bubbles is neglected. Equation 4.3 is neglected because of the uniform small bubble size distribution. In Equation 4.4, the mass transfer term between the large bubbles and the liquid is neglected. In the boundary conditions, Equation 4.9 is neglected. Figure 4.5 is the schematic representation of the model for the bubbly flow condition. The model equations for the four regions (L1, L2, SB1 and SB2) are as follows:

Upflow region of small bubbles (SB1)

$$\tau_{g1}\frac{\partial C_{g1}}{\partial t}+\frac{\partial C_{g1}}{\partial x}+\frac{K_{g12}}{1+r_{g12}}(C_{g1}-C_{g2})-(\frac{V_{l1}}{V_{l1}+V_{l2}^{1}})(k_la)^{S}(HC_{l1}-C_{g1})\tau_{g1}$$
$$-(\frac{V_{l2}^{1}}{V_{l1}+V_{l2}^{1}})(k_la)^{S}(HC_{l2}-C_{g1})\tau_{g1}=0 \qquad (4.31)$$

Downflow region of small bubbles (SB2)

$$\tau_{g2}\frac{\partial C_{g2}}{\partial t}-\frac{\partial C_{g2}}{\partial x}-\frac{K_{g12}}{r_{g12}}(C_{g1}-C_{g2})-(k_la)^{S}(HC_{l2}-C_{g2})\tau_{g2}=0 \qquad (4.32)$$

Upflow region of liquid

$$\tau_{l1}\frac{\partial C_{l1}}{\partial t}+\frac{\partial C_{l1}}{\partial x}+\frac{K_{l12}}{1+r_{l12}}(C_{l1}-C_{l2})+\frac{V_{g1}-V_{g1}^{1}}{V_{l1}}(k_la)^{S}(HC_{l1}-C_{g1})\tau_{l1}$$
$$+R_{l1}\tau_{l1}=0 \qquad (4.33)$$

Downflow region of liquid

$$\tau_{l2}\frac{\partial C_{l2}}{\partial t}-\frac{\partial C_{l2}}{\partial x}-\frac{K_{l12}}{r_{l12}}(C_{l1}-C_{l2})+\frac{V_{g2}}{V_{l2}}\left(\frac{V_{g2}}{V_{g2}+V_{g1}^{1}}\right)(k_l a)^{s}(HC_{l2}-C_{g2})\tau_{l2}$$

$$+\frac{V_{g1}^{1}}{V_{l2}}\left(\frac{V_{g1}^{1}}{V_{g2}+V_{g1}^{1}}\right)(k_l a)^{s}(HC_{l2}-C_{g1})\tau_{l2}+R_{l2}\tau_{l2}=0 \qquad (4.34)$$

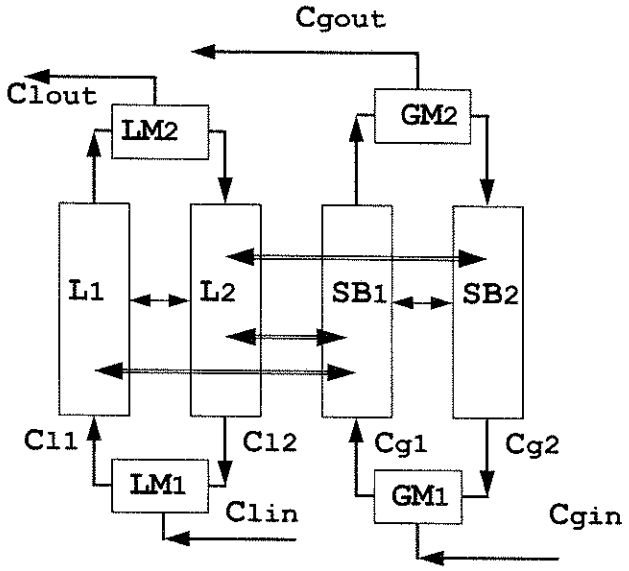

FIGURE 4-5. Schematic Diagram of Two Phase Recycle with Cross Flow Model in Bubbly Flow Regime

4.3 Computational Method

An implicit finite difference method with backward differences in spatial coordinate is used to numerically calculate the concentration profiles along the longitudinal direction of the bubble column, the concentration profiles in different regions (SB1, SB2, LB, L1 and L2) as well as concentration profiles with time on stream.

5. Mathematical Model for the Subcases of TRCFM

Here, we will show that the mathematical model for the subcases of TRCFM can be used in bubble columns. The following cases are considered:

1. A subcase of TRCFM to deal with liquid phase mixing with liquid phase chemical reactions. The objectives are to assess the effect of reaction rate constants and different reaction schemes on the concentration distribution and conversion profiles in both upflow and downflow regions.

2. Use of a subcase of TRCFM to study liquid tracer step and impulse responses in various regions of the column subject to tracer injections at the bottom, the top and the middle of the bubble column.

3. A subcase of TRCFM to represent gas phase mixing.

5.1 Subcase of TRCFM for Liquid Phase Mixing with Chemical Reactions.

It is assumed that liquid reactant is introduced at the bottom of the bubble column reactor. During chemical reaction, the gas hold up is assumed to be constant by assuming that the concentration of liquid reactants and products is small enough as compared with

the concentration of the inert gas carrier. A first order reaction is assumed. The liquid velocity profile is assumed to be independent of chemical reaction because of low concentration for both reactants and products. Due to high turbulent intensity, the exchange coefficient between the reactants in the upflow and downflow regions is assumed to be the same as the exchange coefficient between the products in the upflow and downflow regions. The following Sections of 5.1.1, 5.1.2 and 5.1.3 illustrate three cases of typical linear chemical reaction schemes. The more complicated reaction schemes such as non-linear reaction scheme can be readily handled. A schematic representation of the model for a single irreversible liquid phase reaction $A \xrightarrow{k1} B$ is shown in Figure 5-1 as applied to a bubble column system.

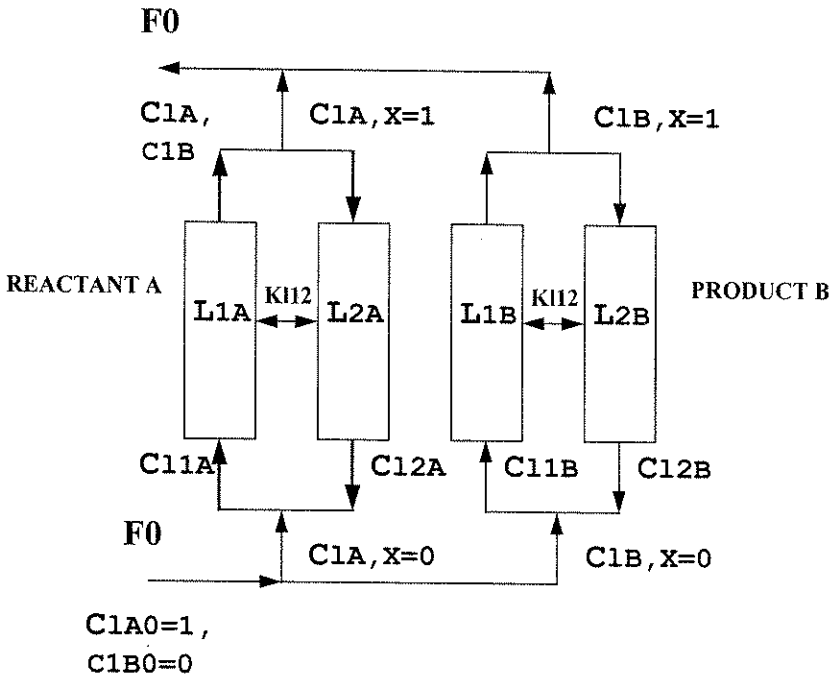

FIGURE 5-1. Schematic Diagram of Liquid Phase Recycle with Cross Flow Model for Single Irreversible Reaction ($A \xrightarrow{k1} B$)

5.1.1 Single Irreversible Reaction

Mathematical models:

For a single irreversible reaction $A \xrightarrow{k1} B$ involving non-volatile liquid reactant A injected into the bottom of the bubble column, the reaction takes place in the liquid phase and the liquid phase product B is produced. The mass balance for both reactant A and product B in the upflow and downflow regions yields the following four partial differential equations and their initial and boundary conditions.

For reactant A in the upflow region.

$$\tau_{l1}\frac{\partial C_{l1a}}{\partial t}+\frac{\partial C_{l1a}}{\partial x}+\frac{K_{l12}}{1+r_{l12}}(C_{l1a}-C_{l2a})+\tau_{l1}k_1C_{l1a}=0 \qquad (5.1)$$

where $\tau_{l1}, K_{l12}, r_{l12}, k_1$ are the mean residence time in the upflow region for the liquid phase, the dimensionless exchange coefficient between upflow and downflow regions, the recycle ratio (which is defined as the ratio of liquid phase volumetric flowrate in the downflow region to the inlet volumetric flowrate of the liquid), the volumetric first order reaction rate constant.

For reactant A in the downflow region

$$\tau_{l2}\frac{\partial C_{l2a}}{\partial t}-\frac{\partial C_{l2a}}{\partial x}-\frac{K_{l12}}{r_{l12}}(C_{l1a}-C_{l2a})+\tau_{l2}k_1C_{l2a}=0 \qquad (5.2)$$

where τ_{l2} is the mean residence time in the downflow region of liquid phase in bubble column.

For product B in the upflow region

$$\tau_{l1}\frac{\partial C_{l1b}}{\partial t}+\frac{\partial C_{l1b}}{\partial x}+\frac{K_{l12}}{1+r_{l12}}(C_{l1b}-C_{l2b})-\tau_{l1}k_1C_{l1a}=0 \tag{5.3}$$

For product B in the downflow region

$$\tau_{l2}\frac{\partial C_{l2b}}{\partial t}-\frac{\partial C_{l2b}}{\partial x}-\frac{K_{l12}}{r_{l12}}(C_{l1b}-C_{l2b})-\tau_{l2}k_1C_{l2a}=0 \tag{5.4}$$

Initial conditions

$$t=0, \qquad C_{l1a}=C_{l2a}=C_{l1b}=C_{l2b}=0, \qquad C_{l0a}=1 \tag{5.5}$$

Boundary conditions

$$x=0, \qquad C_{l1a}=\frac{1}{1+r_{l12}}(C_{l0a}+r_{l12}C_{l2a}),$$
$$C_{l1b}=\frac{r_{l12}C_{l2b}}{1+r_{l12}} \tag{5.6}$$

$$x=1, \qquad C_{l1a}=C_{l2a}, \qquad C_{l1b}=C_{l2b} \tag{5.7}$$

5.1.2 Consecutive (Series) Reactions

Mathematical models:

For a non-volatile liquid reactant species A injected into the bottom of the bubble column, the reaction takes place and the intermediate liquid phase product B and final

liquid phase product C are both produced. The first order reaction scheme is written as $A \xrightarrow{k1} B \xrightarrow{k2} C$. The mass balance on reactant A and product B and C in both upflow and downflow regions yields the following six partial differential equations and their initial and boundary conditions.

For reactant A in the upflow region.

$$\tau_{l1}\frac{\partial C_{l1a}}{\partial t}+\frac{\partial C_{l1a}}{\partial x}+\frac{K_{l12}}{1+r_{l12}}(C_{l1a}-C_{l2a})+\tau_{l1}k_1C_{l1a}=0 \tag{5.8}$$

For reactant A in the downflow region

$$\tau_{l2}\frac{\partial C_{l2a}}{\partial t}-\frac{\partial C_{l2a}}{\partial x}-\frac{K_{l12}}{r_{l12}}(C_{l1a}-C_{l2a})+\tau_{l2}k_1C_{l2a}=0 \tag{5.9}$$

For intermediate product B in the upflow region

$$\tau_{l1}\frac{\partial C_{l1b}}{\partial t}+\frac{\partial C_{l1b}}{\partial x}+\frac{K_{l12}}{1+r_{l12}}(C_{l1b}-C_{l2b})-\tau_{l1}k_1C_{l1a}+\tau_{l1}k_2C_{l1b}=0 \tag{5.10}$$

For intermediate product B in the downflow region

$$\tau_{l2}\frac{\partial C_{l2b}}{\partial t}-\frac{\partial C_{l2b}}{\partial x}-\frac{K_{l12}}{r_{l12}}(C_{l1b}-C_{l2b})+\tau_{l2}k_2C_{l2b}-\tau_{l2}k_1C_{l2a}=0 \tag{5.11}$$

For product C in the upflow region

$$\tau_{l1}\frac{\partial C_{l1c}}{\partial t}+\frac{\partial C_{l1c}}{\partial x}+\frac{K_{l12}}{1+r_{l12}}(C_{l1c}-C_{l2c})-\tau_{l1}k_2C_{l1b}=0 \tag{5.12}$$

For product C in the downflow region

$$\tau_{l2}\frac{\partial C_{l2c}}{\partial t}-\frac{\partial C_{l2c}}{\partial x}-\frac{K_{l12}}{r_{l12}}(C_{l1c}-C_{l2c})-\tau_{l2}k_2C_{l2b}=0 \tag{5.13}$$

Initial conditions

$$t=0,\qquad C_{l1a}=C_{l2a}=C_{l1b}=C_{l2b}=C_{l1c}=C_{l2c}=0,\qquad C_{l0a}=1 \tag{5.14}$$

Boundary conditions

$$x=0,\qquad C_{l1a}=\frac{1}{1+r_{l12}}(C_{l0a}+r_{l12}C_{l2a}),$$

$$C_{l1b}=\frac{r_{l12}C_{l2b}}{1+r_{l12}},\quad C_{l1c}=\frac{r_{l12}C_{l2c}}{1+r_{l12}} \tag{5.15}$$

$$x=1,\qquad C_{l1a}=C_{l2a},\qquad C_{l1b}=C_{l2b},\qquad C_{l1c}=C_{l2c} \tag{5.16}$$

5.1.3 Parallel Reactions

Mathematical models:

For a non-volatile liquid reactant species A injected into the bottom of the bubble column, the parallel reactions take place and the liquid phase product B and C are produced. The first order parallel reaction scheme is $A\xrightarrow{k1}B$, $A\xrightarrow{k2}C$. The mass balance of reactant A and product B and C in both upflow and downflow regions yields the following six partial differential equations and their initial and boundary conditions.

For reactant A in the upflow region

$$\tau_{l1}\frac{\partial C_{l1a}}{\partial t}+\frac{\partial C_{l1a}}{\partial x}+\frac{K_{l12}}{1+r_{l12}}(C_{l1a}-C_{l2a})+\tau_{l1}(k_1+k_2)C_{l1a}=0 \qquad (5.17)$$

For reactant A in the downflow region

$$\tau_{l2}\frac{\partial C_{l2a}}{\partial t}-\frac{\partial C_{l2a}}{\partial x}-\frac{K_{l12}}{r_{l12}}(C_{l1a}-C_{l2a})+\tau_{l2}(k_1+k_2)C_{l2a}=0 \qquad (5.18)$$

For product B in the upflow region

$$\tau_{l1}\frac{\partial C_{l1b}}{\partial t}+\frac{\partial C_{l1b}}{\partial x}+\frac{K_{l12}}{1+r_{l12}}(C_{l1b}-C_{l2b})-\tau_{l1}k_1C_{l1a}=0 \qquad (5.19)$$

For product B in the downflow region

$$\tau_{l2}\frac{\partial C_{l2b}}{\partial t}-\frac{\partial C_{l2b}}{\partial x}-\frac{K_{l12}}{r_{l12}}(C_{l1b}-C_{l2b})£-\tau_{l2}k_1C_{l2a}=0 \qquad (5.20)$$

For product C in the upflow region

$$\tau_{l1}\frac{\partial C_{l1c}}{\partial t}+\frac{\partial C_{l1c}}{\partial x}+\frac{K_{l12}}{1+r_{l12}}(C_{l1c}-C_{l2c})-\tau_{l1}k_2C_{l1a}=0 \qquad (5.21)$$

For product C in the downflow region

$$\tau_{l2}\frac{\partial C_{l2c}}{\partial t}-\frac{\partial C_{l2c}}{\partial x}-\frac{K_{l12}}{r_{l12}}(C_{l1c}-C_{l2c})-\tau_{l2}k_2C_{l2a}=0 \qquad (5.22)$$

Initial conditions

$$t = 0, \qquad C_{l1a} = C_{l2a} = C_{l1b} = C_{l2b} = C_{l1c} = C_{l2c} = 0, \qquad C_{l0a} = 1 \tag{5.23}$$

Boundary conditions

$$x = 0, \qquad C_{l1a} = \frac{1}{1 + r_{l12}}(C_{l0a} + r_{l12} C_{l2a}),$$

$$C_{l1b} = \frac{r_{l12} C_{l2b}}{1 + r_{l12}}, C_{l1c} = \frac{r_{l12} C_{l2c}}{1 + r_{l12}} \tag{5.24}$$

$$x = 1, \qquad C_{l1a} = C_{l2a}, \qquad C_{l1b} = C_{l2b} \qquad C_{l1c} = C_{l2c} \tag{5.25}$$

5.2 Tracer Response Prediction for the Injection of Tracer at the Middle of the Bubble Column

Suppose a non-volatile liquid tracer A is injected in the upflow region of the liquid phase at the middle of the bubble column (dimensionless position, x = 0.5) (see Figure 5-2).

The mass balance for a liquid tracer A in the upper section of both the upflow and the downflow regions, and the lower section of the upflow and the downflow regions in the bubble column, yields the following four partial differential equations and their associated initial and boundary conditions.

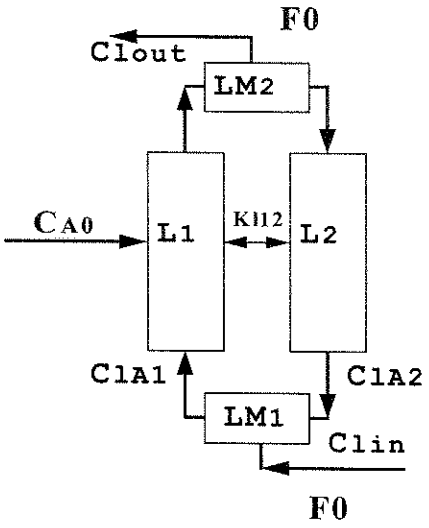

FIGURE 5-2. Schematic Diagram of Recycle with Cross Flow Model for Tracer Injected in the Middle of a Bubble Column

Lower section of upflow region

$0 \le x < 0.5$

$$\tau_{l1}\frac{\partial C_{l1a}}{\partial t}+\frac{\partial C_{l1a}}{\partial x}+\frac{K_{l12}}{1+r_{l12}}(C_{l1a}-C_{l2a})=0 \tag{5.26}$$

Upper section of upflow region

$x \ge 0.5$

$$\tau_{l1}\frac{\partial C_{l1a'}}{\partial t}+\frac{\partial C_{l1a'}}{\partial x}+\frac{K_{l12}}{1+r_{l12}}(C_{l1a'}-C_{l2a'})=0 \tag{5.27}$$

Lower section of downflow region

$0 \le x < 0.5$

$$\tau_{l1}\frac{\partial C_{l2a}}{\partial t} - \frac{\partial C_{l2a}}{\partial x} - \frac{K_{l12}}{r_{l12}}(C_{l1a} - C_{l2a}) = 0 \tag{5.28}$$

Upper section of downflow region

$x \ge 0.5$

$$\tau_{l1}\frac{\partial C_{l2a'}}{\partial t} - \frac{\partial C_{l2a'}}{\partial x} - \frac{K_{l12}}{r_{l12}}(C_{l1a'} - C_{l2a'}) = 0 \tag{5.29}$$

Initial conditions

$$t = 0, \qquad C_{l1a} = C_{l2a} = C_{l2a'} = 0, \qquad C_{l1a}' = \delta(x - 0.5) \tag{5.30}$$

where $\delta(x - 0.5)$ is the delta function for the liquid tracer injected in the middle of upper flow region of the bubble column reactor.

Boundary conditions

t > 0

$$x = 0, \qquad C_{l1a} = \frac{r_{l12}C_{l2a}}{1 + r_{l12}} \tag{5.31}$$

$$x = 0.5, \quad C_{l2a} = C_{l2a'} \tag{5.32}$$

$$x = 1, \qquad C_{l1a'} = C_{l2a'}, \tag{5.33}$$

5.3 Subcase of TRCFM for Gas Phase Mixing

It is assumed that a non-soluble gas tracer is injected into the bottom of the bubble column. The flow regime in the bubble column can be assumed to be of two types:
1. Churn turbulent regime; 2. Bubble flow regime.

5.3.1 Churn Turbulent Regime

In churn turbulent regime, a bimodal bubble size distribution is assumed. Five regions are encountered (see Figure 5-3): Large bubble upflow region; small bubble upflow region; small bubble downflow region; gas inlet distributor zone and gas outlet disengagement zone. In the TRCFM developed in the last Chapter, since gas tracer is non-soluble, the model equations in the liquid phase can be neglected. Therefore, the model equations can be described as follows:

Upflow region of small bubbles (SB1)

$$\tau_{g1}\frac{\partial C_{g1}}{\partial t}+\frac{\partial C_{g1}}{\partial x}+\frac{K_{g12}}{1+r_{g12}}(C_{g1}-C_{g2})+K_{g13}(C_{g1}-C_{g3})=0 \tag{5.34}$$

Downflow region of small bubbles (SB2)

$$\tau_{g2}\frac{\partial C_{g2}}{\partial t}-\frac{\partial C_{g2}}{\partial x}-\frac{K_{g12}}{r_{g12}}(C_{g1}-C_{g2})=0 \tag{5.35}$$

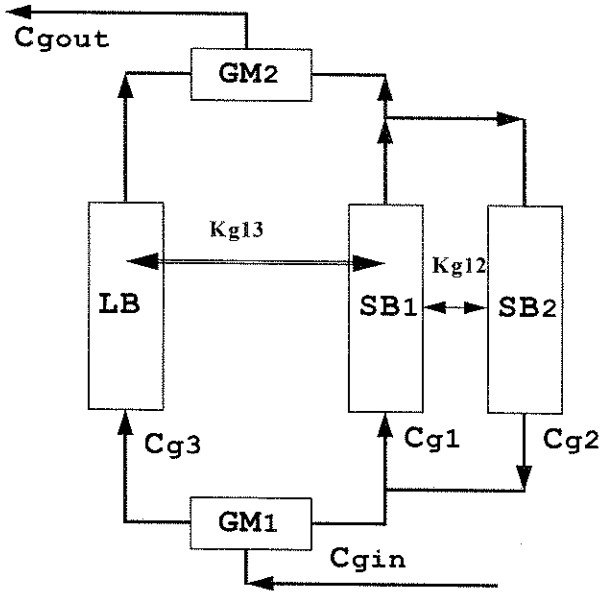

FIGURE 5-3. Schematic Diagram of Gas Phase Recycle with Cross Flow Model in Churn Turbulent Regime

Upflow region of large bubbles (LB)

$$\tau_{g3}\frac{\partial C_{g3}}{\partial t}+\frac{\partial C_{g3}}{\partial x}+K_{g13}(C_{g3}-C_{g1})=0 \qquad (5.36)$$

Initial conditions are presented in Equation 5.37 for a step injection of tracer into the gas phase at the bottom of the bubble column.

$t=0$

$$C_{g1}=C_{g2}=C_{g3}=0 \quad \textit{and} \quad C_{g0}=H(t) \qquad (5.37)$$

Boundary conditions are given by Equations 5.38, 5.39 for the small bubbles, for the large bubbles at the bottom of the bubble column, and by Equations 5.40 for the small bubbles at the top of the column.

$x = 0$

$$C_{g1} = \frac{1}{1+r_{g12}}(C_{g0} + r_{g12}C_{g2}) \tag{5.38}$$

$$C_{g3} = C_{g0} \tag{5.39}$$

$x = 1$

$$C_{g1} = C_{g2}, \quad C_{l1} = C_{l2} \tag{5.40}$$

5.3.2 Bubbly Flow Regime

Uniform bubble size is assumed and only small bubbles exist. Therefore, the interaction term between large and small bubbles in Equation 5.34 is neglected. Equation 5.36 and Equation 5.39 are neglected. Figure 5-4 is a schematic to represent gas phase mixing in bubbly flow regime.

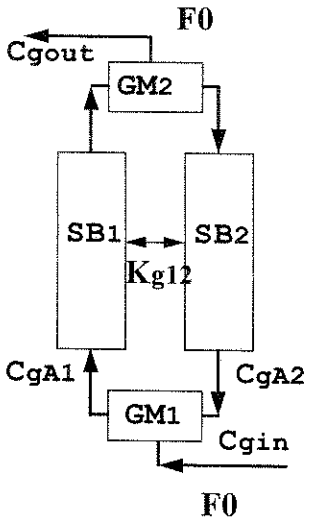

FIGURE 5-4. Schematic Diagram of Gas Phase Recycle with Cross Flow Model in Bubbly Flow Regime

6. Evaluation of Model Parameters

6.1 Model Parameters

In the last two Chapters, the physical basis and the mathematical formulation of TRCFM were described. The developed model requires a number of parameters but most of them can be determined either from available experimental data or via phenomenological correlations. Solving the model equations requires the knowledge of the mean residence times for the gas and the liquid in each region (SB1, SB2, LB, L1 and L2) and the recycle ratio of the small bubbles and the liquid; the knowledge of the volume of both gas and liquid in each region ($V_{g1}, V_{g2}, V_{g3}, V_{g1}^{1}, V_{l1}, V_{l2}$ *and* V_{l2}^{1}); the knowledge of exchange coefficients between the liquid in upflow and downflow, between the small bubbles in upflow and downflow and between the large bubbles and the small bubbles in upflow, as well as the knowledge of mass transfer contribution (mass transfer coefficients and weighing factors to describe the relative contribution of mass transfer) between the large bubbles and the liquid in upflow, between the small bubbles in upflow and the liquid in upflow, between the small bubbles in upflow and the liquid in downflow and between the small bubbles in downflow and the liquid in downflow. In this chapter, we discuss how most of the parameters can be estimated based on the available physical evidence.

Figure 6-1 represents a schematic of the methodology involved and the correlations and the experimental data needed to evaluate the model parameters.

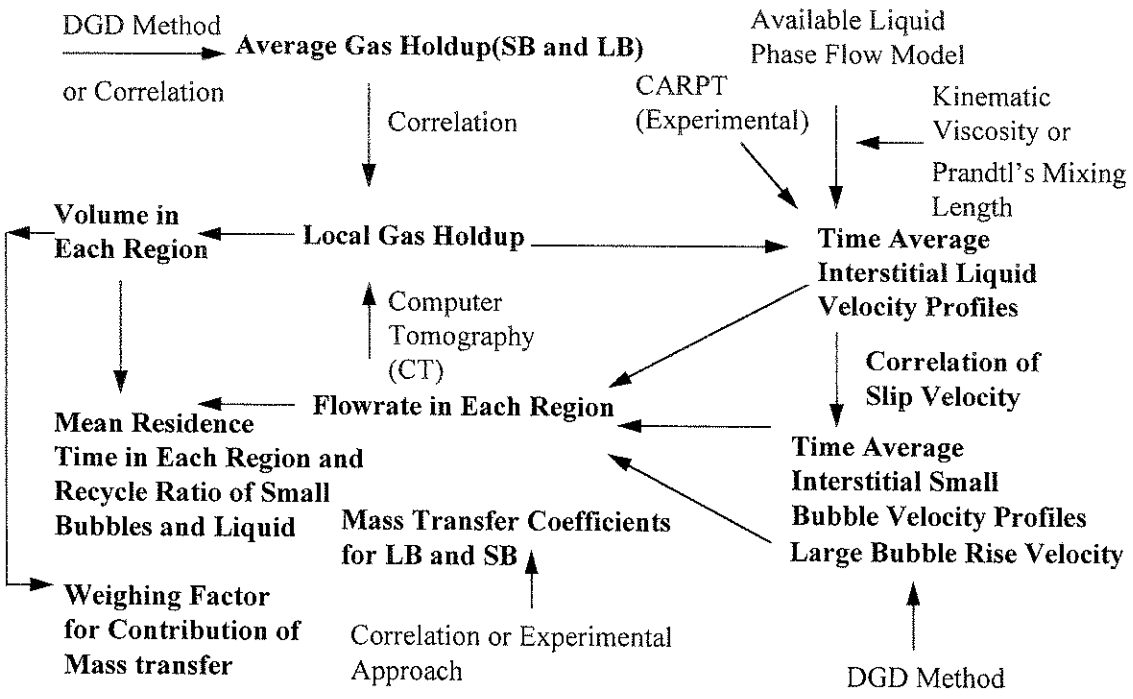

Figure 6-1. Procedures for Calculating Model Parameters

As seen from Figure 6-1, in order to determine the mean residence time in each region and the recycle ratio, one needs the volume and the flowrate for each phase in each region. The volume in each region can be determined by integration along both radial and longitudinal directions if the local holdup profiles are known. The local holdup profiles can be obtained either through experimental methods, such as Computer Tomography (Kumar et al. (1994)) or via available correlations if the average overall gas holdup is known. The overall average gas holdup and the average holdups of large and small bubbles can be determined from the dynamic gas disengagement method (DGD) or from some available correlations which will be discussed later. The flowrate of liquid and small bubbles in each region can be determined by integration along the radius if the time averaged interstitial liquid and gas velocity profiles are known. The time averaged interstitial liquid velocity profile can be determined either through experiments, such as Computer Aided Radioactive Particle Tracking (CARPT) (Devanathan et al. (1990)), or

via some correlations based on kinematic viscosity theory (Ueyama and Miyauchi (1979) and Anderson and Rice(1989)) or Prandtl's mixing length theory (Kumar et al. (1994)). The pertinent mathematical formulation will be discussed in the following sections. The evaluation of time averaged interstitial small bubble velocity profile requires the knowledge of the time averaged interstitial liquid velocity profile and the slip velocity between the small bubbles and the liquid. The slip velocity can be determined either from existing correlations, or via experiments using conductivity or optical probes. The large bubble rise velocity can be determined from dynamic gas disengagement method (DGD). The mass transfer coefficients for large and small bubbles can be determined from experiments or available correlations. The weighing factor of the mass transfer contribution can be determined if the volume in each region is known. The determination of the exchange coefficient between the large and small bubbles relies on the work of Modak et al. (1993). Therefore, the only fitting parameters in the model are the exchange coefficients between the small bubbles in upflow and downflow and between the liquid in upflow and downflow.

For simplicity, most of the model parameters are determined based on the existing phenomenological and fundamental correlations. Therefore, in summary, we need to know the following: local gas holdup profiles and overall average gas holdup as well as average holdups of small and large bubbles, time averaged interstitial liquid velocity profiles; the slip velocity between the small bubbles and the liquid so that the time average interstitial small bubble velocity can be obtained, the needed mean residence time in each region and the recycle ratio for small bubbles and for the liquid, the volume occupied in each region, and mass transfer coefficients between the small bubbles and the liquid and between the large bubbles and the liquid. Then, the crossmixing parameters for the small bubbles and for the liquid can be used to fit the experimental data.

In the following sections of this Chapter, we discuss the determination of each parameter required for the model.

6.2 Holdup

6.2.1 Average Gas Holdup

Several correlations were developed in the past two decades for the average gas holdup and are summarized in Table 6-1.

TABLE 6-1. Average Gas Holdup Correlation

$\frac{\varepsilon_g}{(1-\varepsilon_g)^4} = 0.2\left(\frac{gD_r^2\rho_l}{\sigma}\right)^{1/8}\left(\frac{gD_r^3\rho_l^2}{\eta_l^2}\right)^{1/12}\left(\frac{u_g}{\sqrt{gD_r}}\right)^{1.0}$ Akita et al. (1973)
$\varepsilon_g = 0.505u_g^{0.47}\left(\frac{0.072}{\sigma}\right)^{2/3}\left(\frac{0.001}{\eta_l}\right)^{0.05}$ Hikita et al. (1974)
$\varepsilon_g = 0.89\left(\frac{H_l}{D_r}\right)^{0.036(-15.7+\log K)}\left(\frac{d_b}{D_r}\right)^{0.3}\left(\frac{u_g}{gd_b}\right)^{0.025(2.6+\log K)}$ $K^{0.047} - 0.05 \qquad d_b = 0.003(m) \qquad K = \frac{\rho_l\sigma^3}{g\eta_l^4}$ Gestrich et al. (1975)
$\frac{\varepsilon_g}{1-\varepsilon_g} = 0.115\left(\frac{\rho_l u_g^3}{\eta_l g}\frac{\rho_l}{\rho_l-\rho_g}\right)^{0.23}$ Bach et al. (1978)
$\varepsilon_g = 0.672\left(\frac{U_g\eta_l}{\sigma}\right)^{0.578}\left(\frac{\eta_l^4 g}{\rho_l\sigma^3}\right)^{-0.131}\left(\frac{\rho_g}{\rho_l}\right)^{0.062}\left(\frac{\eta_g}{\eta_l}\right)^{0.107}$ Hikita et al. (1980)
$\frac{\varepsilon_g}{(1-\varepsilon_g)} = 0.4\left(\frac{U_g\eta_l}{\sigma}\right)^{0.87}\left(\frac{\eta_l^4 g}{\rho_l\sigma^3}\right)^{-0.27}\left(\frac{\rho_g}{\rho_l}\right)^{0.17}$ Hammer et al. (1984)
$\frac{\varepsilon_g}{(1-\varepsilon_g)} = 1.44U_g^{0.87}\rho_g^{0.12}\sigma^{-0.16\exp(P)}$ $P \ in \ MPa$ $\sigma \ in \ mN/m$ Idogawa et al.(1985)

TABLE 6-1. Average Gas Holdup Correlation (Continued)

$\varepsilon_g = 296 U_g^{0.44} \rho_l^{-0.98} \sigma^{-0.16} \rho_g^{0.19} + 0.009$ Relly et al. (1986)
$\varepsilon_g = 0.20 \left(\frac{g D_r^2 \rho_l}{\sigma} \right)^{-0.13} \left(\frac{g D_r^3 \rho_l^2}{\eta_l^2} \right)^{0.13} \left(\frac{u_g}{\sqrt{g D_r}} \right)^{0.54}$ Schumpe et al. (1987)
$\frac{\varepsilon_g}{1-\varepsilon_g} = 0.0625 \left(\frac{\rho_l u_g^3}{\eta_l g} \right)^{1/4}$ Kawase et al. (1992)
$\varepsilon = \varepsilon_{large} + \varepsilon_{small}$, $\varepsilon_{small} = \varepsilon_{trans} = \exp(-193 \rho_g^{-0.61} \mu_l^{0.5} \sigma^{0.11})$ $\varepsilon_{large} = \frac{U_g - U_{trans}}{u_{large}}$, $U_{trans} = 2.25 \varepsilon_{trans} \frac{\sigma}{\mu_l} \left(\frac{\sigma^3 \rho_l}{g \mu_l^4} \right)^{-0.273} \left(\frac{\rho_l}{\rho_g} \right)^{0.33}$ $\frac{u_{large} \mu_l}{\sigma} = 2.25 \left(\frac{\sigma^3 \rho_l}{g \mu_l^4} \right)^{-0.273} \left(\frac{\rho_l}{\rho_g} \right)^{0.03} + 2.4 \left(\frac{(U - U_{trans}) \mu_l}{\sigma} \right)^{0.757}$ $\left(\frac{\sigma^3 \rho_l}{g \mu_l^4} \right)^{-0.077} \left(\frac{\rho_l}{\rho_g} \right)^{0.077}$ Wilkinson et al.(1992)
$\varepsilon_g (1 - \varepsilon_g) = 2.849 \left(\frac{\rho_g^{0.04} u_g}{\sigma^{0.12}} \right)$ Relly et al. (1994)
$\varepsilon_g = 129 \left(\frac{u_g \eta_l}{\sigma} \right)^{0.99} \left(\frac{\eta_l^4 g}{\rho_l \sigma^3} \right)^{-0.123} \left(\frac{\rho_g}{\rho_l} \right)^{0.187} \left(\frac{\eta_g}{\eta_l} \right)^{0.343} \left(\frac{d_{orif}}{D_r} \right)^{-0.089}$ Sotelo et al. (1994)
$\varepsilon = \varepsilon_{trans} + \varepsilon_{large}$; $\varepsilon_{large} = A(U - U_{trans})^{4/5}; U \geq U_{trans}$ $-\varepsilon^2 \frac{\partial v_0}{\partial \varepsilon} \frac{\partial}{\partial \varepsilon} \left[\left(\rho_g + \frac{1}{2} \rho_l m_0 \right) v_o \right] \geq - \left[\frac{\partial P_e}{\partial \varepsilon} + \frac{12 \pi a \mu_l}{\frac{4}{3} \pi a^3} \frac{1}{(1-\varepsilon)^n} \delta_e \right]$ for calculating transition gas holdup, A is a function of column diameter   Krishna et al.(1994)

For our model, it is necessary to distinguish between the holdups of large and small bubbles. Vermeer and Krishna (1981), Relly et al. (1986), Schumpe and Deckwer (1988), Shetty et al. (1992), Wilkinson et al. (1992), Hoefsloot and Krishna (1993), Krishna et al. (1994) and Krishna and Ellenberger (1995), addressed this issue and made extensive studies for holdups of both large and small bubbles. The dynamic gas disengagement method (DGD) was often used to obtain the data. The major findings can be summarized as follows:

1. The effect of increased gas density is to largely increase gas holdup. The two distinct flow regimes were proposed, churn turbulent regime (heterogeneous regime) and bubbly flow regime (homogeneous regime).

In the homogeneous regime, $U_g < U_{trans}$ (U_{trans} is the superficial gas velocity at transition point from homogeneous regime to heterogeneous regime). The overall average holdup is equal to the average holdup of small bubbles and is given by:

$$\varepsilon = \frac{U}{V_{small}} \tag{6.1}$$

where V_{small} is the rising velocity of the small bubbles.

In the heterogeneous regime, $U_g > U_{trans}$. Large and small bubbles coexist, the correlations proposed by Wilkinson et al. (1992) may be used to calculate the large and small bubble holdups separately.

2. Gas holdup varies linearly with the superficial gas velocity until the transition point is reached (U_{trans}).

3. At $U_g > U_{trans}$, the holdup of small bubbles is assumed to be equal to the total gas holdup at $U_g = U_{trans}$. Additional holdup is attributed to large bubbles. The increase in

superficial gas velocity in this regime affects significantly the large bubble holdup and, consequently, total gas holdup.

Biesheuvel and Gorissen (1990) presented a theoretical analysis of the stability of homogeneous bubbly flow subject to a void fraction disturbance. They developed the following criterion for instability of the homogeneous bubbly flow.

$$-\varepsilon^2 \frac{\partial v_0}{\partial \varepsilon} \frac{\partial}{\partial \varepsilon}\left[\left(\rho_G + \frac{1}{2}\rho_L m_0\right) v_0\right] \geq -\left[\frac{\partial p_e}{\partial \varepsilon} + \frac{12\pi a \mu_L}{(4/3)\pi a^3} \frac{1}{(1-\varepsilon)^p} \delta_e\right] \tag{6.2}$$

where v_0 is the velocity of the bubble swarm in the zero volume frame, this velocity is related to the single, isolated bubble rise velocity.

$$v_0 = v_\infty (1-\varepsilon)^p \tag{6.3}$$

In the laboratory fixed reference frame, the bubble swarm velocity is (Wallis, 1969):

$$U_{swarm} = \frac{U}{\varepsilon} = U_\infty (1-\varepsilon)^n \tag{6.4}$$

where the Richardsen-Zaki exponent n = p-1.

In Biesheuvel and Goriesan's (1990) model, they assume p = 2, n = 1 and they claimed that U_{trans} decreases slightly with the increase in gas density. But, unfortunately, their model cannot explain the experimental data of Krishna et al. (1993) who claimed that U_{trans} increases with the increase in gas density.

Krishna et al. (1993) modified the above model and claimed that the Richardson-Zaki exponent n is shown to be an important parameter in determining the stability of homogeneous bubbly flow in bubble columns. With the increase in gas density, the exponent n decreases. Physically this means that the increase in gas density results in the decrease of the interaction between neighboring bubbles and consequently, reduces the chance of the propagation of instabilities.

Besides correlations described above, the average small and large bubble holdups can also be determined by dynamic gas disengagement (DGD) method. In this work, the average holdups are obtained from this approach.

6.2.2 Local Holdup

In the past two decades, different correlations were proposed for radial distribution of the gas holdup in bubble columns, most of which are summarized in Table 6-2.

TABLE 6-2. Local Gas Holdup Correlation

Petrick (1959)	$\varepsilon_g / \varepsilon_c = 1-(r/R)^n$	$n = 0.024 U_l^{0.66/\varepsilon}$
Bankoff (1960)	$\varepsilon_g / \varepsilon_c = (r/R)^{1/n}$	$\bar{\varepsilon}_g / \varepsilon_c = 2n^2/(n+1)(2n+1)$
Zuber & Findlay (1965)	$\frac{\varepsilon_g - \varepsilon_w}{\varepsilon_c - \varepsilon_w} = 1-(r/R)^n$	$\overline{\varepsilon_g} / \varepsilon_c = \frac{n}{n+2}$
Kobayashi & Kanegae (1970)	$\varepsilon_g / \varepsilon_c = S^{1/as} + nse^{-as}$	$S = 1 - r/R$ a, n,α are constants
Miyauchi et al. (1981)	$\varepsilon_g = \overline{\varepsilon_g} \frac{n+2}{n}(1-(r/R)^n)$	n fitted to the data
Myers (1986)	$\varepsilon_g = 2\overline{\varepsilon_g}(1-(r/R)^2)$	n=2

In addition, local gas holdup can also be determined experimentally. Kumar et al.(1994) used CT (Computer Tomography) to successfully measure the local gas holdup profiles.

In this work, Miyauchi et al.'s approach (1981) was used and n is assumed to be equal to 2.

6.3 One Dimensional Liquid Phase Flow Model

Several models have been developed for liquid recirculation in the fully developed region of a tall bubble column based on the one dimensional flow assumption.

1. The first correlation for the velocity profile in the bubble column system was proposed by Ueyama and Miyauchi (1979). In their model, the authors made an assumption that there is a laminar sublayer δ near the wall which is small enough so that the liquid downward velocity at r =δ is approximately equal to the wall velocity. They developed the following equations:

$$\frac{u_l + |u_w|}{u_0 + |u_w|} = \left[1 - \left(\frac{r}{R}\right)^2\right]^2 \tag{6.5}$$

$$u_0 = \frac{gD^2\varepsilon_g}{192\nu_t}\left(\frac{4 - 3\varepsilon_g}{1 - \varepsilon_g}\right) + \frac{U_l}{1 - \varepsilon_g} \tag{6.6}$$

$$|u_w| = \frac{gD^2\varepsilon_g}{192\nu_t}\left(\frac{2 - 3\varepsilon_g}{1 - \varepsilon_g}\right) - \frac{U_l}{1 - \varepsilon_g} \tag{6.7}$$

where D, column diameter, m; g, acceleration of gravity, m/s^2;

U_L, superficial liquid velocity, m/s; u_o, centerline interstitial liquid velocity, m/s;

$|u_w|$, absolute value of the interstitial axial liquid velocity near column wall, m/s.

$U_l = 0$, if the liquid is in batch state.

In Ueyama and Miyauchi's (1979) approach, the velocity in the core is matched to the universal velocity profile of the single phase turbulent pipe flow at the wall. The specification of the wall shear stress involves an empirical constant.

2. Anderson and Rice (1989) proposed a similar model. The difference is essentially that the setting of the boundary condition is based on physical reasoning and no empirical constant is involved.

The maximum downward velocity based on their approach is:

$$u_l(\xi = \lambda) = \frac{gR^2 \overline{\varepsilon_g}}{4\upsilon_m \lambda^2}(\lambda^2 - 1 - 2\lambda^2 \ln \lambda) \tag{6.8}$$

where $\lambda = \sqrt{\frac{\bar{\varepsilon}}{(1-p')}}$, p'= dimensionless pressure gradient.

3. In Luo and Sevendsen (1991)'s model, the boundary condition at the wall is set implicitly rather than explicitly like in Anderson's (1989) or Ueyama's (1979) approach. Richard's correlation for eddy viscosity was used in the model. This is the main difference from other models in which any correlation of eddy viscosity could be used.

4. Kumar et al. (1994) proposed a liquid recirculation model and used the Prandtl's mixing length theory as well as the eddy viscosity approach to achieve closure of the one dimensional momentum balance. They claimed that the scale up based on the mixing length theory is possible when the consistent set of data for liquid velocity and gas void fraction is obtained. They demonstrated this based on the experimental data using CARPT (Computer Automated Radioactive Particle Tracking) and CT (Computer Tomography).

Here, two different approaches for shear stress and liquid velocity are briefly described:

Eddy viscosity:

Using the Boussinesq's (1896) hypothesis, the constitutive equations for the shear stress are given as:

In the core region,

$$\tau_{rz}(\xi) = -\frac{\upsilon_t \rho_l}{R}\left(\frac{du_l}{d\xi}\right) \qquad \xi \le \lambda \tag{6.9}$$

In the wall region,

$$\tau^*_{rz}(\xi) = -\frac{\upsilon_m \rho_l}{R}\left(\frac{du_l}{d\xi}\right) \qquad \xi \ge \lambda \tag{6.10}$$

Boundary conditions:

$$\xi = \lambda, \qquad u_l = u_l^* \tag{6.11}$$

$$\xi = 1, \qquad u_l = 0 \tag{6.12}$$

The liquid velocity profile in these two regions is:

$$u_l(\xi) = \frac{gR^2\bar{\varepsilon}}{2\upsilon_t}\left[\frac{m-(m+2)\left(\frac{\xi}{\lambda}\right)^2+2\left(\frac{\xi}{\lambda}\right)^{(m+\lambda)}}{m(m+2)}\right] + u_\lambda \qquad \xi \le \lambda \tag{6.13}$$

$$u_l^{\xi}(\xi) = \frac{gR^2\bar{\varepsilon}}{4\upsilon_m\lambda^2}(\xi^2 - 1 - 2\lambda^2 \ln\xi) \qquad \xi \ge \lambda \tag{6.14}$$

Prantdl's mixing length:

The expression for shear stress is given as:

$$\tau_{rz}(\xi) = -\frac{\upsilon_m \rho_l}{R}\left(\frac{du_l}{d\xi}\right) + \rho_l \frac{l^2(\xi)}{R^2}\left(-\frac{du_l}{d\xi}\right)^2 \qquad \xi \le \lambda \tag{6.15}$$

$$\tau^*_{rz}(\xi) = -\frac{\upsilon_m \rho_l}{R}\left(\frac{du_l}{d\xi}\right) \qquad \xi \ge \lambda \tag{6.16}$$

Combining Equation 6.15, 6.16 with the boundary conditions specified by Equation 6.11 and 6.12, the equations for the liquid velocity profiles can, therefore, be obtained as:

$$u_l(\xi) = u_\lambda - \frac{\upsilon_m R}{2}\int_\xi^\lambda \frac{1-\sqrt{1+\dfrac{2gRl^2(\xi')\beta(\xi')}{\upsilon_m^2}}}{l^2(\xi)}d\xi', \qquad for \xi \le \lambda \tag{6.17}$$

$$u^*_l(\xi) = \frac{gR^2\bar{\varepsilon}}{4\upsilon_m \lambda^2}(\xi^2 - 1 - 2\lambda^2 \ln\xi); \qquad for \xi \ge \lambda \tag{6.18}$$

A radial power law equation of an axi-symmetric distribution of the void fraction is expressed as:

$$\varepsilon = \bar{\varepsilon}\frac{m+2}{m}(1 - c\xi^m) \tag{6.19}$$

where m is an arbitrary constant, c is a parameter that allows for the possibility of non-zero void fraction close to the wall.

An iterative procedure is involved for obtaining the liquid velocity profile as follows: Assume m in Equation 6.19 is available which best fits the void fraction data. A value of λ is assumed, the maximum downward liquid velocity is evaluated using Equation 6.8. The liquid velocity is calculated using Equations 6.15 and 6.16, if the model based on the Prandtl's mixing length is used. The computed velocity and void fraction profiles need to

satisfy the mass balance, given by Equation 6.19, which provides an iteration procedure for the parameter λ.

$$\int_0^{\lambda}(1-\varepsilon(\xi))u_l(\xi)\xi d\xi + \int_{\lambda}^{1} u_l^*(\xi)\xi d\xi = U_l \tag{6.20}$$

For the Prandtl's mixing length approach, several correlations for the mixing length were proposed.

1. For the bubble generated turbulence (Geary and Rice, (1992)).

$$l(\xi) = \frac{d_b \varepsilon(\xi)}{\bar{\varepsilon}} \tag{6.21}$$

2. For the wall generated turbulence, the single pipe correlation for the mixing length given by Nikuradse (Schlichting (1979)) was suggested:

$$l(\xi) = 0.14 - 0.08\xi^2 - 0.06\xi^4 \tag{6.22}$$

3. Kawase and Tokunage (1991) proposed an empirical equation to characterize the mixing length in bubble columns.

$$l = 0.045 U_g^{-0.38} D_c \tag{6.23}$$

4. Kumar et al. (1994), based on the experimental data from CARPT, used the regression

process to propose the following mixing length dependence on dimensionless radial position ξ, where a, b, c, d and e are obtained by a nonlinear regression process.

$$l(\xi) = \frac{a(1-\xi)}{(\xi+b)^c} + d(1-\xi)^e \tag{6.24}$$

For turbulent kinematic viscosity, different correlations were proposed and listed in Table 6-3 as follows:

TABLE 6-3. Correlation for Turbulent Kinematic Viscosity

Authors	Correlation
Miyauchi & Shyu (1970)	$\nu_t = 0.05 D_c^{1.8}$
Miyauchi & Ueyama (1979)	$\nu_t = 0.128 D_c^{1.7} \rho_l$
Miyauchi et al. (1981)	$\nu_t = 0.160 U_g^{1/6} D_c^{1.5}$
Kojima et al. (1980)	$\nu_t = 0.053 D_c^{1.77}$
Riquarts (1982)	$\nu_t = 0.011 D_c^{3/4} U_g^{3/8} \nu_l^{-1/8} g^3 \rho_l$
Sekizawa et al. (1983)	$\nu_t = 0.265 D_c^{1.5} \rho_l$
Kauase & Moo Young (1986)	$\nu_t = 0.00184 D_c^{4/3} U_g^{1/3} g^{1/3} \rho_l$

In this paper, for simplicity, Ueyama and Miyauchi (1979)'s one dimensional liquid flow model together with Miyauchi's (1981) turbulent kinematic viscosity correlation is used to obtain the liquid velocity profile in the bubble column reactor.

6.4 Slip Velocity

The slip velocity here is defined as the relative velocity between the rising small bubbles and liquid at a local point. It is assumed here to be independent of local position

in the column. In other words, for the given operating conditions of the bubble column system, it is assumed that a unique slip velocity exists which connects the interstitial velocity of small bubbles and of the liquid at a given point. The slip velocity is assumed to be a function of average gas holdup. The typical correlations for slip velocity are:

1. Lockett and Kirkpatrick (1975) correlation

$$u_s = 0.164(1-\varepsilon_g)^{1.39}(1+2.55\varepsilon_g^3) \tag{6.25}$$

For single small bubble size between 0.5 and 4.5 mm, Field and Davidson (1980) have successfully applied the above correlation in the axial dispersion model and satisfactory results were obtained.

2. Tsuneo's correlation (1983)

$$u_S = 87.125\varepsilon_g^{-0.440}(1-A_r)^{0.550} \pm 0.0194|u_l|^{1.94} \tag{6.26}$$

It is reported that large set of experimental data were used to develop the above correlation.

3. Experimentally, it is possible to use optical probes or conductivity probes to measure the bubble rise velocity so that the slip velocity can be determined. But the research in this field needs to be improved to get more accurate results.

Here, Lochett and Kirkpatrick's correlation is used to calculate the slip velocity and, therefore, the interstitial velocity of small bubbles is determined from both the slip velocity correlation and liquid phase one dimensional flow model.

6.5 Mean Residence Time in Various Regions

As it is seen from Figure 4-3 for continuous flow of gas and liquid, the bubble column is divided into nine regions including inlet and outlet liquid mixing zones, distribution and disengagement zones (LM1, LM2, GM1, GM2) with assumed negligible residence time. The mean residence times in the remaining five regions (SB1, SB2, LB, L1, L2) can be found as follows:

$$\tau_{g1} = \frac{V_{g1}}{Q_{g1}} = \frac{Gas\ \ Volume\ \ in\ \ \text{Re}gion\ \ SB1\ \ (Upflow\ \ of\ \ Small\ \ Bubbles)}{Volumetric\ \ Gas\ \ Flowrate\ \ in\ \ \text{Re}gion\ \ SB1} \tag{6.27}$$

$$\tau_{g2} = \frac{V_{g2}}{Q_{g2}} = \frac{Gas\ \ Volume\ \ in\ \ \text{Re}gion\ \ SB2\,(Downflow\ \ of\ \ Small\ \ Bubbles)}{Volumetric\ \ Gas\ \ Flowrate\ \ in\ \ \text{Re}gion\ \ SB2} \tag{6.28}$$

$$\tau_{g3} = \frac{V_{g3}}{Q_{g3}} = \frac{Gas\ \ Volume\ \ in\ \ \text{Re}gion\ \ LB\,(Upflow\,of\ \text{Large}\ \ Bubbles)}{Volumetric\ \ Gas\ \ Flowrate\ \ in\ \ \text{Re}gion\ \ LB} \tag{6.29}$$

$$\tau_{l1} = \frac{V_{l1}}{Q_{l1}} = \frac{Liquid\ \ Volume\ \ in\ \ \text{Re}gion\ \ L1\,(Upflow\ \ of\ \ Liquid)}{Volumetric\ \ Liquid\ \ Flowrate\ \ in\ \ \text{Re}gion\ \ L1} \tag{6.30}$$

$$\tau_{l2} = \frac{V_{l2}}{Q_{l2}} = \frac{Liquid\ \ Volume\ \ in\ \ \text{Re}gion\ \ L2\,(Downflow\ \ of\ \ Liquid)}{Volumetric\ \ Liquid\ \ Flowrate\ \ in\ \ \text{Re}gion\ \ L2} \tag{6.31}$$

Hochman and McCord (1970) claimed that the mean residence times can also be determined by the direct measurement of the flow field. This technique, of course, would certainly be applicable in the bubble column systems using Computer Automated Radioactive Particle Tracking (CARPT) and Computer Tomography (CT) developed by Devanathan et al. (1990) and Kumar et al. (1994). However, since several one dimensional models for determining interstitial liquid velocity and some correlations for slip velocity are available, Myers (1986) has already applied this successfully for investigating the liquid phase backmixing in bubble column systems. Therefore, here, we extend Myers' approach (1986) and apply it to two phase bubble column system in both bubbly flow and churn turbulent regimes.

The small bubble interstitial velocity profile can be determined directly from the liquid interstitial velocity profile and slip velocity while plug flow is assumed for large bubbles. The relationship between the interstitial velocity of the small bubbles and the liquid at the same radial position can be described as:

$$u_g = u_s + u_l \tag{6.32}$$

Due to the turbulent recirculation of both liquid and small bubbles, there exists a radial position where the interstitial velocity of the liquid is equal to zero (we set $u_l = 0$ @ r = r'). In the same manner, there may also be a radial position where the interstitial velocity of small bubbles is equal to zero as well (we set $u_g = 0$ @ r = r"). As discussed previously, u_s is the slip velocity and is assumed to be constant along the radial direction of the bubble column. However, the model structure can also incorporate a slip velocity as a function of radial position if, later, it is indicated that such modification is needed. At present, based on constant slip velocity, for the upflow region of the small bubbles (SB1 region), by triple integration of local holdup profiles along the radial, azimuthal and longitudinal directions of the column and double integration of the interstitial velocity profile of small bubbles along the radial and azimuthal directions, the following mathematical expression for the mean residence time is derived:

$$\tau_{gl} = \frac{\pi R^2 L\overline{\varepsilon_{gs}} - \int_0^{L}\int_0^{2\pi}\int_{r"(u_g=0)}^{R} \varepsilon_g r\,dr\,d\theta\,dz}{\pi R^2 (U_g - U_{gl}) + \int_0^{2\pi}\int_{r"(u_g=0)}^{R} |u_g|\varepsilon_g r\,dr\,d\theta} \tag{6.33}$$

where L is the test level in the bubble column, m.

$\overline{\varepsilon_{gs}}$ is the average holdup of small bubbles

$\overline{\varepsilon_{gl}}$ is the average holdup of large bubbles

ε_g is local gas holdup.

U_{gl} is the superficial velocity of large bubbles.

By dynamic gas disengagement (DGD) method (Shetty et al. (1992)), the large bubble rise velocity can be determined. A mass balance across any cross-section of the column gives the following expression for calculating the superficial velocity of large bubbles:

$$\frac{U_{gl}}{\overline{\varepsilon_{gl}}} - \frac{U_l}{1-\overline{\varepsilon_{gl}}} = U_{lbr} \tag{6.34}$$

where U_{lbr} is the rise velocity of the large bubbles.

Similarly, for the down flow region of small bubbles(SB2) , by triple integration of holdup profiles along the radial, azimuthal and longitudinal directions and double integration of the interstitial velocity profile of small bubbles along the radial and azimuthal directions, the mean residence time is:

$$\tau_{g2} = \frac{\int_0^{L}\int_0^{2\pi}\int_{r''(u_g=0)}^{R} \varepsilon_g r dr d\theta dz}{\int_0^{2\pi}\int_{r''(u_g=0)}^{R} |u_g| \varepsilon r dr d\theta} \tag{6.35}$$

For large bubbles, which are assumed to rise upwards in plug flow near the center of the bubble column, the mean residence time in the upflow region of large bubbles (LB region) is:

$$\tau_{g3} = \frac{L\overline{\varepsilon_{gl}}}{U_{gl}} \tag{6.36}$$

By triple integration of the local holdup profiles in space and double integration of the interstitial liquid velocity profile along the cross section of the column, the mean residence time in the upflow region of the liquid (L1) is:

$$\tau_{l1} = \frac{\int_0^{L} \int_0^{2\pi} \int_0^{r'(u_l=0)} (1-\varepsilon_g) r dr d\theta dz}{\pi R^2 U_l + \int_0^{2\pi} \int_{r'(u_l=0)}^{R} |u_l|(1-\varepsilon_g) r dr d\theta} \tag{6.37}$$

Similarly, by triple integration of the local holdup profiles along the whole column and double integration of the interstitial liquid velocity profile along the cross section of the column for the downflow region of the liquid (L2), the mean residence time is:

$$\tau_{l2} = \frac{\int_0^{L} \int_0^{2\pi} \int_{r'(u_l=0)}^{R} (1-\varepsilon_g) r dr d\theta dz}{\int_0^{2\pi} \int_{r'(u_l=0)}^{R} |u_l|(1-\varepsilon_g) r dr d\theta} \tag{6.38}$$

6.6 Recycle Ratio for Small Bubbles and Liquid

For small bubbles, the recycle ratio (r_{g12}) is defined as the ratio of the flowrate of small bubbles in the downflow region (SB2) to the inlet feed flowrate of the small bubbles (inlet gas flowrate from which the flowrate of large bubbles is subtracted). For continuous flow of the liquid phase, the liquid recycle ratio (r_{l12}) is defined as the ratio of the flowrate of the liquid in the downflow region (L2) to the inlet flowrate of the liquid. Mathematically, the recycle ratios for small bubbles and liquid are defined as:

$$r_{g12} = \frac{R_1}{Q_g - Q_{g3}} = \frac{Volumetric \quad Gas \quad \text{Re}cycle(SB2) \quad Flowrate}{Volumetric \quad Small \quad Bubble(SB1+SB2) \quad Flowrate} \tag{6.39}$$

$$r_{l12} = \frac{R_2}{Q_l} = \frac{Volumetric \quad Liquid \quad \text{Re}cycle(L2) \quad Flowrate}{Volumetric \quad Liquid \quad Flowrate} \tag{6.40}$$

and can be computed as follows:

$$r_{g12} = \frac{\int_0^{2\pi} \int_{r''(u_g=0)}^{R} |u_g| \varepsilon_g r dr d\theta}{\pi R^2 (U_g - U_{gl})} \tag{6.41}$$

$$r_{l12} = \frac{\int_0^{2\pi} \int_{r'(u_l=0)}^{R} |u_l| (1-\varepsilon_g) r dr d\theta}{\pi R^2 U_L} \tag{6.42}$$

For the batch mode operation in the liquid phase, the recycle ratio for the liquid does not exist as previously defined.

6.7 Crossmixing Coefficient for Both Gas and Liquid Phase

For a two phase bubble column system in heterogeneous churn turbulent regime or in homogeneous bubbly flow regime, due to the shear stress between the upflow of the small bubbles and the downflow of the small bubbles, and between the upflow of the liquid and the downflow of the liquid (refer to Figure 4-3), the communication and exchange between SB1 and SB2 and between L1 and L2 can be described by crossmixing parameters called "exchange coefficients". They are described separately for gas and liquid.

The dimensionless crossmixing coefficients for the small bubbles K_{g12} and for the liquid K_{l12} are defined as:

$$K_{g12} = \frac{k_{g12}\ L}{Q_g - Q_{g3}} = \frac{Volumetric\ \ Small\ \ Bubble\ \ Crossmixing\ \ Rate}{Volumetric\ \ Gas\ \ (Small\ \ Bubble)\ \ Flowrate} \tag{6.43}$$

$$K_{l12} = \frac{k_{l12}\ L}{Q_l} = \frac{Volumetric\ \ Liquid\ \ Crossmixing\ \ Rate}{Volumetric\ \ Liquid\ \ Flowrate} \tag{6.44}$$

For batch liquid, the crossmixing coefficient is:

$$K'_{l12} = \frac{k'_{l12}\ L}{Q_{l1}} = \frac{k'_{l12}\ L}{Q_{l2}} = \frac{Volumetric\ \ Liquid\ \ Crossmixing\ \ Rate}{Volumetric\ \ Liquid\ \ Flowrate\ \ in\ \ \mathrm{Re}gion\ \ L_1\ \ or\ \ L_2} \tag{6.45}$$

where k_{g12} is the dimensional exchange coefficient (m^2 / s) or simply called " exchange coefficient" for small bubbles, k_{l12} is the exchange coefficient (m^2 / s) for the liquid in continuous liquid flow mode, k'_{l12} is the exchange coefficient (m^2 / s) for the liquid in batch mode of operation.

In churn turbulent regime, due to the interaction between the large and small bubbles, the dimensionless crossmixing parameter is defined as:

$$K_{g13} = \frac{k_{g13} L}{Q_g} \tag{6.46}$$

where k_{g13} is the exchange coefficient (m^2 / s) between the large and the small bubbles and Q_g is the total volumetric gas flowrate, (m^3 / s).

It was found through regression analysis by Modak et al. (1993) that the interaction between the large and small bubbles is so strong that the crossmixing coefficient between the large and small bubbles is a very large number. This implies that the concentrations in the upflow region of the small bubbles and in the upflow region of the large bubbles are quite close to each other. The above assumption is used to perform model simulation.

6.8 Volume of Each Region

Since the average holdup of gas and liquid in each region is known, the total holdup distribution can be determined from the local holdup correlation discussed in Section 6.1, and the radial position for the small bubbles or the liquid where the interstitial velocity becomes zero can, therefore, be calculated through the one dimensional liquid phase flow model and the slip velocity discussed in Section 6.3. The volume in each region can then be determined accordingly by integration of local holdup profiles.

Gas regions

The volume of large bubbles (LB) is:

$$V_{g3} = \pi R^2 L\overline{\varepsilon_{gl}} \tag{6.47}$$

where $\overline{\varepsilon_{gl}}$ is the average large bubble holdup which can be determined by dynamic gas disengagement (DGD) method or by the correlations from Wilkinson et al. (1992) or Krishna et al. (1994) (See Table 6-1).

The volume of small bubbles in the upflow region (SB1) is:

$$V_{g1} = \pi R^2 L\overline{\varepsilon_{gs}} - \int_{r''(u_g=0)}^{R} 2\pi r L \varepsilon_g dr \tag{6.48}$$

where $\overline{\varepsilon_{gs}}$ is the average small bubble holdup determined by DGD method or by correlations from Wilkinson et al. (1992) or Krishna et al. (1994) (See Table 6-1).

The volume of small bubbles in the downflow region (SB2) is:

$$V_{g2} = \int_{r''(u_g=0)}^{R} 2\pi r L \varepsilon_g dr \tag{6.49}$$

The volume of small bubbles in the upflow region where the liquid interstitial velocity is less than zero is:

$$V'_{g1} = \int_{r'(u_r=0)}^{r''(u_g=0)} 2\pi r L \varepsilon_g dr \tag{6.50}$$

Liquid regions

The volume of liquid in the upflow region (L1) is:

$$V_{l1} = \int_{0}^{r'(u_l=0)} 2\pi r L (1-\varepsilon_g) dr \tag{6.51}$$

The volume of liquid in the downflow region (L2) is:

$$V_{l2} = \int_{r'(u_l=0)}^{R} 2\pi r L (1-\varepsilon_g) dr \tag{6.52}$$

The volume of liquid in the downflow region where the small bubble interstitial velocity is greater than zero is:

$$V_{l2}^{1} = \int_{r'(u_l=0)}^{r''(u_g=0)} 2\pi r L(1-\varepsilon_g)dr \tag{6.53}$$

6.9 Mass Transfer Coefficient and Interfacial Area

Considerable studies for different correlations have been reported for mass transfer in bubble column systems. In Table 6-4 some reported correlations for mass transfer coefficients as a function of gas and liquid properties are summarized based on their date of publication.

Among them, Akita and Yoshida's (1973) correlation relies on the measurement of bubble diameters and gas hold up, but, it was only tested for gas hold up $\varepsilon < 0.14$. Gestrich and Krauss (1975) compared the literature data with known correlation for the interfacial area and developed a new correlation which fits the data better than previously reported correlation. The data covered is for superficial gas velocity less than 0.6 m/s and $0.56*10^{6} < \frac{\rho_L \sigma^3}{g\eta_L^4} < 0.18*10^{12}$. Later, a new correlation based on Hikita's (1981) work was developed and gas hold up correlation was also proposed. Calderbrank and Moo-Young (1961) first developed the correlations for large and small bubbles for mass transfer coefficient as well as interfacial area for an air water system, and Shah and Joseph (1985) pointed out its applicability based on the good fit for their system. Kawase et al. (1987) derived a semi-theoretical correlation for Newtonian and pseudo-plastic fluids based on Higbie's penetration theory as well as Kolmogoroff's theory of isotropic turbulence. By fitting their own, as well as literature data, as a function of the flow behavior index n, the constant B has been found as follows:

$$B = 0.0645n^{1.5} \quad \text{with} \quad \eta_{eff} = k\gamma_{eff}^{n-1} \tag{6.54}$$

TABLE 6-4. Mass Transfer Coefficient Correlations

$$\frac{k_L a d_R^2}{D_L} = 0.6\left(\frac{\mu_L}{\rho_L D_L}\right)^{0.5}\left(\frac{g d_R^2 \rho_L}{\sigma}\right)^{0.62}\left(\frac{g d_R^3 \rho_L^2}{\mu_L}\right)^{0.31} \varepsilon_G^{1.1}$$

or $Sh = 0.6 Sc^{0.5} Bo^{0.62} Ga^{0.31} \varepsilon_G^{1.1}$

Akita and Yoshida (1973)

$$a = 2600\left(\frac{H_L}{D_r}\right)^{-0.3}\left(\frac{\rho_l \sigma^3}{g\eta_l^4}\right)^{-0.003} \varepsilon$$

Gestrich and Krauss (1975)

$$\frac{k_l a u_G}{g} = 14.9 f\left(\frac{u_G \mu_L}{\sigma}\right)^{1.76}\left(\frac{\mu_L^4 g}{\rho_L \sigma^3}\right)^{-0.248}\left(\frac{\mu_G}{\mu_L}\right)^{0.243}\left(\frac{\mu_L}{\rho_L D}\right)^{-0.604}$$

Hikita et al. (1981)

Small Bubble

$$(k_L)^s = 0.31\left(\frac{\Delta\rho\mu_L g}{\rho_L^2}\right)^{1/3} Sc^{-2/3}$$

Large Bubble

$$(k_L)^g = 0.42\left(\frac{\Delta\rho\mu_L g}{\rho_L^2}\right)^{1/3} Sc^{-1/2}$$

Interfacial areas

$$a^S = \frac{6\varepsilon_g^S}{d_S}$$

Interfacial areas

$$a^L = \frac{6\varepsilon_g^L}{d_L}$$

Calderbrank and Moo-Young (1961) and Joseph and Shah (1985)

$$\frac{k_l a D_r^2}{D_l} = \frac{12}{\sqrt{\pi}} B\left(\frac{\eta_l D_l}{\rho_l}\right)^{1/2}\left(\frac{\rho_l u_g D_r}{\eta_l}\right)^{3/4}\left(\frac{u_g}{\sqrt{g D_r}}\right)^{7/60}\left(\frac{g D_r^2 \rho_l}{\sigma}\right)^{3/5}$$

Kawase et al. (1987)

TABLE 6-4. Mass Transfer Coefficient Correlations (Continued)

$\left(\frac{k_L a d_B^2}{D_L}\right) = 0.62\left(\frac{\mu_L}{\rho_L D_L}\right)^{0.5}\left(\frac{g\rho_L d_B^2}{\sigma}\right)^{0.33}\left(\frac{g\rho_L^2 d_B^3}{\mu_L^2}\right)^{0.29}\left(\frac{u_G}{\sqrt{g d_B}}\right)^{0.68}\left(\frac{\rho_G}{\rho_L}\right)^{0.04}$ Ozturk et al.(1987)
$Sh' = 0.018 Sc^{0.50} Bo^{0.20} Ga^{0.62} Fr^{0.51}(1+0.12Wi)^{-1}$ Suh et al.(1991)
$\frac{(k_L a)_{\rho G2}}{(k_L a)_{\rho G1}} = \left(\frac{(\varepsilon G)_{\rho G2}}{(\varepsilon G)_{\rho G1}}\right)^n$ Wilkinson (1991)
$\frac{g k_l d_{sm}^2}{\sigma} = 8.8\left(\frac{u_g \eta_l}{\sigma}\right)^{-0.04}\left(\frac{\sigma^3 \rho_l}{g\eta_l^4}\right)^{-0.12}\left(\frac{\rho_l}{\rho_g}\right)^{0.22}$ Wilkinson and Haringa (1994)
$\frac{k_l a u_g}{g} = 16.9\left(\frac{u_g \eta_l}{\sigma}\right)^{2.14}\left(\frac{\eta_l^4 g}{\rho_l \sigma^3}\right)^{-0.518}\left(\frac{\eta_g}{\eta_l}\right)^{0.074}\left(\frac{\eta_l}{\rho_l D_l}\right)^{-0.038}\left(\frac{d_{orif}}{D_r}\right)^{0.908}$ Sotelo et al. (1994)

For Newtonian fluids, n is equal to 1, implying that B=0.0645. However, from their work, it follows that B, as determined from experiments, has values from 0.0388 to 0.104 for Newtonian liquids depending on the column diameter and the physical properties of the liquid phase.

Suh et al. (1991) investigated the volumetric mass transfer coefficient in four sucrose solutions and proposed a correlation (refer to Table 6-4) for three highly viscous liquids

with the viscosity greater than 11.4 mPa.s, where churn turbulent or slug flow prevailed throughout the whole measurements. For the low viscous solution with $\mu_l = 2.6\text{mPa.s}$, the bubbly flow was always present due to the low superficial gas velocity. It was found that the dependence of the volumetric mass transfer coefficient for this particular liquid solution on the superficial gas velocity was about $u_g^{0.4}$. The conclusion of their analysis is that the mass transfer coefficient in the heterogeneous regime is more affected by the gas velocity than that in the homogeneous regime.

Wilkinson et al. (1991) analyzed their high pressure bubble column system data and extracted the information of pressure effects on mass transfer coefficient. A correlation was developed. In 1994, they also studied the influence of gas and liquid physical properties on bubble diameters in a column with an internal diameter of 0.15 m and a liquid level of 1.5 m. By means of regression analysis, they developed the dimensionless equation presented in Table 6-4.

It was found that the various correlations in Table 6-4 usually can only fit their own experimental data. For gas holdup, both negative and positive exponents for the density of liquid were reported in Table 6-4. Therefore, we conclude that the influence of the liquid properties is also not well understood yet, many discrepancies are found in the literature so far.

Henceforth, the more general correlation for mass transfer coefficient needs to be discovered. In this work, we used Joseph and Shah (1985)'s correlation to fit Shetty et al.'s experimental data (1992).

7. Simulation Results for Various Subcases of TRCFM

The implicit finite difference method with backward differences was used to solve the partial differential equations of the proposed models for the cases of single reaction, series reaction and parallel reaction schemes (refer to Figure 5-1 for a single irreversible reaction). The conditions used for prediction of concentration profiles are from Myers et al.'s (1987) experimental data as follows: superficial gas velocity = 0.1 m/s, superficial liquid velocity = 0.01 m/s, gas hold up = 0.181, column diameter = 0.19 m and the height of the column = 2.44 m. Since the superficial gas velocity is 0.1 m/s, churn turbulent flow prevails. Ueyama and Miyauchi's (1979) one dimensional liquid flow model is applied together with Miyauchi's (1981) correlation for kinematic viscosity to calculate the liquid radial velocity profile. The calculated mean residence time for the upflow region is 7.614 (sec), the calculated mean residence time for the downflow region is 12.211(sec) and the calculated recycle ratio is 9.632. The dimensionless exchange coefficient is assumed to be 135 in the model simulation based on the fit with experimental data of Myer et al.(1987) which will be discussed in Chapter 8. This dimensionless exchange coefficient corresponds to a value of 1.57E-2 m^2 / s for the dimensional exchange coefficient). The liquid reactant and product species are assumed to be nonvolatile.

7.1 Concentration Distribution and Conversion Profiles for a Single Reaction

For case 1, several different reaction rate constants are tested, k = 0.005(s^{-1}), k = 0.1(s^{-1}). It is clear from Figure 7-1 to 7-4 that, with the increase of the reaction rate constant, the steady state reactant concentration is decreased and the product concentration is increased. When k = 0.1 (s^{-1}), nearly all the reactant is consumed at x = 1.0 and even at x = 0.5 as well. This implies that half of the volume of this bubble column reactor is sufficient for achieving the same amount of product. But, this is not the case with k = 0.005 (s^{-1}) because of the lower reaction rate constant. For steady state condition, the location point far away from the tracer inlet has a higher product concentration and, hence, a higher conversion for this reaction Cb (x=0.1) < Cb (x=0.5) < Cb (x=1.0).

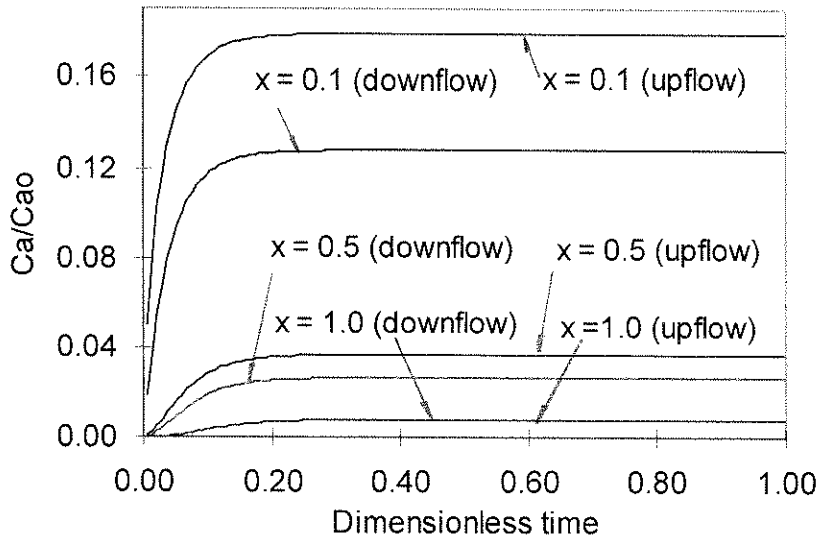

FIGURE 7-1. Reactant Concentration Distribution in the Upflow and the Downflow Regions along the Height of the Column as a Function of Time,

$A \xrightarrow{k} B, k = 0.1s^{-1}$ **(Step Input of Reactant)**

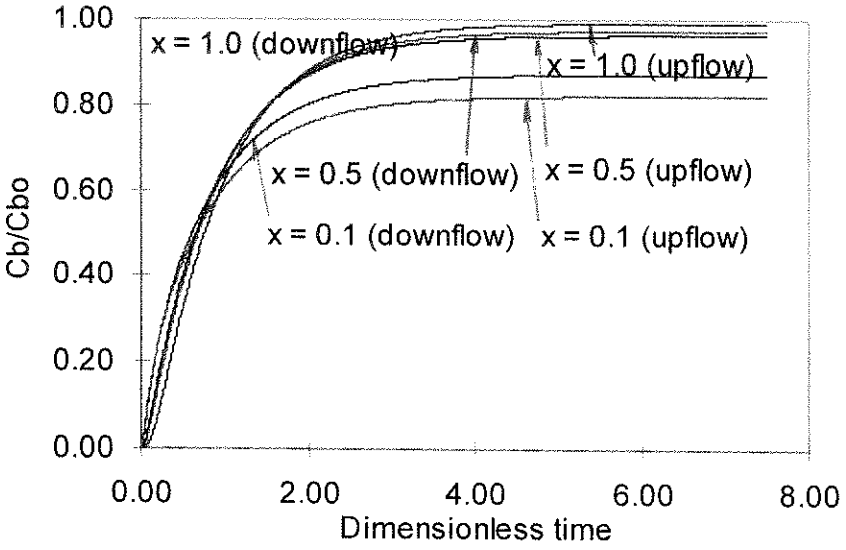

FIGURE 7-2. Product Concentration Distribution in the Upflow and the Downflow Regions along the Height of the Column as a Function of Time,

$A \xrightarrow{k} B, k = 0.1s^{-1}$ **(Step Input of Reactant)**

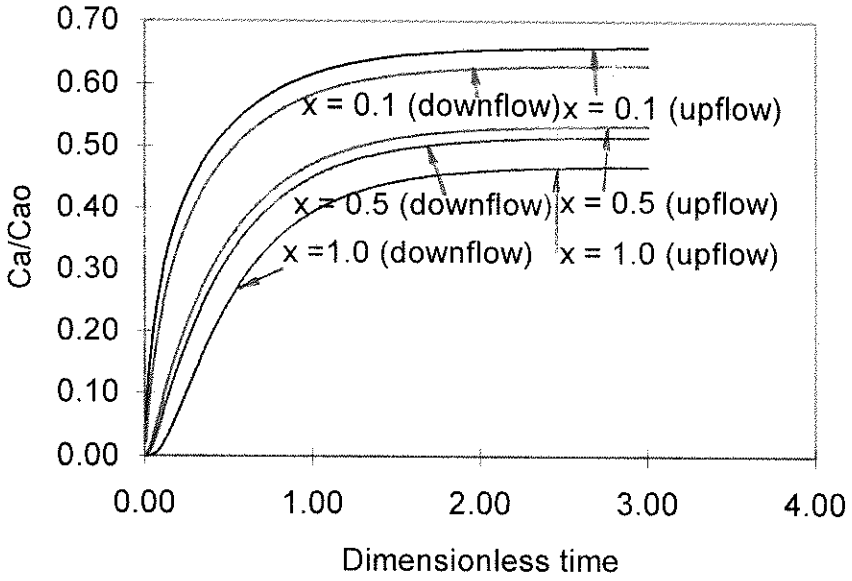

FIGURE 7-3. Reactant Concentration Distribution in the Upflow and the Downflow Regions along the Height of the Column as a Function of Time,

$A \xrightarrow{k} B, k = 0.005s^{-1}$ **(Step Input of Reactant)**

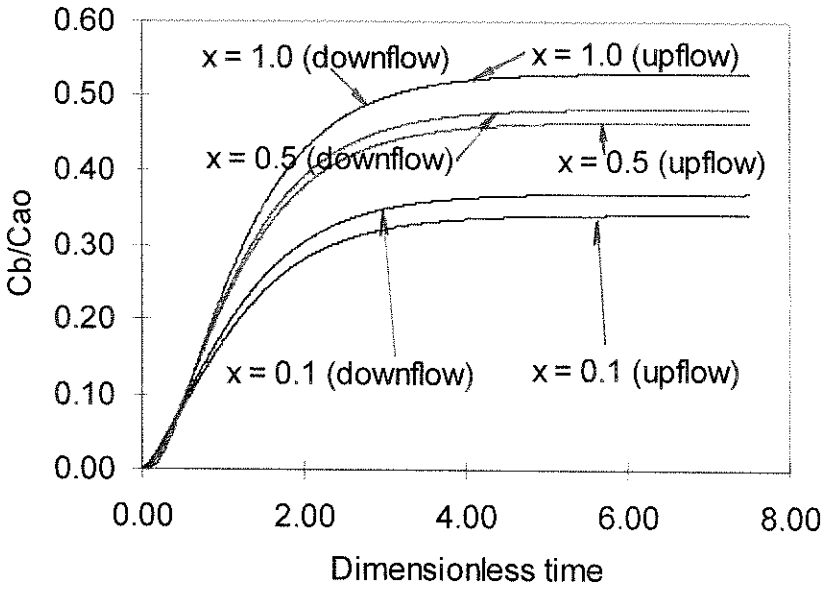

FIGURE 7-4. Product Concentration Distribution in the Upflow and the Downflow Regions along the Height of the Column as a Function of Time, $A \xrightarrow{k} B, k = 0.005 s^{-1}$ **(Step Input of Reactant)**

Under the steady state conditions, the concentration of reactants and conversion for different rate constants (k = 0.1, 0.05, 0.005 1/s) as a function of axial position in the column and in various flow regions are shown in Figure 7-5 and 7-6. The steady state concentration of the reactant drops and the conversion increases with the increase in the longitudinal height of the column. The changes in concentration and conversion are higher at points closer to the bottom of the column and lower when far away from the bottom of the column. The magnitude of the rate constants affects the conversion and reactant concentration profiles. Conversion in the column is always higher in the downflow region than that in the upflow region, which is to be expected since the reactant reaching any axial location has more time to react in the downflow region. Clearly, even at large recycle ratio and cross flow exchange coefficient, the spatial concentration difference exists and perfect CSTR behavior is never reached, this is due to the convection term in the model equations.

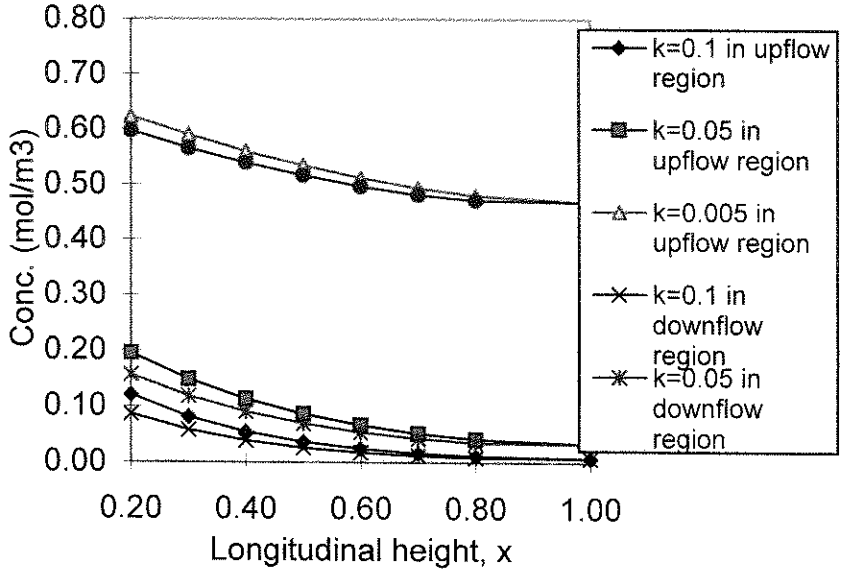

FIGURE 7-5. Steady State Reactant Concentration Profiles for Different Rate Constants as a Function of Longitudinal Height of the Column for Single Irreversible Reaction

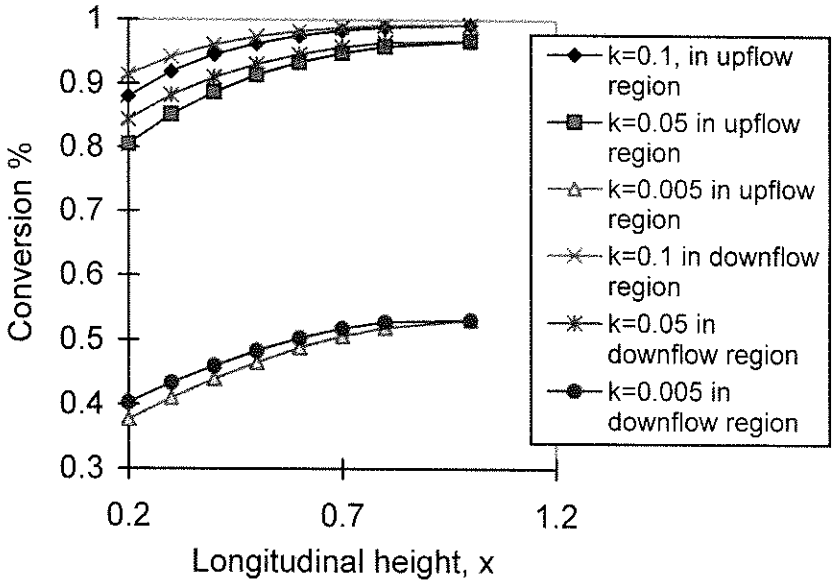

FIGURE 7-6. Conversion as a Function of Height in the Bubble Column for a Single Irreversible Reaction

7.2 Concentration Distribution and Conversion Profiles for Series Reactions

For the series reaction scheme where the values of reaction rate constant are k1 = 0.02 (s^{-1}) and k2 = 0.005 (s^{-1}), the prediction of concentration profiles with time on stream and at different locations is illustrated in Figure 7-7 to 7-9. It is evident that the steady state concentration is higher for intermediate product B than product C. The higher steady state concentration of the intermediate product is due to the higher reaction rate constant k1 and lower reaction rate constant k2. The reactant concentration is the lowest at the outlet of the column and the highest at the inlet of the column. These results are quite realistic.

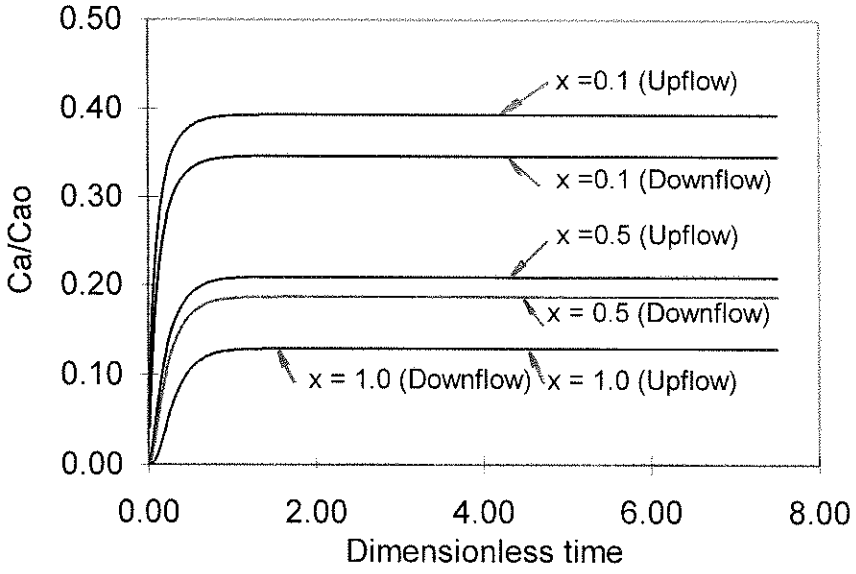

FIGURE 7-7. Reactant Concentration Distribution in the Upflow and the Downflow Regions along the Vertical Position of the Bubble Column as a Function of Time on Stream,

$$A \xrightarrow{k_1} B \xrightarrow{k_2} C, \quad k_1 = 0.02 s^{-1}, k_2 = 0.005 s^{-1}$$

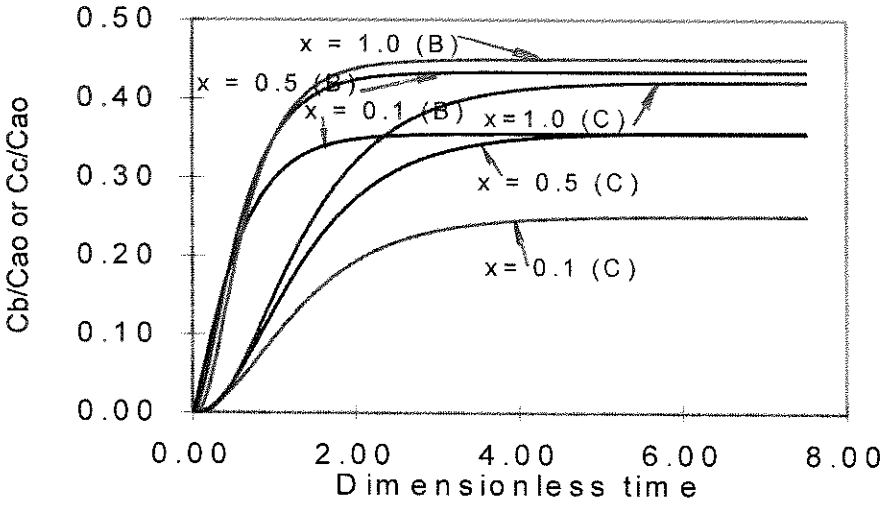

FIGURE 7-8. Intermediate Product B and Product C Concentration Distribution in the Upflow Region along the Vertical Position of the Bubble Column as a Function of Time on Stream,

$$A \xrightarrow{k_1} B \xrightarrow{k_2} C, \quad k_1 = 0.02 s^{-1}, k_2 = 0.005 s^{-1}$$

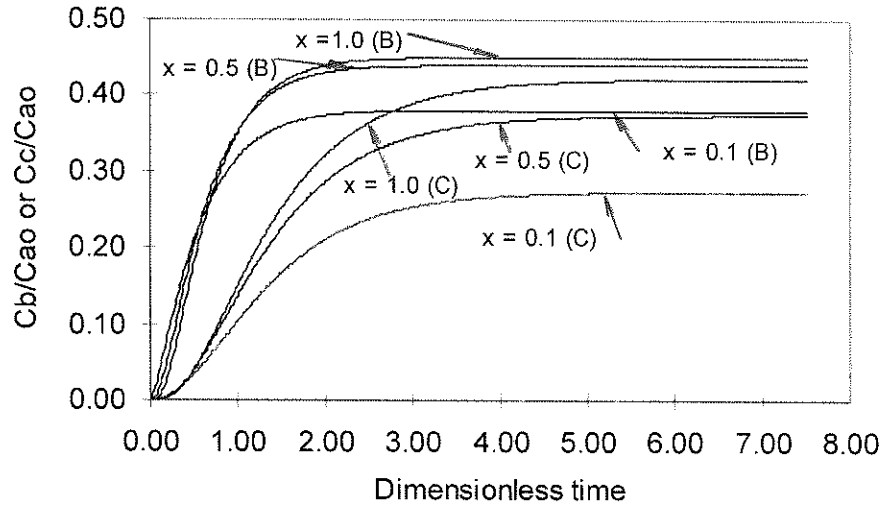

FIGURE 7-9. Intermediate Product B and Product C Concentration Distribution in the Downflow Region along the Vertical Position of the Bubble Column as a Function of Time on Stream,

$$A \xrightarrow{k_1} B \xrightarrow{k_2} C, \quad k_1 = 0.02 s^{-1}, k_2 = 0.005 s^{-1}$$

The steady state for the reactant concentration and conversion is illustrated in Figure 7-10. Similarly to the single reaction case discussed in section 7.1, the change in concentration and conversion is higher near the bottom of the column than away from the bottom region. It is also found from the above cases that, below the outlet of the bubble column, the steady state concentration of reactant in the upflow region is always a little bit higher than that in the downflow region, whereas the steady state concentration of product in the upflow region is always a little bit lower than that in the downflow region. The reason is the longer residence time in the downflow region.

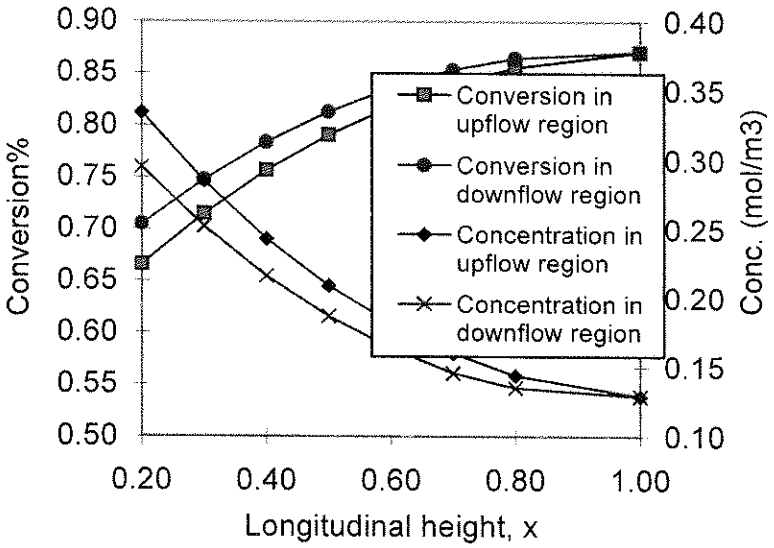

FIGURE 7-10. Conversion and Reactant Concentration as a Function of Height in the Column for Series Reactions,

$$A \xrightarrow{k_1} B \xrightarrow{k_2} C, \quad k_1 = 0.02\,s^{-1}, k_2 = 0.005\,s^{-1}$$

7.3 Concentration Distribution and Conversion Profiles for Parallel Reactions

For the parallel reaction scheme where the values of reaction rate constant for reaction $A \xrightarrow{k1} B$ are k1 = 0.2 (s^{-1}) and reaction $A \xrightarrow{k2} C$ are k2 = 0.05

(s^{-1}), the predictions of reactant and product concentration profiles with time on stream and at different locations are illustrated from Figure 7-11 to 7-13. The higher the reaction rate constant is, the higher the steady state concentration of product is. Therefore, the steady state concentration of product B is greater than that of product C.

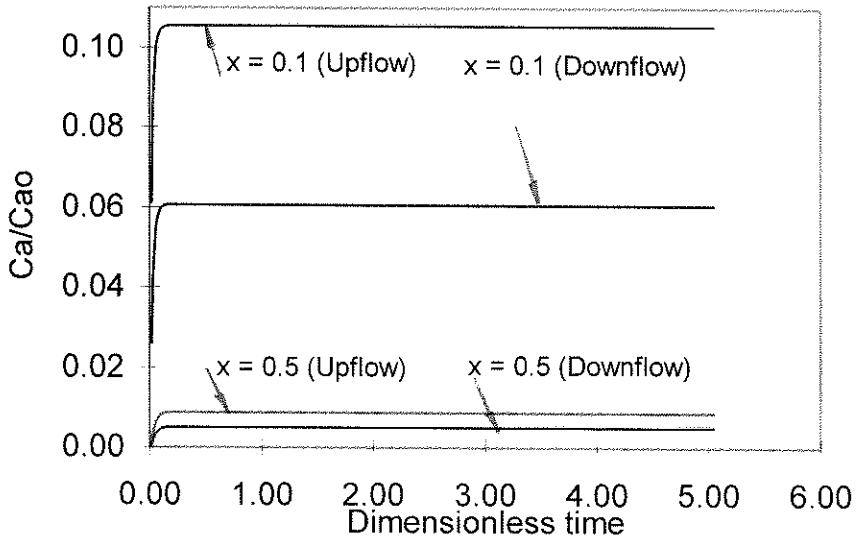

FIGURE 7-11. Reactant Concentration Distribution in the Upflow and the Downflow Regions along the Vertical Position of the Bubble Column as a Function of Time on Stream, $A \xrightarrow{k_1} B, A \xrightarrow{k_2} C, \quad k_1 = 0.2\,s^{-1}, k_2 = 0.05\,s^{-1}$

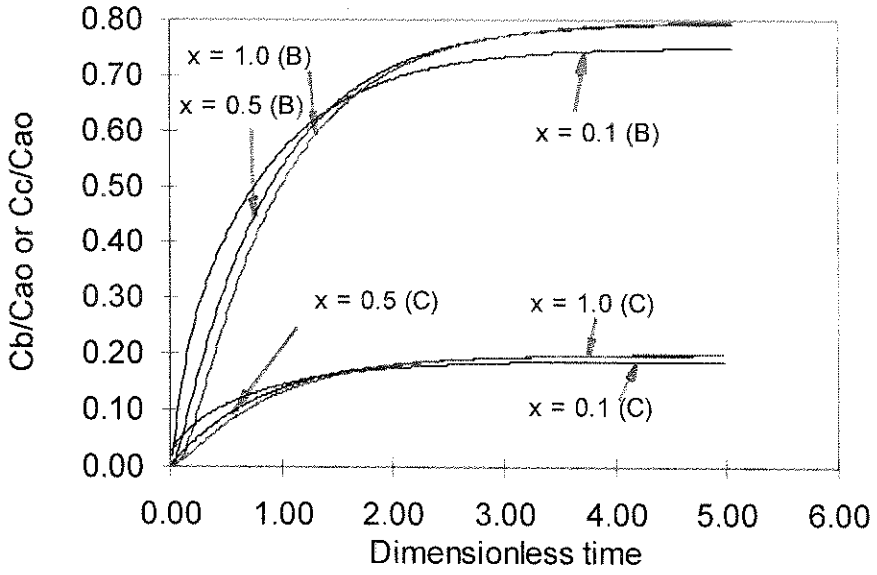

FIGURE 7-12. Product B and C Concentration Distribution in the Upflow Region along the Vertical Position of the Bubble Column as a Function of Time on Stream, $A \xrightarrow{k_1} B, A \xrightarrow{k_2} C, \quad k_1 = 0.2\,s^{-1}, k_2 = 0.05\,s^{-1}$

Similar results to that of the series reaction case are found for the conversion and the steady state concentration of reactant profiles. See Figure 7-14.

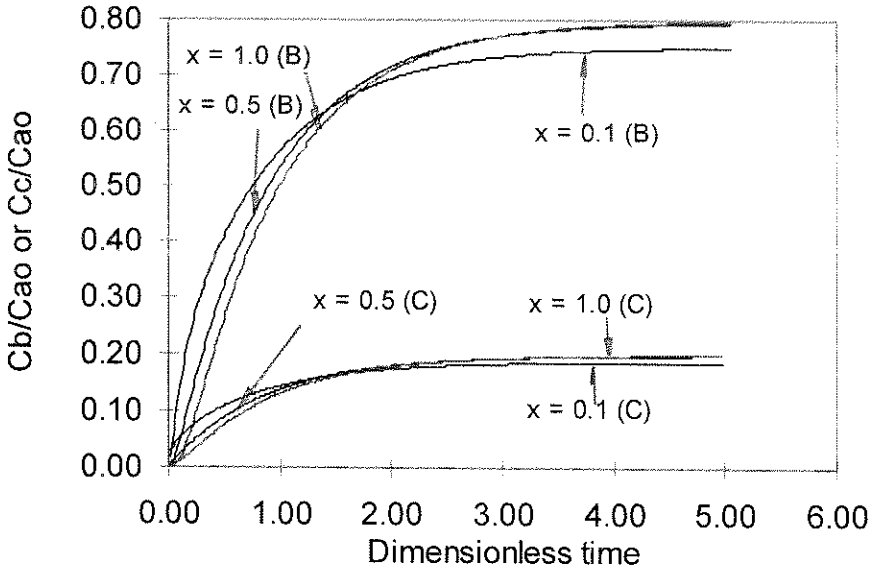

FIGURE 7-13. Product B and C Concentration Distribution in the Downflow Region along the Vertical Position of the Bubble Column as a Function of Time on Stream, $A \xrightarrow{k_1} B, A \xrightarrow{k_2} C, \quad k_1 = 0.2\,s^{-1}, k_2 = 0.05\,s^{-1}$

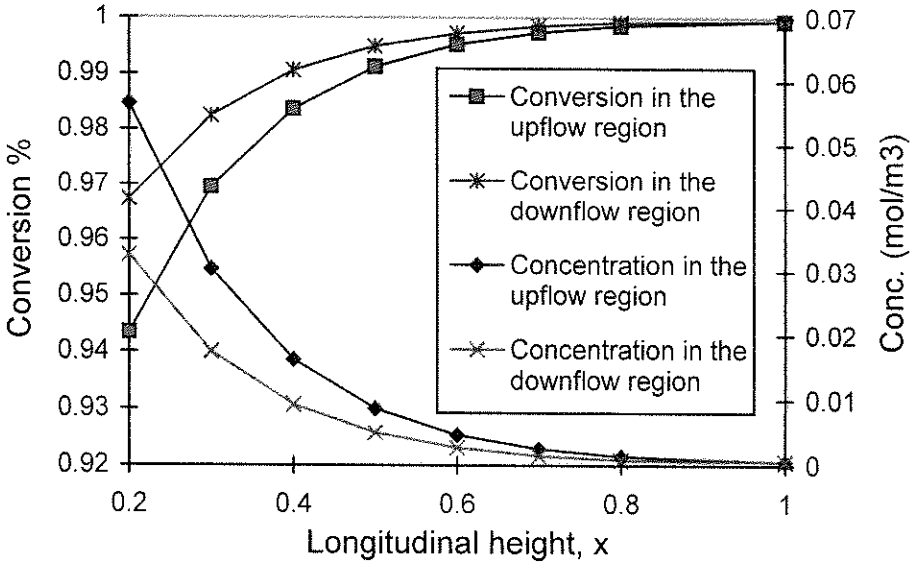

FIGURE 7-14. Conversion and Concentration versus Vertical Positions along the Column for Parallel Reactions

7.4 Concentration Distribution for the Tracer Injected in the Middle of the Bubble Column

The same operating conditions as those in Section 7.1 are assumed. The tracer is assumed to be injected at the middle point of the bubble column and no chemical reaction is involved (refer to Figure 5-2).

Figure 7-15 and 7-16 illustrate liquid tracer responses obtained from the liquid tracer injected in the upflow region in the middle of the bubble column. In the upflow region at $x > 0.5$, the concentration increases with time on stream and the concentration increases faster as the measurement location is closer to the tracer injecting point and vice versa. At steady state condition, all the concentration profiles at $x > 0.5$, approach 1. However, at $x < 0.5$, the situation is different, due to the liquid inlet at $x = 0$ which dilutes the concentration of the tracer injected at a steady rate at $x=0.5$ for all locations at $x < 0.5$ so that the steady state concentration is less than 1. The further the measurement point is from the injection point at $x < 0.5$, the lower the steady state concentration is. In addition, it is also found that, for the upflow and the downflow regions at $x > 0.5$ but below the outlet of the bubble column, before the tracer reaches steady state condition, the concentration is higher in the upflow region than that in the downflow region. But, at $x < 0.5$, the concentration goes up faster in the downflow region than in the upflow region and, therefore, the steady state concentration is higher in the downflow region than that in the upflow region.

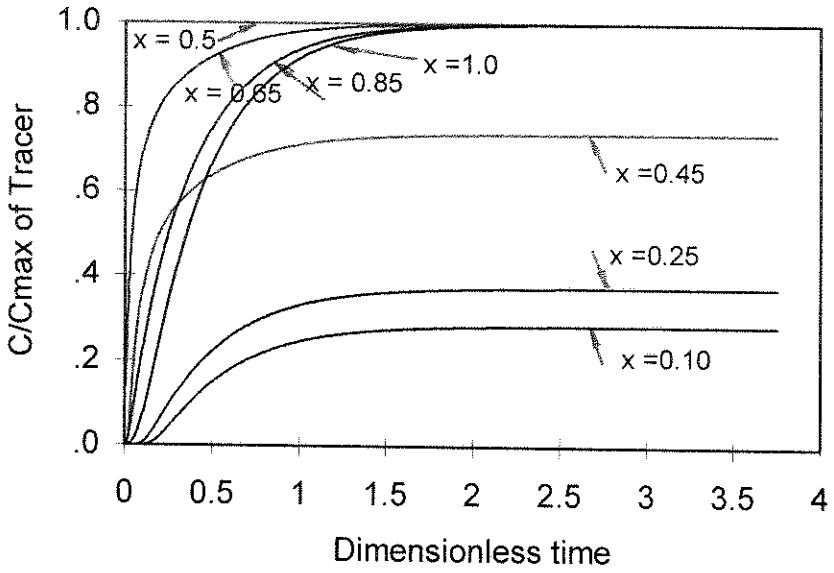

FIGURE 7-15. Tracer Response in the Upflow Region of the Column with Tracer Injection in the Middle of the Column

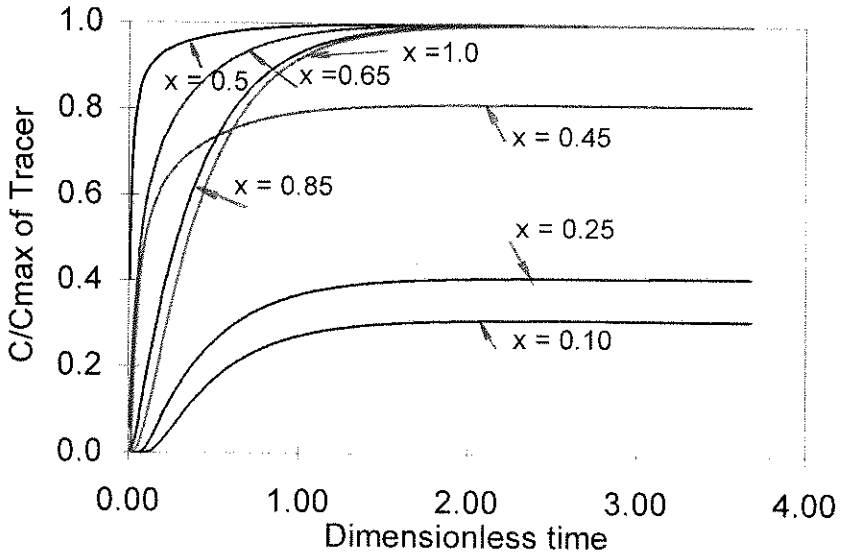

FIGURE 7-16. Tracer Response in the Downflow Region of the Column with Tracer Injection in the Middle of the Column

The cross sectional average tracer concentration at a fixed vertical position can be defined as follows:

$$\overline{C_l} = \frac{\int_0^{2\pi}\int_0^{R}(1-\varepsilon_g)C_l\, r dr d\theta}{\int_0^{2\pi}\int_0^{R} r dr d\theta} \tag{7.1}$$

In TRCFM model, for either upflow or downflow region of liquid, at a given longitudinal position, the local concentration is assumed to be independent of the radial position in that region. By weighted average in upflow and downflow regions, the above Equation can be simplified as follows:

$$\overline{C_l} = \frac{V_{l1}}{(V_{l1}+V_{l2})}C_{l1} + \frac{V_{l2}}{(V_{l1}+V_{l2})}C_{l2} \tag{7.2}$$

where V_{l1}, V_{l2} are the volume of the liquid in upflow and downflow regions and can be determined by Equation 6.51 and 6.52 in Chapter 6.

Figure 7-17 shows the cross sectional average concentration distribution versus time on stream along different vertical locations

This result is useful since the cross sectional average tracer concentration along the column may be related to the response of scintillation detectors by using radioactive tracer measurements such as CARPT (Devanathan et al. 1990). This method may also be used for future interpretation of Laporte tracer runs for Air Product & Chemical (1990).

The concentration differences in both upflow and downflow regions can also be verified experimentally by radioactive tracer measurements. By injecting radioactive tracer in the middle of the bubble column with one experiment in the upflow region

of the liquid and another experiment in the downflow region of the liquid. The scintillation detectors are located both above the tracer injection points and below the tracer injection points. The different responses of the detectors indicate the different cross sectional average concentration for these two experiments.

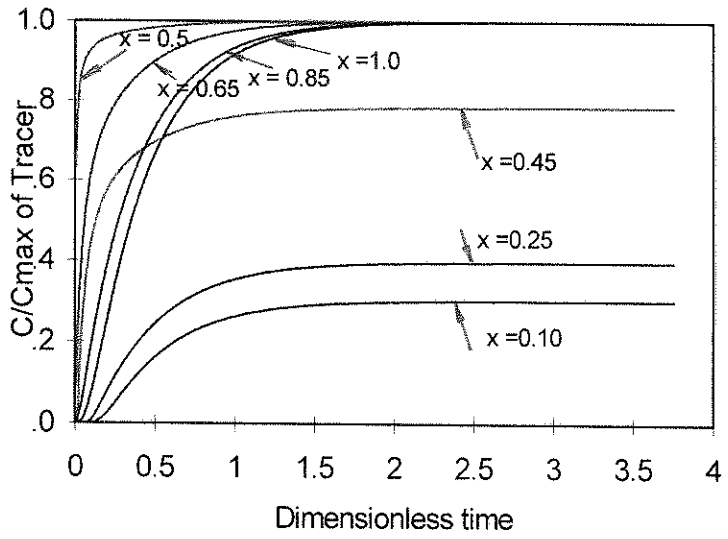

FIGURE 7-17. Cross Sectional Average Tracer Concentration versus Time on Stream with Tracer Injection in the Middle of the Column

7.5 Concentration Distribution of Impulse Liquid Tracer Injected at the Bottom of the Column for Continuous Flow of Gas and Batch Liquid Operation

Under continuous flow of gas and batch liquid operation, the gas enters at the bottom of the bubble column. The operating conditions are assumed as follows: Superficial gas velocity, 0.1 m/s; diameter of the column, 0.19 m; height of the column, 2.44 m; average gas holdup, 0.181; dimensionless exchange coefficient, 135. Using one dimensional liquid flow model of Ueyama and Miyauchi (1979), the calculated mean residence time in the upflow region of the liquid is 7.713 (sec), the

calculated mean residence time in the downflow region of the liquid is 11.537 (sec). A pulse of non volatile liquid tracer is injected at the bottom and near the center of the column (located in the upflow region of the liquid). Using RCFM, the impulse tracer responses at different vertical positions and in different regions (upflow and downflow) are illustrated in Figure 7-18 for the upflow region and Figure 7-19 for the downflow region, respectively.

It is seen that the "overshoot" response happens near the bottom of the column (close to the inlet of pulse tracer position) and the "overshoot" tracer response appears both in the upflow and downflow regions. From Figure 7-18 and 7-19, the peak concentration of the "overshoot" tracer response for the same vertical position is always a little bit higher for the upflow region of the liquid than that for the downflow region of the liquid. "overshoot" response doesn't appear much in both upflow and downflow regions when the vertical position is far away from the bottom. These overshoot phenomena were also found from Air Product & Chemical's report for Laporte tracer runs in slurry bubble column reactors (1990). A quantitative comparison is needed for further validation. But, for ADM model, it is impossible to simulate the "overshoot" behavior. This result indicates the need of this model.

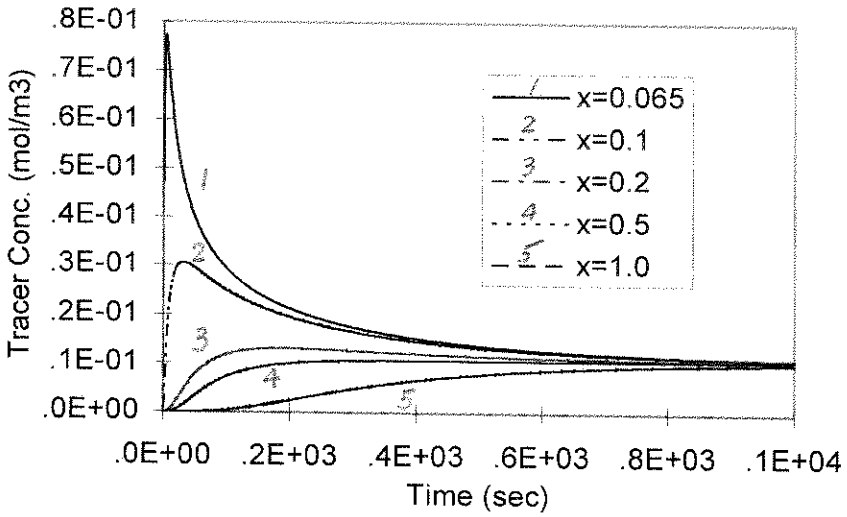

FIGURE 7-18. Prediction of Concentration Profiles in the Upflow Region of the Liquid for the Impulse Liquid Tracer Response in the Batch Liquid Operation by Using RCFM Model

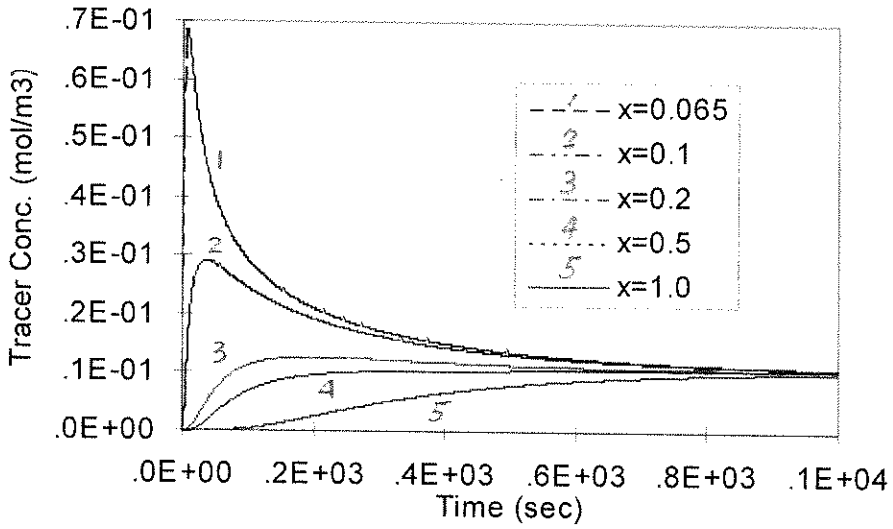

FIGURE 7-19. Prediction of Concentration Profiles in the Downflow Region of the Liquid for the Impulse Liquid Tracer Response in the Batch Liquid Operation by Using RCFM Model

From Figure 7-18 and 7-19, it is also found that the tracer concentration at different positions finally approaches the same concentration. Under the steady state condition, tracer concentration becomes uniform in the bubble column. This result reflects reality.

Similar to Section 7-5, the cross sectional average concentration can also be calculated (refer to Equation 7.1 and 7.2). Figure 7-20 is the cross sectional average tracer concentration response versus time on stream at different vertical position in the column. This result may be applied for comparing with the scintillation detector responses by radioactive tracer measurements for future interpretation of Laporte tracer data (1990).

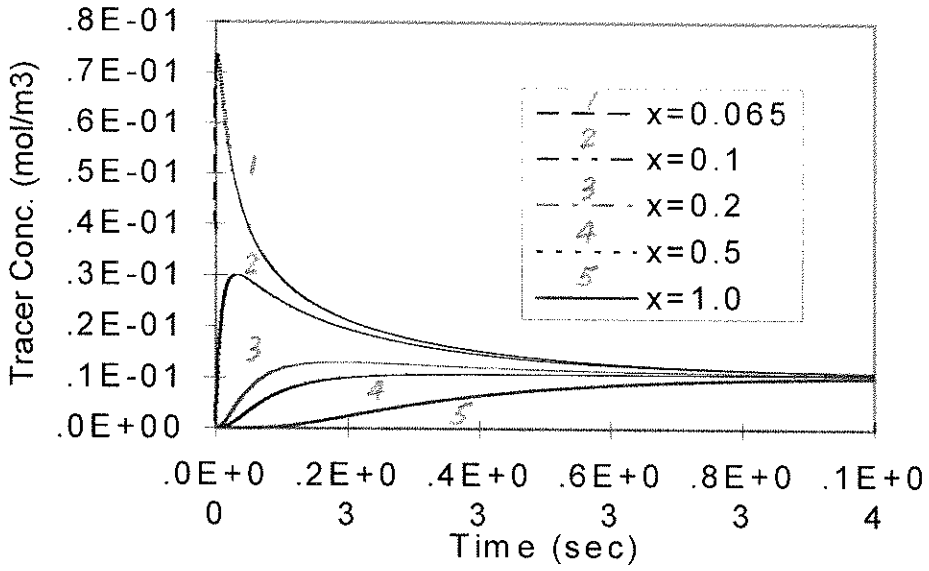

FIGURE 7-20. Cross Sectional Average Tracer Concentration versus Time on Stream with a Pulse of Tracer Injected at the Bottom of the Column in the Batch Liquid Operation

8. Application of TRCFM

8.1 Application of the Subcases of TRCFM for Gas or Liquid Phase Mixing

8.1.1 Myers et al. (1987)'s Tracer Data for Liquid Phase Mixing

The liquid tracer response in air-water bubble column system was obtained experimentally by Myers et al. (1987). Air and water were introduced into the bottom of the bubble column and a pulse of methylene blue liquid tracer was injected into the bottom of the column. Other operating conditions are as follows: superficial gas velocity of 0.1 m/s, superficial liquid velocity of 0.01 m/s and average total gas hold up of 0.181, column diameter of 0.19 m and column height of 2.44 m. Based on the one dimensional liquid flow model from Ueyama and Miyauchi (1979), the calculated mean residence times in the upflow and downflow regions are 12.211 (sec) and 7.614 (sec), respectively, and the calculated recycle ratio is 9.632.

The liquid phase recycle with cross flow model (RCFM) is used to match the experimental data. By changing the exchange coefficient between the upflow and the downflow regions, it is found that the best fit is achieved when dimensionless exchange coefficient equals 135 or dimensional exchange coefficient is 0.0157 m^2 / s. The quality of fit for dimensionless pulse response in the air-water system is illustrated in Figure 8-1. The impulse tracer data response is presented by the E(t) curve. The slug and cell model,

developed by Myers et al. (1987), and the RCFM are both used to fit the data. Excellent fit is achieved for both of the models. This indicates again that RCFM is a good choice for modeling liquid phase mixing.

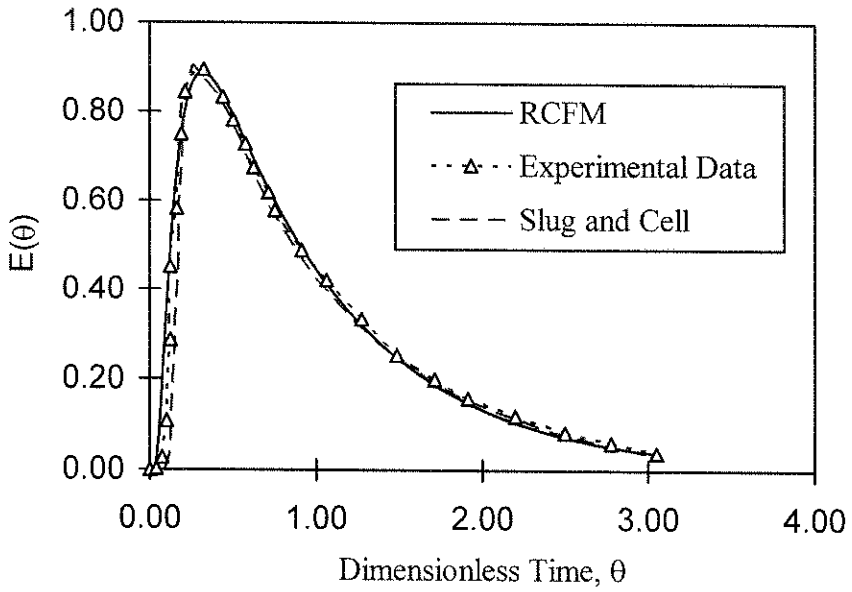

FIGURE 8-1. Comparison of the RCFM, Slug and Cell Model Predictions with Myers et al. (1987)'s Experimental Data in Air-Water System (Continuous Flow of Gas and Liquid)

8.1.2 Towell and Ackermann (1972)'s Tracer Data for Gas Phase Mixing

In the two phase bubble column system, as was pointed out by Vermeer and Krishna (1981), the homogeneous regime is maintained when the superficial gas velocity is approximately less than 0.07 m/s. The recirculation of the liquid also results in the

circulation of the small bubbles. The reason is that the interstitial small bubble velocity and interstitial liquid velocity are related by the slip velocity. The slip velocity is not high enough and can't offset the downflow of the liquid in the annular region. Therefore, the motion of the small bubbles is similar to the motion of the liquid, that is: upflow in the core of the bubble column and downflow in the annual region, refer to Figure 5-4. As shown in Section 8.1.1, a subcase of TRCFM (RCFM) is a good choice for modeling liquid phase mixing. But, its applicability for gas phase mixing is unknown. In addition, an overview of the past literature reveals that modeling of gas phase mixing is much less reported than that of liquid phase mixing. Therefore, here, the RCFM (Subcase of TRCFM) is tested for gas phase mixing.

The step down tracer response data was from Towell and Ackerman (1972). Two sets of experimental runs were included. The Freon gas tracer was used in the experiments. It is regarded as a non-soluble gas tracer. Air and water were introduced into the bottom of the bubble column.

In case A, the bubble column had a superficial gas velocity of 0.0326 m/s (bubbly flow regime), a superficial liquid velocity of 0.0135 m/s and gas holdup was 0.133, the column had a diameter of 0.406 m and the height of the column was 3.42 m. The calculated mean residence time for upflow region of the small bubbles is 8.418 sec. The calculated mean residence time for downflow region of the small bubbles is 21.327 sec. The recycle ratio is 0.1059.

In case B, the bubble column had a superficial gas velocity of 0.0344 m/s (bubbly flow regime), a superficial liquid velocity of 0.0072 m/s and gas holdup was 0.139. The column had a diameter of 1.280 m and the height of the column was 5.11 m. The calculated mean residence time for upflow region of the small bubbles is 12.292 (sec).

The calculated residence time for downflow region of the small bubbles is 18.313 (sec). The recycle ratio is 0.2746.

As the superficial gas velocity is quite low, it is safe to assume that the homogeneous flow regime prevails. Therefore, uniform bubble size (small bubbles) distribution is assumed. The small bubbles are assumed to go upward in the core of bubble column and go downward near the wall.

The comparison between the step down gas tracer response data and the prediction from the proposed model is shown in Figure 8-2 for case A and Figure 8-3 for case B. It is noteworthy that the normalized tracer concentration is plotted against dimensionless time ($U_g t / L\varepsilon_g$) in Figure 8-2 and Figure 8-3. The concentration was normalized with the initial step value of the concentration. The best fit is found when the dimensionless exchange coefficients are 1.05 for case A and 0.9 for case B. It is shown that excellent result is achieved for case A and satisfactory result can be achieved for case B. This indicates that the (RCFM) can be applied not only for modeling liquid phase mixing but also for modeling gas phase mixing in the bubble column system. The suitability of model for both gas and liquid phase mixing is, therefore, examined next.

8.2 Applications of TRCFM for Two Phase Mixing with Mass Transfer

8.2.1 Shetty et al. (1992)'s Data for a Small Size Bubble Column

Shetty et al. (1992) performed a series of gas tracer experiments in a cylindrical column of 0.15 m inside diameter in an air-water system. The height of the bubble column was 3 m. The column was operated at atmospheric pressure.

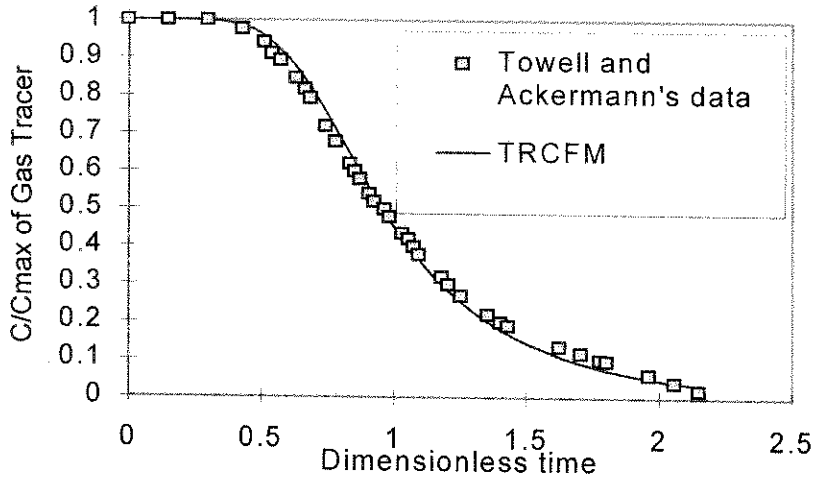

FIGURE 8-2. Comparison of Towell and Ackermann (1972)'s Data with TRCFM Simulation Results (Superficial Gas Velocity = 0.0326 m/s, Superficial Liquid Velocity = 0.0135 m/s, D = 0.4064 m, H=3.42 m, Gas Holdup = 0.133, Kg12 = 1.05, Freon Gas Tracer, Air Water System)

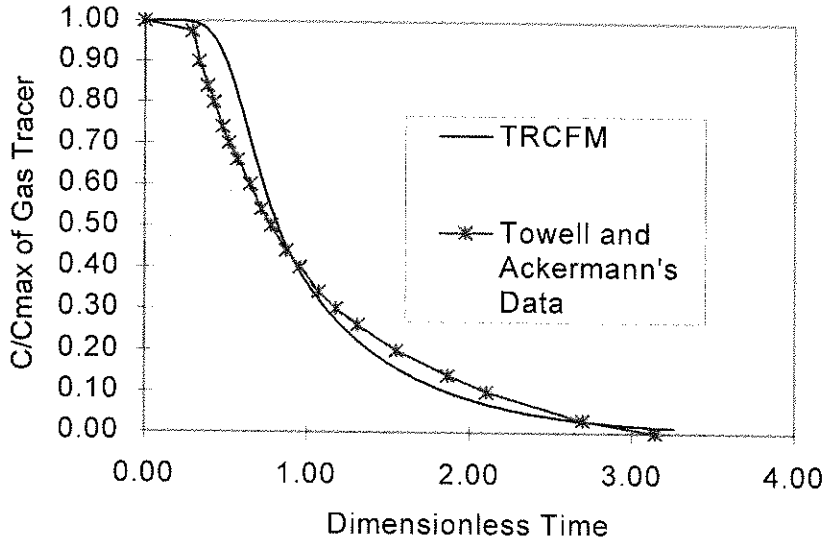

FIGURE 8-3. Comparison of Towell and Ackermann (1972)'s Data with TRCFM Simulation Results (Superficial Gas Velocity = 0.0344 m/s, Superficial Liquid Velocity = 0.0072 m/s, D = 1.067 m, H=5.11 m, Gas Holdup = 0.139, Kg12 = 0.9, Freon Gas Tracer, Air Water System)

A sensitive quadruple mass spectrometer was used to measure the tracer concentration for the gas phase exiting the funnel. Sampling was done by a 50 μm diameter capillary inlet probe. Helium was used as gas tracer.

It was concluded by Shah and Joseph (1985) that the assumption made by most of the previous investigators in neglecting the mass transfer of Helium to water is not reasonable since neglecting the mass transfer contribution can only be justified for the dimensionless Henry's coefficient greater than 1000. For Helium in water at ambient temperature condition, the reported Henry's coefficient is equal to 106 $mol/m^3(gas)*m^3(liquid)/mol$ (Shetty et al.(1992)). Therefore, it can only be classified as a soluble tracer.

The overall gas hold up was determined from the steady state pressure profile obtained by using eight pressure transducers along the column height. The hold up of small bubbles was calculated from the steady state pressure difference after a shut down in the gas supply to the column.

The superficial gas velocity in this experiment was 0.15 (m/s). Therefore, the churn turbulent regime prevails. The superficial liquid velocity was 0.011 (m/s).

The experimental data is as follows: The dimensionless Henry's coefficient, H=106 ($mol/m^3(gas)*m^3(liquid)/mol$), the average small bubble hold up, $\overline{\varepsilon_s} = 0.117$, the average large bubble hold up, $\overline{\varepsilon_l} = 0.063$, the total average gas hold up, $\overline{\varepsilon_g} = 0.18$, the superficial gas velocity, $u_g = 0.15$ (m/s), the superficial liquid velocity, $u_l = 0.011$ (m/s), the column had a diameter of 0.15 m, the height of the bubble column was 3 m.

Shetty et al. (1992) used the axial dispersion model (ADM) with two bubble size distribution to fit the experimental data. They assumed that the large bubbles go upward in plug flow and both the small bubbles and the liquid phase follow ADM due to backmixing, but the interaction among the large and small bubbles was neglected in their model.

The TRCFM was used based on Shetty et al.'s (1992) experimental data above.

The liquid velocity profile is calculated by assuming Ueyama and Miyauchi's (1979) one dimensional model. The Lockett and Kirkpatrick (1989)'s correlation for slip velocity is used in the model. The interstitial velocity for the small bubbles can, then, be calculated according to the slip velocity and the liquid interstitial velocity. The small bubble and large bubble hold up values were from Shetty et al.'s (1992) experiments.

As was pointed out by Modak et al.(1993) that the interaction between the large and small bubbles is so strong that the dimensionless exchange coefficient is a very large number. A value of K_{g13} of 1000 and 10000 is used and no difference is found for the concentration profiles (see Figure 8-4). Therefore, it can be safely assumed that K_{g13} of 1000 is numerically large. In this work, K_{g13} of 10000 is used as the dimensionless exchange coefficient between the large and small bubbles to perform simulation.

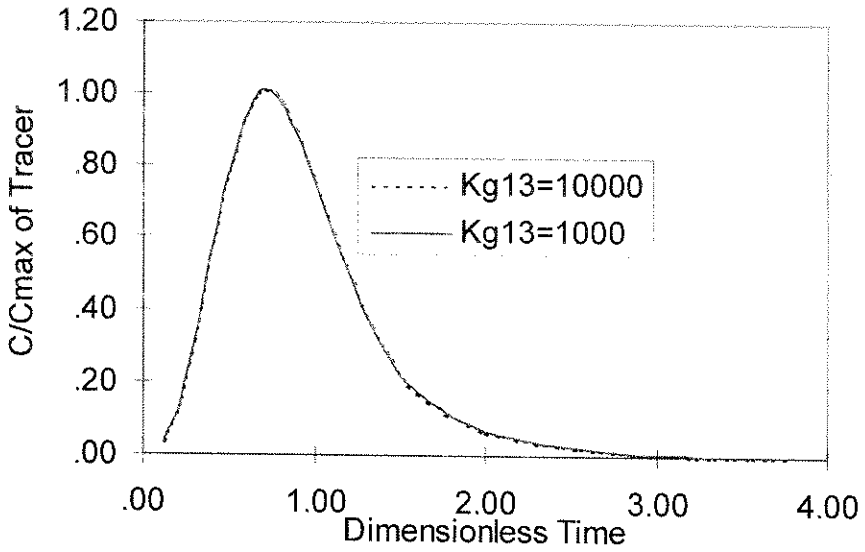

FIGURE 8-4. Effect of Interaction Between Large and Small Bubbles (K_{g13} = 1000 and K_{g13} = 10000) on the Tracer Curves

The correlation for mass transfer coefficient from Shah and Joseph (1985) is used to match the experimental data. The dimensionless exchange coefficients for small bubbles (SB1 and SB2) and for liquid (L1 and L2) are 1.75 and 80 for the best fit of the tracer curves at the outlet of the bubble column. The normalization procedure for the impulse response tracer curves was discussed in Section 4.2.1.1. In summary, the following parameters were estimated (see Table 8-1).

TABLE 8-1. Summary of Parameters Used to Fit Shetty et al. (1992)'s Experimental Data by Using TRCFM Model

Parameter	Units	Value
τ_{g1}	s	3.87
τ_{g2}	s	47.19
τ_{g3}	s	1.97
τ_{l1}	s	10.16
τ_{l2}	s	16.58
r_{g12}		0.0215
r_{l12}		7.10
K_{g12}		1.75
K_{l12}		80
k_{g12}	m^2 / s	40.50E-3
k_{l12}	m^2 / s	57.57E-3
$(k_l a)^l$	1/s	0.0234
$(k_l a)^s$	1/s	0.1039
H	$mol / m^3(gas) * m^3(liquid) / mol$	106

The comparison of experimental data with simulation results for TRCFM and ADM is presented in Figure 8-5.

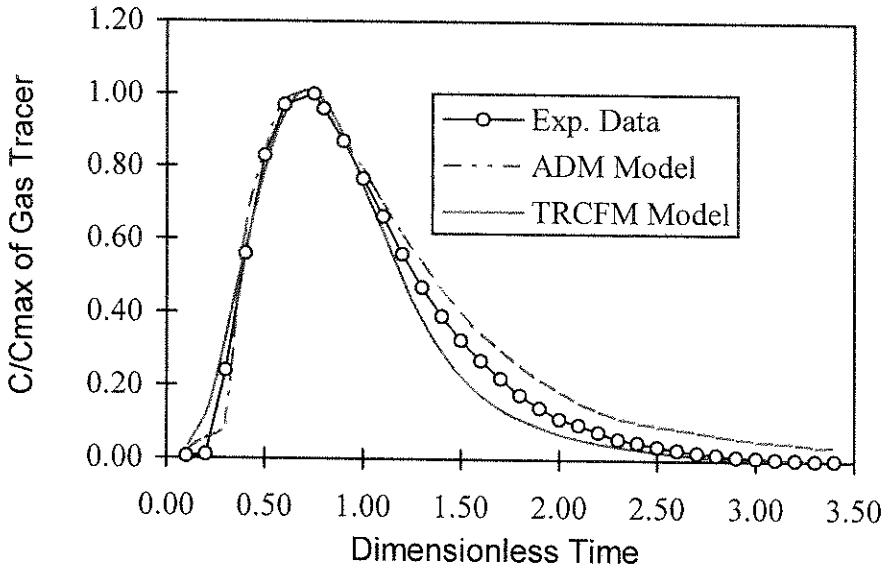

FIGURE 8-5. Comparison of TRCFM, ADM Simulation Results at the Outlet of the Column with Shetty et al. (1992)'s Experimental Data. For simulation of TRCFM, $K_{g12} = 1.75$, $K_{l12} = 80$, $(k_la)^l = 0.0234$ 1/s, $(k_la)^s = 0.1039$ 1/s

It is clear that a satisfactory fit can be achieved with the TRCFM. Although an almost equivalent fit can also be achieved by the axial dispersion model (ADM), the axial dispersion model lacks the physical basis to describe gas and liquid phase mixing in bubble column reactor.

8.2.2 Field and Davidson (1980)'s Data for a Large Size Bubble Column

Another set of experimental data was from Field and Davidson (1980). In their experiments, a large bubble column was used, and the diameter of the column was as large as 3.2 m, the aerated liquid height was as high as 18.9 m. Temperature in the system was 370-410 K. The superficial liquid velocity was 0.034 m/s, the superficial gas velocity

was 0.052 m/s. A radioactive gas tracer, Ar41, was used so that the detection devices could be placed externally to the column. Detectors were placed at the inlet and outlet. The detectors were scintillation counters connected to rate meters and a UV recorder. Radioactive Argon was mixed with compressed nitrogen and injected into the air feed system. As Ar41 has a finite solubility in the liquid, there was an exchange of tracer between the gas and the liquid.

The system was air-organic liquid system containing mostly paraffin. As the superficial gas velocity was 0.05 m/s in this experiment, it can still be assumed that bubbly flow regime prevails (refer to Figure 4-5). Therefore, uniform small size bubbles are assumed, the average hold up was taken as 0.34 which was determined from the reported experiments.

In summary, the physical properties and operating conditions were:

The diameter of the column was 3.2 m, the aerated liquid height was 18.9 m, the operating temperature was 370-410 K, the superficial liquid velocity, u_l was 0.034 m/s, the superficial gas velocity, u_g was 0.052 m/s, the average gas hold up, $\overline{\varepsilon_g}$ =0.34, therefore, the average small bubble hold up, $\overline{\varepsilon_{gs}} = 0.34$. The liquid viscosity, μl = 0.3 cp, the liquid density, $\rho_l = 800\ kg/m^3$.

Field and Davidson (1980) used ADM for both gas and liquid phases. Following Ostergaard and Michelson (1969), the interface mass transfer was neglected in their model.

The TRCFM is used based on Figure 4-5 for bubbly flow regime. A uniform small size of bubbles is assumed due to low superficial gas velocity. Backmixing of small

bubbles and liquid is assumed. Since Ar41 has finite solubility in the liquid, it is not a good assumption to simplify the model by neglecting the mass transfer term through assuming equilibrium between the phases in Field and Davidson's (1980) analysis. Actually, Van Vuuren (1988) criticized their analysis and it was found that the Henry's coefficient for Ar41 in paraffin is about 5.4 and the mass transfer term needs to be included. Therefore, in TRCFM, the coupling of the phase is considered through the mass transfer coefficient. The one dimensional liquid flow model from Ueyama and Miyauchi (1979) is used. The best fit is achieved for Henry's coefficient of 6 and mass transfer coefficient of 0.005 1/s. It is found that the value of Henry's coefficient used is quite close to the number reported by Van Vuuren (1988).

In summary, the following parameters are used in order to achieve the best fit (see Table 8-2).

TABLE 8-2. Summary of Parameters Used to Fit Field and Davidson (1980) 's Experimental Data (1980) by Using TRCFM Model

Parameter	Units	Value
τ_{g1}	sec	37.08
τ_{g2}	sec	18.17
τ_{l1}	sec	7.46
τ_{l2}	sec	12.68
r_{g12}		1.566
r_{l12}		17.948
K_{g12}		11
K_{l12}		7
k_{g12}	m^2 / s	0.242
k_{l12}	m^2 / s	0.101
$(k_l a)^s$	1/s	0.005
H	$mol / m^3(gas) * m^3(liquid) / mol$	6.0

Figure 8-6 shows the comparison between TRCFM results and the experimental data. It is shown that TRCFM fits this set of experiment data satisfactory. The normalized procedure of impulse response tracer curves can be referred to Section 4.2.1.1.

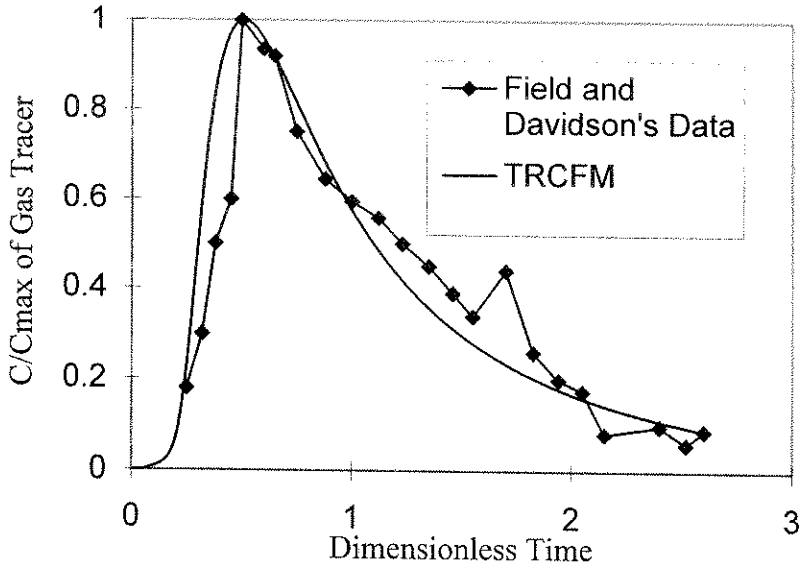

FIGURE 8-6. Comparison of Field and Davidson's Experimental Data of Soluble Gas Tracer (1980) at the Outlet of the Bubble Column with TRCFM Simulation Results (Continuous Flow of Gas and Liquid)

8.2.3 Some Predictions

8.2.3.1 Concentration Profiles in Each Region

The concentration profiles in the upflow and downflow regions of small bubbles are shown in Figure 8-7 to 8-11 for Shetty et al.'s (1992) data. It is clear that the concentration of the tracer is higher in the upflow region than that in the downflow region at the same longitudinal position in the bubble column. This result is similar to the result for the RCFM prediction with chemical reactions. This is due to a longer residence time in the downflow region of small bubbles. The same result is observed for the concentration curves of upflow region of liquid and downflow region of liquid because of longer residence time in the downflow region of the liquid than that in the upflow

region of the liquid. (refer to Figure 8-7, 8-8, 8-9 and Figure 8-10 and 8-11 for Shetty et al.'s data).

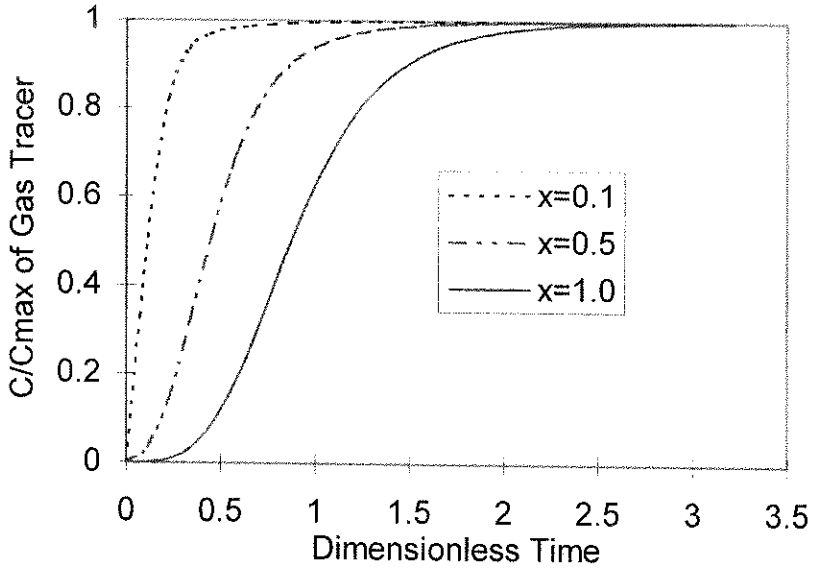

FIGURE 8-7. Soluble Gas Tracer Step Response of Small Bubbles in the Upflow Region along the Height of the Bubble Column Based on TRCFM and Operating Conditions from Shetty et al. (1992)

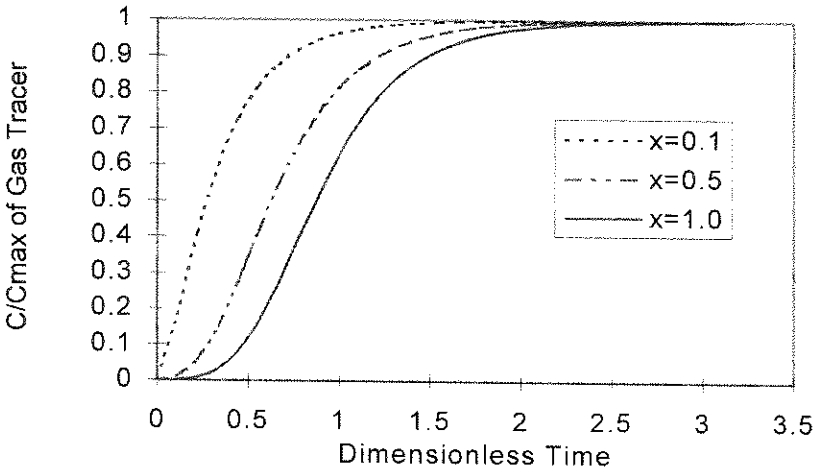

FIGURE 8-8. Soluble Gas Tracer Step Response of Small Bubbles in the Downflow Region along the Height of the Bubble Column Based on TRCFM and Operating Conditions from Shetty et al. (1992)

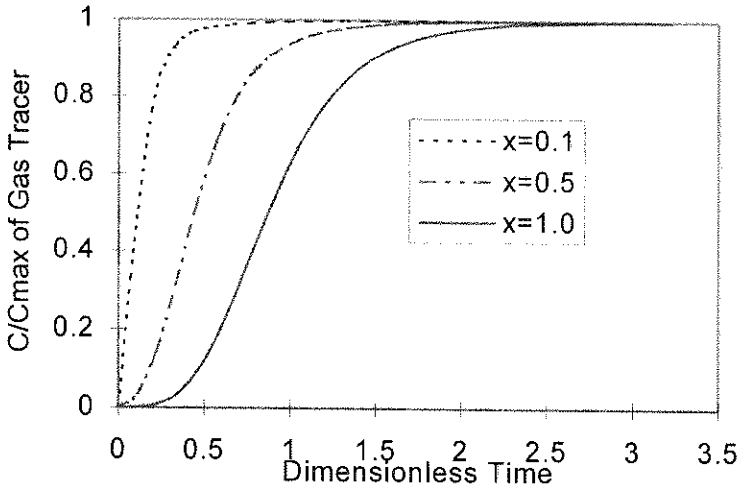

FIGURE 8-9. Soluble Gas Tracer Step Response of Large Bubbles in the Upflow Region along the Height of the Bubble Column Based on TRCFM and Operating Conditions from Shetty et al. (1992)

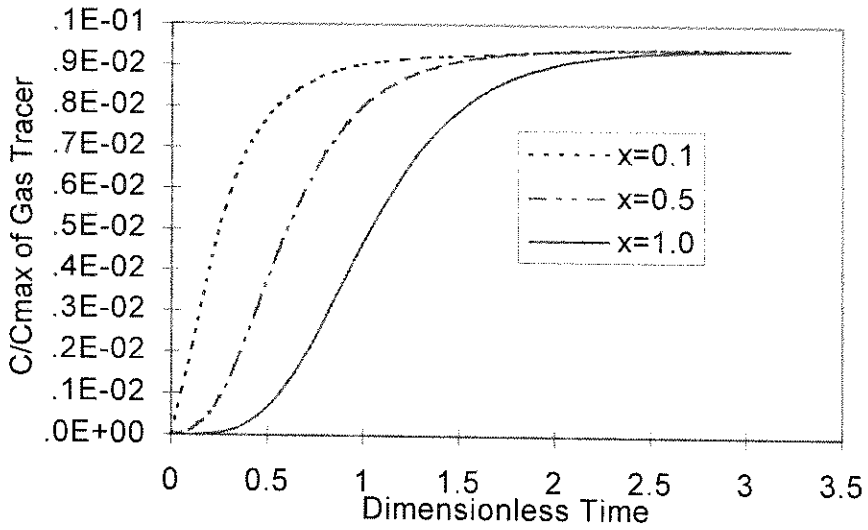

FIGURE 8-10. Soluble Gas Tracer Step Response of Liquid in the Upflow Region along the Height of the Bubble Column Based on TRCFM and Operating Conditions from Shetty et al. (1992)

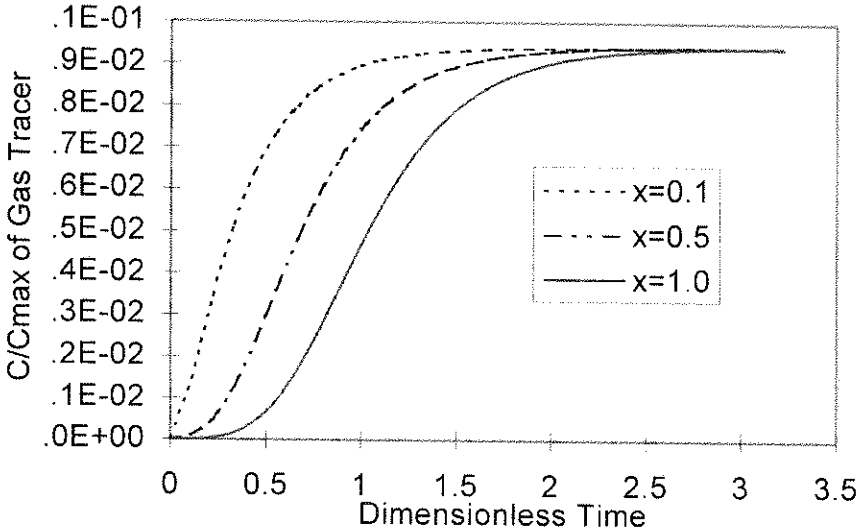

FIGURE 8-11. Soluble Gas Tracer Step Response of Liquid in the Downflow Region along the Height of the Bubble Column Based on TRCFM and Operating Conditions from Shetty et al. (1992)

The almost identical tracer curves of large and small bubbles indicate strong interaction (coalescence and break-up) and mixing between the large and small bubbles.

8.2.3.2 Concentration Profiles Along Longitudinal Direction

Using Shetty et al.'s experimental operating conditions (1992) for the TRCFM, the tracer response curves are presented in Figure 8-7 to 8-11 at x =0.1, 0.5, 1.0. The normalized response to step input, C/Cmax of tracer curves in different regions such as SB1, SB2, L1, L2 and LB are presented in Figure 8-7 to 8-11, respectively. It is found that the contour of the tracer curves moves to the increasing values of time on stream as x increases. It is also seen that, for a step injection of tracer represented by a Heaviside's step function, the normalized step response curves for the gas tracer approach 1 at large times and the normalized tracer curves for the liquid go to a value which approaches 1/H, where H is Henry's constant. This means that the equilibrium between the phases is nearly achieved close to the outlet of the bubble column ($HC_l - C_g \approx 0$).

The concentration profiles obtained as a response to an impulse gas tracer input are shown in Figure 8-12 to 8-16, respectively. The curves become broader with the increase of axial position indicating increased backmixing. With one dimensional ADM, it is impossible to obtain these results for different regions. This is the limitation of the conventional one dimensional ADM. The normalized procedure of impulse response tracer curves is referred to Section 4.2.1.1.

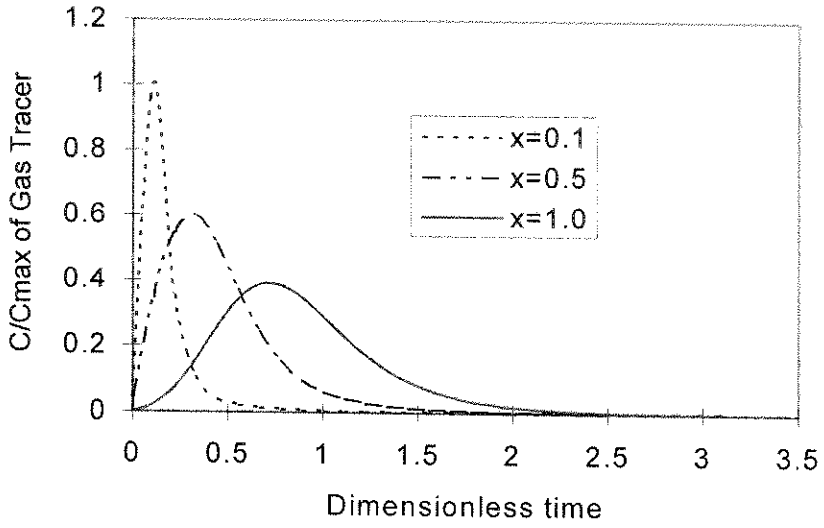

FIGURE 8-12. TRCFM Prediction of Impulse Soluble Gas Tracer Response for the Small Bubbles in Upflow Region at Different Vertical Positions in the Bubble Column (Operating Conditions from Shetty et al. (1992))

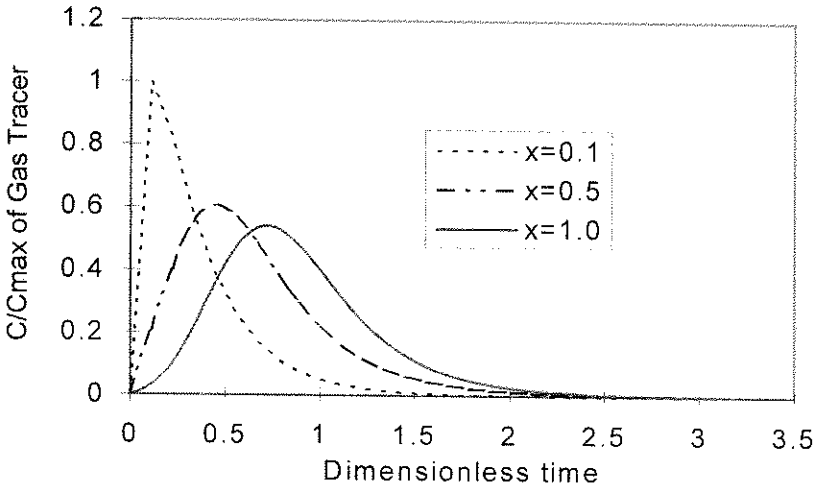

FIGURE 8-13. TRCFM Prediction of Impulse Soluble Gas Tracer Response for the Small Bubbles in Downflow Region at Different Vertical Positions in the Bubble Column (Operating Conditions from Shetty et al. (1992))

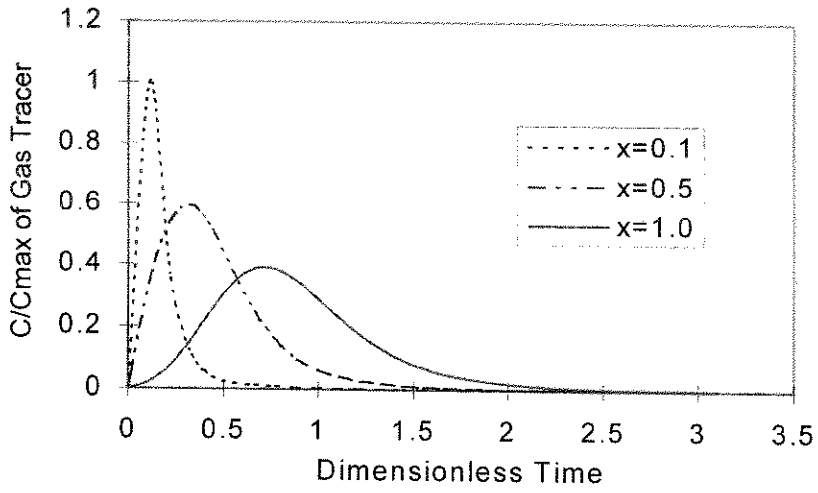

FIGURE 8-14. TRCFM Prediction of Impulse Soluble Gas Tracer Response for the Large Bubbles in Upflow Region at Different Vertical Positions in the Bubble Column (Operating Conditions from Shetty et al. (1992))

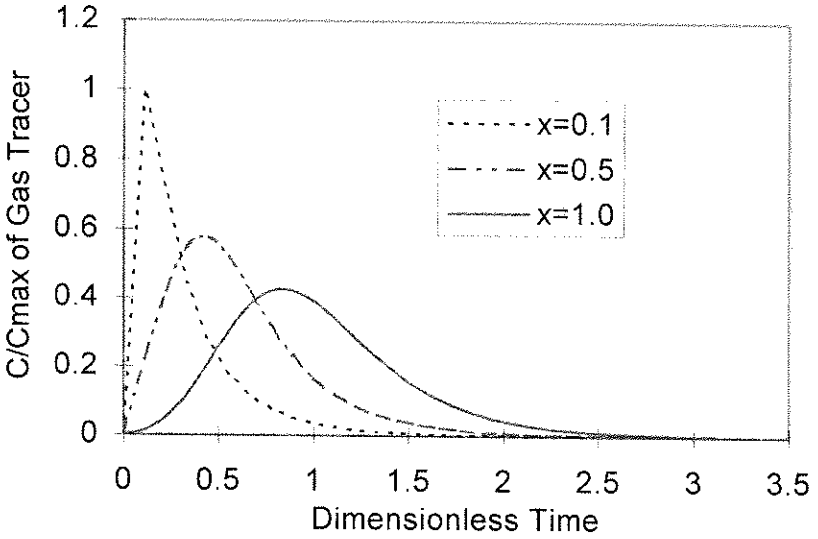

FIGURE 8-15. TRCFM Prediction of Impulse Soluble Gas Tracer Response for the Liquid in Upflow Region at Different Vertical Positions in the Bubble Column (Operating Conditions from Shetty et al. (1992))

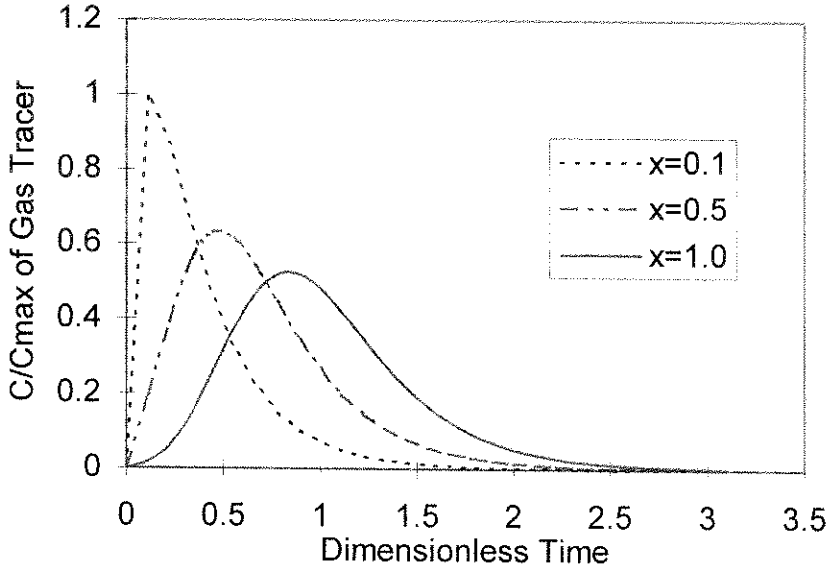

FIGURE 8-16. TRCFM Prediction of Impulse Soluble Gas Tracer Response for the Liquid in Downflow Region at Different Vertical Positions in the Bubble Column (Operating Conditions from Shetty et al. (1992))

8.2.3.3 Solubility Effect

The effect of solubility of the gas tracer on the tracer curves is studied using Field and Davidson's data (1980) with different gas tracer solubility of H = 6, 12, 24, 100 $mol/m^3(gas)*m^3(liquid)/mol$. The dimensionless exchange coefficient for the small bubbles, $K_1 = 12$, the dimensionless exchange coefficient for the liquid, $K_2 = 8$, (similar to the fitting parameters from Field and Davidson (1980)'s experimental data), the mass transfer coefficient, $k_l a$ = 0.0065 1/s. The results are illustrated in Figure 8-17. It is evident that the solubility of the tracer does affect the tracer curve. The higher the solubility (lower H values) is , the longer the tail of the tracer curve is. The tracer curve drops slower with increasing solubility. In addition, the time to achieve the peak value of the impulse tracer response curve is almost identical for all three cases. The result with "long tail" in the case of high solubility is consistent with Vermeer and Krishna's

experimental result (1981) during their experiment of using soluble Argon 41, CH_4 *and* CO_2 tracer in turpentine liquid system. This indicates that the solubility has an impact on the tracer curves. The correction for solubility effect is needed in order to achieve more accurate result during tracer study. Cmax is the maximum tracer concentration in the outlet of the column for a pulse injection of tracer for different gas solubility.

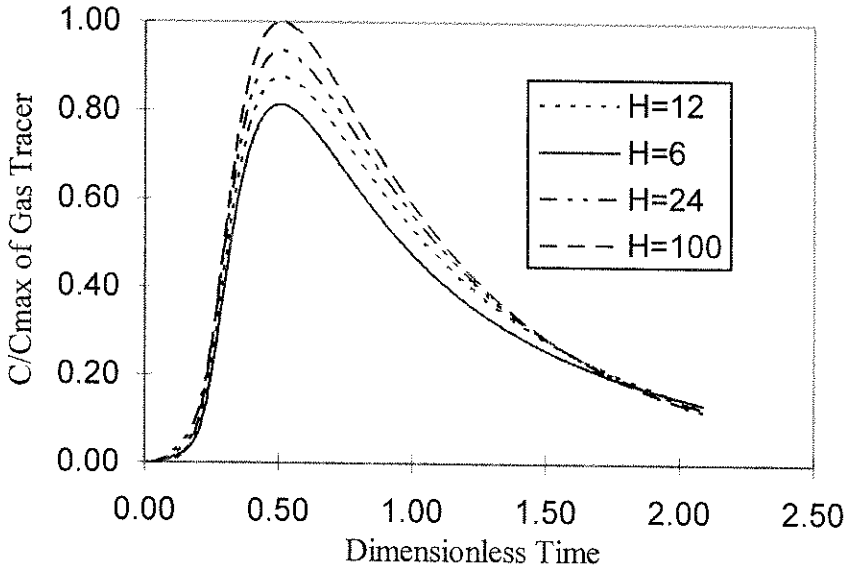

FIGURE 8-17. Solubility Effect on the Gas Tracer Curves at the Outlet of the Column based on TRCFM Model

8.2.3.4 Effect of Mass Transfer Coefficient

The mass transfer coefficient has effects on the tracer response are illustrated in Figure 8-18. Most of the operating conditions used are based on Field and Davidson's (1980) experimental conditions. The dimensionless exchange coefficients for the upflow

and the downflow of small bubbles and for the upflow and the downflow of liquid are chosen as 12 and 8, respectively.

The different values of mass transfer coefficient $k_l a$ of 0.65, 0.065 and 0.0065 1/s are applied in the model equation. It is assumed that Henry's coefficient is as small as 6 $mol/m^3(gas)*m^3(liquid)/mol$. This indicates that gas is quite soluble. It is shown that the tracer curves moves to the increasing values of time as the value of mass transfer coefficients decreases. Furthermore, the tails of the impulse tracer curves become longer with the increasing values of mass transfer coefficients. More interestingly, with the increase in mass transfer coefficient, the 'second small hump' occurs with the high value of mass transfer coefficient ($k_l a$ of 0.65 1/s) when dimensionless time ranges from 0.4 to 0.6. As we know the gas tracer with such low Henry's coefficient is highly soluble. This second peak is consistent with Vermeer and Krishna's (1981) experimental data by using soluble Ar, CH_4 or CO_2 as a gas tracer in the solvent turpentine 5. These phenomena also appear in Air Products & Chemicals, 1990 to DOE's report for their interpretation of tracer curves for the Laporte slurry bubble column reactors. The simulated mass transfer coefficient used was the same magnitude as that is used in the simulation of $k_l a = 0.65$ 1/s (Toseland et al.(1994)). Up to now, the second peak of tracer curves hasn't been reported by using conventional mixing model such as ADM. But, this can be handled by TRCFM, which indicates the applicability of this model.

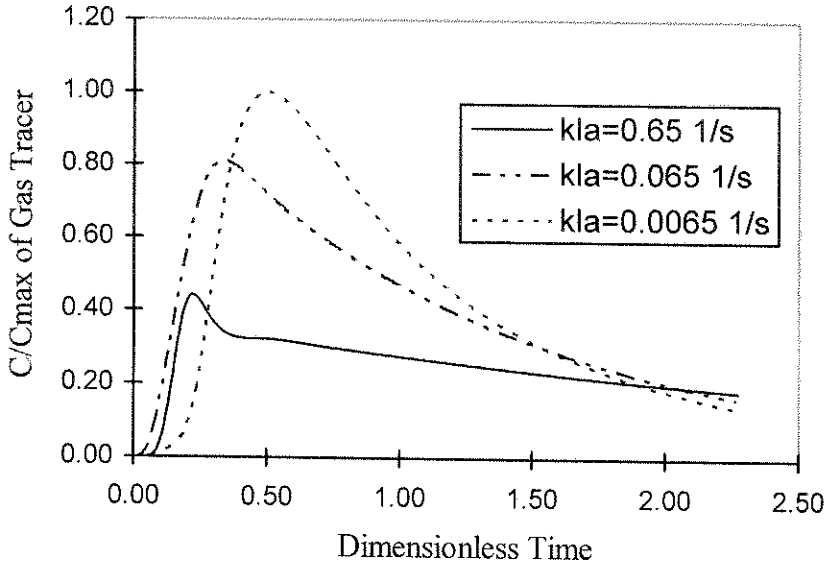

FIGURE 8-18. Effect of Mass Transfer Coefficients on the Impulse Soluble Gas Tracer Curves at the Outlet of the Column based on TRCFM

9. Conclusions

The proposed "Two Phase Recycle (Recirculation) with Cross Flow Model (TRCFM)" is a good choice for modeling both gas and liquid phase mixing. It fits the current experimental data for both large and small bubble columns well. TRCFM is applicable for either churn turbulent regime or bubbly flow regime in the bubble column reactors. These are the two common flow regimes in the current operation of industrial bubble columns. Definitely, it has significant potential for future modeling of the industrial bubble columns reactors.

Based on the findings discussed above, in summary, TRCFM has the following advantages:

It is more physical than conventional ADM because the bimodal bubble size distribution is incorporated in the model. The gas and liquid upflow and downflow are included. Therefore, the backmixing is modeled based on the observed flow pattern. Different concentration profiles in different regions can be determined, which is impossible for the conventional ADM to achieve. The different mixing behavior of large and small bubbles is described in the model. Various interactions between the large and the small bubbles, between the liquid in the upflow region and the liquid in the downflow region, between the small bubbles in the upflow region and the small bubbles in the downflow region are incorporated in the model. The liquid phase reaction may also be incorporated in the model. The coupling of the phases is brought in through the mass

transfer coefficient. A weighting function is defined to represent the contribution of mass transfer for different size of bubbles or the same size of bubbles in different regions. All these considerations make the TRCFM reflect realty. In some sense, this model is " two dimensional".

In addition, the RCFM (subcase of TRCFM) has been successfully applied for both gas and liquid phase mixing. The good fit of the RCFM with Myers et al.'s (1987) experimental data indicates once again that RCFM can be used for investigating liquid phase mixing in the bubble column system. The comparison of RCFM with Towell and Ackerman (1972)'s gas tracer data in a medium size bubble column indicates that RCFM can also be extended for modeling gas phase mixing.

The predicted results of the liquid phase recycle with cross flow model (subcase of TRCFM) with different chemical reaction schemes seems quite realistic. The same realistic result is apparent from the model prediction for the tracer injected in the middle of the bubble column. If, later, these can be verified experimentally, the proposed model will have important advantages over the conventional ADM in modeling the concentration distribution in the bubble column.

The difference of concentration profiles in the upflow and downflow indicates that it is important to consider this effect during experimental tracer study or chemical reaction study in order to obtain the local concentration more accurately. That is to say, the average concentration at a given height of the bubble column may be quite different from the local concentration at the same height. More detailed experimental technique is needed to verify these results.

Simulation of mass transfer coefficients and solubility effects on the impulse tracer curves indicates TRCFM model mimics the experimental discoveries. The experimental observations such as tracer's "second peak" has never been simulated successfully by conventional model such as ADM.

Simulation of pulse liquid tracer response under the continuous flow of gas and batch liquid operation reveals the " overshoot" response near the tracer injection position. This result is consistent with Laporte tracer runs (Air Product, 1990). For ADM, it is impossible to simulate such behavior.

10. Recommendation for Future Work

The even better fit with experimental data may be achieved by adding axial turbulent diffusion terms in the SB1, SB2, L1 and L2 regions instead of assuming plug flow with crossmixing as done in our model. But, how to treat four additional eddy diffusion coefficients theoretically or experimentally needs to be further studied. The average turbulent eddy diffusivity in the liquid phase may be used for the axial dispersion coefficients in the upflow region of the liquid and the downflow region of the liquid. It was found by Degaleesan et al. (1996) that eddy diffusivity may also be obtained from CARPT in their laboratory. By averaging the radial eddy diffusivities in the upflow region of the liquid phase and the downflow region of the liquid phase, the eddy diffusion coefficients of the liquid phase may be obtained in L1 and L2 regions. The average value of the radial eddy diffusivity at the point of inversion (the point where the interstitial liquid velocity is zero) may be used as an estimate of exchange coefficient between the upflow of liquid and the downflow of the liquid. A similar theory needs to be exploited to obtain the axial dispersion coefficients of small bubbles in both the upflow and the downflow regions as well as the exchange coefficient between the upflow of small bubbles and the downflow of small bubbles.

In addition, the mean residence time in the four mixing zones (LM1, LM2, GM1 and GM2, refer to Figure 4-3) may be considered in order to have more accurate results. In our current model, we assume negligible mean residence time. How to determine the volumes and flow pattern in these four zones is a subject for further investigation.

The correlations of mass transfer coefficient and interfacial areas need to be further developed to match the data with various operating conditions. Most of the existing correlations from different authors usually can only be applied for their operating conditions (refer to Table 6-4).

The new experimental apparatus needs to be developed such as optical probe or conductivity probe to obtain the bubble rise velocity and bubble size distribution.

The more accurate result may be achieved by experimentally determining liquid interstitial velocity profile and holdup distribution such as CARPT together with CT developed in CREL laboratory (Devanathan et al. (1990) and Kumar et al. (1994)) instead of using empirical correlations.

Since TRCFM can explain some experimental observation such as "long tail", "second peak" for soluble gas tracer and "overshoot" response for liquid tracer during batch mode operation of the liquid, the quantitative validation of TRCFM with those experimental data such as tracer curves for the Laporte bubble column reactor is needed (Air Product & Chemical (1990) and Toseland et al. (1994)).

Finally, if all the above can be achieved, then the population balance equations of the bubble size distribution may be incorporated into the model equations instead of only assuming two bubble classes.

11. References

(1) Air Products & Chemicals Inc. and Chem Systems Inc. *A Report to DOE contract No. DE-AC22-87PC90005*. August 1990.

(2) Anderson, K.G. and R.G. Rice. 1989. *Local turbulence model for predicting circulation rates in bubble columns*. AIChE. J, 35:514-518.

(3) Akita, K., and F.Yoshida. 1973. *Gas hold-up and volumetric mass transfer coefficient in bubble columns, effects of liquid properties*. Ind. Eng. Chem. Process Des. Dev. 12:76.

(4) Bach, H.F., and T. Pilhofer. 1978. *Variation of gas hold-up in bubble columns with physical properties of liquids and operating parameters of columns*. Ger. Chem. Eng. 1:270.

(5) Bankoff, S.G. 1960. *Available density single-fluid model for two-phase flow with particular reference to steam water flow*. J. Heat. Transfer, Trans. ASME. Serres C. 82: 265-272.

(6) Biesheuvel, A. and W. C. M. Gorissen. 1990. *Void fraction disturbances in a uniform bubbly fluid.* Int. J. Multiphase Flow. 16:211.

(7) Biesheuvel, A., S. Spoelstra. 1990. *The added mass coefficient of a dispersion of spherical gas bubbles in liquid.* Int. J. Multiphase Flow. 15:911-924.

(8) Boussinesq, J. 1896. *Theory de'l ecoulement tourbillant et tumultueux des liquides.* Acad. Sci. Paris, 122:1298.

(9) Bukur, D.B., J.G.Daly, S.A.Patel, R.Matheo, and G.B.Tatterson. 1986. *Hydrodynamic parameters for the Fischer-Tropsch Synthesis in bubble column reactors.* Proc. DOE Indirect Liquefaction Contactors Mtg., Monroeville, PA. 126 (Dec.3-4, 1986).

(10) Calderbrank, P. H. and M. B. Moo-Young. 1961. *The continuous phase heat and mass transfer properties of dispersions.* Chem. Engng. Sci. 9(2): 171-174.

(11) Deckwer, W.D., 1985. *Reaktionstechnik in blasensouler*; Verlag Sauerlunder and Salle Asran and Frankfurt a. Main, Germany

(12) Deckwer, W.D., and A. Schumpe. 1993. *Improved tools for bubble column reactor design and scale-up.* Chem. Engng. Sci. 48:889-911.

(13) Degaleesan, S., S. Roy, S.B. Kumar, and M.P. Dudukovic'. 1996. *Liquid mixing based on convection and turbulent dispersion in bubble columns.* Accepted by 14th Chem. React. Eng. Conference.

(14) Devanathan, N., D. Moslemian, and M.P. Dudukovic'. 1990. *Flow mapping in bubble columns using CARPT.* Chem. Engng. Sci. 45:2285-2291.

(15) Dudukovic', M. P. 1987. *Tracer methods in chemical reactors: techniques and applications, Chemical Reactor Design and* Technology (De Lasa, H. ed) NATO Series E: Applied Sciences N-110 (Nijhoff Publishing Co, Dordrecht, Holland).

(16) Field, R.W., and J. F. Davidson. 1980. *Axial dispersion in bubble columns.* Trans I Chem E, 58:228.

(17) Froment, G.F., K.B. Bischoff. 1990. *Chemical Reactor Analysis and Design.* 2nd ed; John Wiley and Sons: New York, 543-547.

(18) Geary, N.W., and R.G.Rice. 1992. *Circulation and scale-up in bubble columns.* AIChE J., 38(1): 76-82.

(19) Gestrich, W., and W. Krauss. 1975. *Die spezifische phasengrenzflache in blasenschichten.* Chem. Engng. Tech. 47:360.

(20) Grienberger,J. and H. Hoffmann. 1992. *Investigations and modeling of bubble column reactors*. Chem. Engng. Sci. 47: 2215-2221.

(21) Hikita, H., S. Asai, K. Tanigawa, and M. Kitao. 1981. *The volumetric mass transfer coefficient in bubble columns.* Chem. Eng. J. 22:61.

(22) Hikita, H., and H. Kikukawa. 1974. *Liquid phase mixing in bubble columns, effect of liquid properties.* Chem. Eng. J. 8:191.

(23) Hill, J.H. 1974. *Radial non-uniformity of velocity and voidage in a bubble column.* Trans. IChemE. 52:1-9.

(24) Hochman, J.M., and J.R. McCord. 1970. *Residence time distribution in recycle systems with crossmixing.* Chem. Engng. Sci. 25:97-107.

(25) Hoefsloot, H.C.J., and R. Krishna, 1993. *Influence of gas density on the stability of homogeneous flow in bubble column.* Ind. Eng. Chem. Res. 32:747-750.

(26) Idogawa, K., K. Ikeda, T. Fukuda, and S. Morooka. 1986. *Behavior of bubbles of the air-water system in a column under high pressure*. Int. Chem. Eng. 26:468.

(27) Idogawa, K., K. Ikeda, T. Fukuda, and S. Morooka, 1987. *Effect of gas and liquid properties on the behavior of bubbles in a column under high pressure*. Int. Chem. Eng. 27:93.

(28) Joseph, S., Y.T. Shah, and B.G. Kelkar. 1985. *A simple experimental technique to measure gas phase dispersion in bubble columns*. Chem. Eng. Comm. 24:105.

(29) Kashiwa, B.A., and R.A. Gore. 1991. *A four equation model for multiphase turbulent flow*. In First Joint ASME/ JSME Fluids Engineering Conference.

(30) Kawaoe, M., T. Otake, and R.D. Robinson. 1988. *Gas phase mixing in bubble column*. Journal of Chem Eng. of Japan. 22 (2): 136-142.

(31) Kawase, Y., B. Halard, and M.M. Young. 1987. *Theoretical prediction of volumetric mass transfer coefficients in bubble columns for Newtonian and non-Newtonian fluid.* Chem. Engng. Sci. 42:1609.

(32) Kawase, Y. and M. Moo-Young. 1986. *Influence of non-Newtonian flow behavior or mass transfer in bubble columns with and without draft tubes.* Chem. Eng. Comm. 40:67-83.

(33) Kawase, Y., S. Umeno, T. Kumagai. 1992. *The prediction of gas hold up in bubble column reactors: Newtonian and non-Newtonian fluids.* Chem. Eng. J. 51:1.

(34) Kobayasi, Y.I., and N. Kanegae. 1970. *Distribution of local void fraction of air-water two-phase flow in a vertical channel.* Bull. Japan. Soc. Mech. Eng. 13:1005-1012.

(35) Kojima, E., H. Unno, Y. Sato, T. Chida, H. Imai, K. Endo, I. Inoue, J. Kobayashi, H. Kaji, H. Nakanishi, and K. Yamamoto. 1980. *Liquid phase velocity in a 5.5m diameter column.* J. Chem. Engng. Japan, 13:16.

(36) Krishna, R and J. Ellenberger. 1995. *A unified approach to the scale-up of "Fluidized" multiphase reactors.* Trans IChemE. 73(A):217-221.

(37) Krishna, R., J.W.A. DeSwait, D.E. Hennephof, J. Ellenberger, H. C.J. Hoefsloot. 1994. *Influence of increased gas density on hydrodynamics of bubble column reactors.* AIChE J. 40:112.

(38) Krishna, R., P.M. Wilkinson and L.L Van Dierendonck. 1991. *A model for gas holdup in bubble columns incorporating the influence of gas density on flow regime transitions.* Chem. Engng. Sci. 46(10): 2491-2496.

(39) Kumar, S.B., N. Devanathan, D. Moslemian, and M.P. Dudukovic'. 1994. *Effect of scale on liquid recirculation in bubble columns*. Chem. Engng. Sci. 49:5637-5652.

(40) Levenspiel, O., T.J. Fizgerald. 1983. *A Warning on the misuse of the dispersion model*. Chem. Engng. Sci. 38(3): 489-491.

(41) Lockett, M.J. and R. D. Kirkpatrick. 1975. *Ideal bubbly flow and actual flow in bubble columns.* Trans IChem E. 53:267-273.

(42) Lübbert, A. 1991. *Characterization of bioreactors.* in Biotechnology, Edited by H.-J. Rehm and G. Reed, VCH.

(43) Lübbert, A., and A. Lapin. 1994. *Numerical simulation of the dynamics of two phase gas-liquid flows in bubble columns*, Chem. Engng. Sci. 49(21):3661-3674.

(44) Lübbert, A., and B. Larson. 1990. *Detailed investigations of the multiphase flow in airlift tower loop reactors.* Chem. Engng. Sci. 45 (10): 3047-3053.

(45) Luo, H. and H.F. Svendsen. 1991. *Turbulent circulation in bubble columns from eddy viscosity distributions of single-phase pipe flow*. Can. J. Chem. Eng. 69:1389-1394.

(46) Menzel, T., Thomas in der Weider, Olive Staudacher, Ondra Wein and Ulfert Onken. 1990. *Reynolds shear stress for modeling of bubble column reactors*. Ind. Eng. Chem Res. 29: 988-994.

(47) Miyauchi, T., S, Furusaki, S. Morooka, and Y. Ikeda. 1981. *Transport phenomena and reaction in fluidized catalysts beds*, in Advances in Chemical Engineering. 11:275-448.

(48) Miyauchi, T. and C.N. Shyu. 1970. *Flow of fluid in gas bubble columns*, Kagaka Kogaku, 34:958-964.

(49) Modak, S. Y., V. A.Juvekar, and V. C. Rane. 1993. *Dynamics of the gas phase in bubble column.* Chem. Eng. Technol. 16: 303-306.

(50) Myers, K.J. 1986. *Liquid phase mixing in churn turbulent bubble columns.* D.Sc. Thesis, Washington University, St. Louis, MO.

(51) Myers, K.J., M.P. Dudukovic', and P.A. Ramachandran. 1987. *Modeling of churn -turbulent bubble columns 1: Liquid phase mixing.* Chem. Engng. Sci. 42:2301-2311.

(52) Myers, K. J., Dudukovic', M.P. and Ramachandran, P.A. 1987. *Modeling liquid-phase chemical reactions and interface mass transfer in churn turbulent bubble columns.* Chem. Engng. Sci. 42(11):2757-2766.

(53) Ostergaard, K. and M.L. Michelson. 1969. *On use of imperfect tracer pulse method for determination of holdup and axial mixing.* Can. J. Chem. Eng. 47:107.

(54) Oztork, S. S., A. Schumpe, and W. -D. Decker. 1987. *Organic liquids in bubble columns: Hold-ups and mass transfer coefficients.* AIChE J. 33:1473.

(55) Petrick, M. 1959. *Investigation of two-phase air water flow phenomena.* Tech. Rep. #14. ANL.

(56) Reilly, I.G., D.S. Scott, T. J. W. De Bruijn, and D. McIntyre. 1994. *The role of gas momentum in determining gas hold-up and hydrodynamics flow regimes in bubble column operations.* Can. J. Chem. Eng. 72:3.

(57) Reilly, I.G., D.S. Scott, T. Jain A. De Bruijn, and J. Piskorz, 1986. *A correlation for gas hold up in turbulent coalescing bubble columns*. Can. J. Chem. Eng. 64:705.

(58) Riquarts, H.P. 1982. *Stromungsmechanische modllierung von blasensaulenreak torer*. Chem. Ing. Tech. 54:770.

(59) Schlichting, H. 1979. *Boundary Layer Theory,* New York: McGraw Hill, 11:602-609.

(60) Schumpe, A., and W.D. Deckwer, 1987. *Viscous media in tower bioreactors: Hydrodynamic characteristics and mass transfer properties*. Bioprocess Eng. 2:79.

(61) Shah, Y.T., S. Joseph. 1986. *Errors caused by tracer solubility in the measurement of gas phase axial dispersion.* Can. J. Chem. Eng. 64:380.

(62) Shetty, S.A., M.V. Kantak, and B.G. Kelkar. 1992. *Gas-phase backmixing in bubble-column reactors*. AIChE. J. 38(7): 1013-1026.

(63) Sotelo, J.L., F. J. Benitez, J. Beltran-Heredia, and C. Rodriquez. 1994. *Gas hold up and mass transfer coefficients in bubble columns. 1. porous glass-plate diffusers.* Int. Chem. Eng. 34:82.

(64) Suh, I.-S., A. Schumpe, W.-D. Deckwer, and P. Ponzi. 1984. *Hydrodynamic characteristics of three phase reactors.* Chem. Eng. J. 18:270.

(65) Toseland, B.A., D.M. Brown,. B.S. Zou, and M.P. Dudukovic'. 1994. *Flow patterns in a slurry bubble column reactor under reaction conditions.* Trans IChem E. 73:297-301.

(66) Towell, G.D., and G.H. Ackerman. 1972. *Axial mixing of liquid and gas in large bubble reactors.* 5th European International Symposium Chem. React. Eng. B3-1, Elsenz, Amsterdam.

(67) Ueyama, K. and T. Miyauchi. 1979. *Properties of recirculating turbulent two phase flow in gas bubble columns.* AIChE. J. 25:258-266.

(68) Van Vuuren, D. S. 1988. *The transient response of bubble columns.* Chem. Engng. Sci. 43 (2): 213-220.

(69) Vermeer, D.J. and R. Krishna. 1981. *Hydrodynamics and mass transfer in bubble columns operating in the churn-turbulent regime*. Ind. Eng. Chem. Proc. Des. Dev. 20:475-482.

(70) Wallis, G.B. 1969. *One-Dimensional Two Phase Flow*, McGraw-Hill, New York.

(71) Wilkinson, P.M. 1991. *Physical aspects and scale up of high pressure bubble columns*. Ph.D. Thesis, Rilksuniversiteit Gronigen, the Netherlands.

(72) Wilkinson, P.M., A.P. Spek, and L. L. Van Dierendonck. 1992. *Design parameters estimation for scale up of high pressure bubble columns.* AIChE. J. 38:544.

(73) Wilkinson, P.M., and Herman. Haringa. 1994. *Mass transfer and bubble size in a bubble column under pressure.* Chem. Engng. Sci. 49:1417-1427.

(74) Zuber, N., and J.A. Findlay. 1965. *Average volumetric concentration in two-phase flow systems*. J.Heat Transfer Trans. ASME. 87:453-468.

12. Vita

Biographical items on the author of thesis, Mr. Qingqi Wang.

Graduation Date: August, 1996

1. Born on August 14, 1964 in Shanghai, P. R. China
2. BS, MS in Chemical Engineering from East China University of Science and Technology, Shanghai, P. R. China in 1985 and 1988
3. Process Engineer at Unilab Research Center of Chemical Reaction Engineering at Shanghai Pharmaceutical Industry Design Institute, P. R. China from 1988 to 1993
4. Graduate Student at the University of Rochester, Rochester, NY from 1993 to 1994
5. Graduate Student at Washington University, St. Louis, MO from 1994 to present
6. Senior Process Engineer at KTI Corporation, CA from 1995 to present
7. Member of AIChE
8. List of Publications and Presentations:

"Effect of Internal Diffusion in Porous Catalyst Particles on the Deactivating Kinetics for Second Order Reactions" presented on AIChE Annual meeting, San Francisco, CA in November, 1989 with Guotai Zhang and Zhinan Wu.

"A Study of the Behavior of Coke Formation on the Mordenite Catalyst for the Vapor-Phase Disproportionation of Toluene" Chemical Reaction Engineering and Technology 5(2), 27, 1989, P. R. China with Guotai Zhang and Zhinan Wu.

"On the Development of Packing Tower Liquid Distributor" Pharmaceutical Engineering Design 3, 1, 1989, P. R. China.

"A study on the Deactivating Kinetics for Vapor-Phase Disproportionation of Toluene Over Mordenite Catalyst" Journal of Catalysis 11(6), 483, 1990. with Guotai Zhang and Zhinan Wu.

"Effect of Intraparticle Diffusion on Catalyst Deactivation Kinetics for Second Order Reactions" Journal of Chemical Industry and Engineering 43(1), 82, 1992, P. R. China with Guotai Zhang and Zhinan Wu.

"A Two Phase Recycle with Cross Flow Model for Churn Turbulent Bubble Column Reactors" presented on the 5th World Congress in Chemical Engineering in July, 1996 with M. P. Dudukovic'.

"Progress in Understanding the Fluid Dynamics of Bubble Column Reactors" presented on the First Joint Power and Fuel System Contractors Conference , Pittsburgh, PA in July, 1996 with S. Degaleesan, S. Kumar, M. P. Dudukovic', B. A. Toseland and B. L. Bhatt.

"A Gas and Liquid Phase Mixing with Reaction Model for Churn Turbulent Bubble Column Reactors" to be presented on AIChE Annual Meeting, Chicago, IL in November 1996 with M. P. Dudukovic'.